Final Report

Project Title: Pre-Crash Interactions between Pedestrians and Cyclists and Intelligent Vehicles

September 30, 2018

CENTER FOR AUTOMOTIVE RESEARCH

OVERVIEW

This is the Final Report of the Project

Pre-Crash Interactions between Pedestrians and Cyclists and Intelligent Vehicles

Project Lead: Yaobin Chen

Professor and Chair, Department of Electrical & Computer Engineering
Email: ychen@iupui.edu
Office: 317-274-4032 Fax: 317-274-4493
723 West Michigan Street, SL160; Indianapolis, Indiana 46202-5132

Other Investigators: Donald Fisher (UMass), Umit Ozguner (OSU)

Project Description

This project investigates how autonomous and semi-autonomous vehicle systems can be configured and improved to accommodate pedestrian and bicycle safety. This project comprises both the modeling track and experimental track components, with a specific focus on pre-crash scenarios involving pedestrians and cyclists.

We propose to develop a simulation model for the vehicle pedestrian/cyclist crash testing scenarios building upon the Pre-Scan model developed at IUPUI. We will validate and modify the simulation models using the UTC's driving simulator network and vehicle field tests. We will first consider single vehicles, but extend to scenarios involving two or more vehicles engaging pedestrians and cyclists. One of the most dangerous scenarios for pedestrians is the multiple-threat scenario in which a vehicle approaching a crosswalk cannot see a pedestrian crossing the street because that pedestrian is obscured by another vehicle stopped for the pedestrian. It will be important to determine how vehicles with precrash warning and crash imminent braking (CIB) capabilities perform in these scenarios. We will also develop pedestrian/cyclist crash scenario simulations in which we can incorporate the bioinjury model to predict the pedestrian/cyclist injury for different crash scenarios using computer simulation and the driving simulator. Finally, we will use driving simulation experiment results to refine the simulation model and to inform on safety improvement technologies, such as earlier warning or automated braking. This project will leverage the CrIS UTC team's significant experience with vehicle-pedestrian crash scenarios. IUPUI has been developing and evaluating vehicle-pedestrian pre-crash warning and braking systems. A large amount of vehicle pre-crash performance data will be collected using two 2013-modelyear vehicles with pre-crash warning and CIB capabilities. The data will include the relative motion history of the vehicle and pedestrians, their motion trajectories and speeds, the time and distance that the vehicle pre-crash system starts warning and braking, and the vehicle and mannequin speeds at crash. Similar work is planned for cyclists in 2014.

IUPUI/TASI CrIS UTC Program
Final Report

by

Transportation Active Safety Institute (TASI)

Indiana University-Purdue University Indianapolis (IUPUI)

Contact: Yaobin Chen, Chancellor's Professor and Director of TASI

723 W. Michigan Street SL160, Indianapolis, IN 46202, USA

(317) 274-4032, ychen@iupui.edu

September 18, 2018

Table of Contents

1 Overview

Aims of project:

The TASI/IUPUI's research focus in the Crash Imminent Safety UTC (or CrIS UTC) was on pedestrian and cyclist inventions research for intelligent vehicles and automated driving (Project #5). In addition the TASI team also participated in Project #1 on pre-crash multiple-vehicle experimental analysis using a networked driving simulators located at five partnering institutions. To this end, the TASI team worked on several related research topics that are most relevant to improve the safety of pedestrians and bicyclists. These topics include:

1) Creating a driving simulation model of a pedestrian forward autonomous emergency braking (AEB),
2) Integrating the active safety sensing information in V2V study,
3) Using a dataset developed from the Indiana State Police and linking it with Census information from the American Community Survey to find the incidence related to race, income and poverty status of pedestrians and drivers involved in crashes and the scope for AEB technologies to mitigate them, and
4) Analyzing and mining big data of driving videos for crash avoidance

Following sections will provide a summary of main results from Topics 1) to 4). A detailed report for Topic 4) is given in a separate document (Appendix 1) as a mini-project funded by the Center for a two-year period. A list of related publications from this grant as well as the reprints of these papers are given in Appendix 2.

2 Overall outcomes of the project

2.1 Summary of Overall Outcomes

TASI studied three topics for this project. Topic 1 is to improve the safety of vulnerable road users by creating the Pedestrian AEB models. Topic 2 is to integrate the active safety sensing information in the V2V environment. Topic 3 is the benefit analysis if the bicyclist AEB system.

2.1.1 Topic 1. Improve the safety of vulnerable road users by creating the Pedestrian AEB models

TASI has developed a model of a pedestrian/cyclist automatic emergency braking (AEB) system based on hundreds of vehicle crash-test results from a Toyota CSRC project (non-UTC funded project). The proposed model was implemented using the PreScan simulation tool provided by TASS International. The results have been published in [1, 2]. The model describes the AEB performance based on the vehicle speed, pedestrian speed, pedestrian size, pedestrian motion direction relative to the vehicle motion, and lighting conditions. A bicyclist AEB model was also developed using a Petri-net model, which was described in detail in a Master's thesis [3]. In addition, TASI researchers have developed a preliminary automatic emergency pullover (AEP) system for automated driving with the driver being incapacitated due to sudden medical conditions (such as at heart defibrillation). A driving simulation model for the AEP system was developed and demonstrated on a Real-time Technology (RTI) driving simulator. The result was published in [4]. Details of these studies are in Section 2.2.

2.1.2 Topic 2. Integrate the active safety sensing information in the V2V environment
All possible crash scenarios that a V2V-AEB system can help to avoid and mitigate were studied based on the relative trajectories of the vehicles and bicyclists. The idea is to integrate V2V and AEB capabilities together and communicate the presence of cyclists from the AEB system to other vehicles around the same location. If a vehicle can exchange the cyclist sensing information in real-time, the vehicle can get potential cyclist crash information before itself can sense the cyclist crash, and hence, will have more lead time to respond to a potential crash and to improve safety. It was concluded that there were 98 possible scenarios that the V2V-AEB system can be beneficial for reducing the crash [5]. In order to use the V2V-AEB system, several related problems were investigated. The first problem is the V2V communication about the AEB sensed information. In the current DSRC protocol, there is not a message type that is defined to transmit the AEB sensed information about the vulnerable road users. Therefore, we studied and proposed a message protocol specifically for vehicles to exchange AEB system sensed vulnerable user information. This protocol was simulated and published in [6]. An architecture for simulating the V2V-AEB system was developed. The system modularized the needed functions for V2V-AEB simulation so that different algorithms in a specific part of the V2V-AEB simulation can be tested quickly [6, 7]. Since each vehicle can detect many different objects (vulnerable road users), and there may be many vehicles in the same area detecting the same objects, the number of exchange messages in a V2V network increases quadratically in terms of number of vehicles and number of vulnerable users on the road. We studied potential methods for reducing the unnecessary messages without reducing the performance of the V2V-AEB system [8]. Since the same vulnerable user can be detected by multiple vehicles, and these vehicles can broadcast the trajectory information of the detected objects at the same time, the message-receiving vehicle should be able to determine if different object information received from different vehicles are actually the same object. This is a real problem since the distance sensing error and GPS location errors always exist so that two different vehicles may give two different locations for the same object. Two object clustering methods were proposed to solve this problem [9, 10]. This helps the message-receiving vehicle to reduce the computation load. Seven graduate students worked on this task. The cyclist AEB model was used for vehicles to detect pedestrians and broadcast to other vehicles in the V2V-AEB simulation. Details of these studies are in Section 2.3.

2.1.2 Topic 3. The benefit analysis if the bicyclist AEB system.
In the US, the number of traffic fatalities has had a long term downward trend as a result of advances in the crash worthiness of vehicles. However, these improvements in crash worthiness do little to protect other vulnerable road users such as pedestrians or bicyclists. Several manufacturers have developed a new generation of crash avoidance systems that attempt to recognize and mitigate imminent crashes with non-motorists. While the focus of these systems has been on pedestrians where they can make meaningful contributions to improved safety, recent designs of these systems have recognized mitigating bicyclist crashes as a potential co-benefit. This paper evaluates the performance of one system that is currently available for consumer purchase. Because the vehicle manufacturer does not claim effectiveness for their system under all crash geometries, we focus our attention on the crash scenario that has the highest social cost in

the US: the cyclist and vehicle on parallel paths being struck from behind. Our analysis of co benefits examines the ability to reduce three measures: number of crashes, fatalities, and a comprehensive measure for social cost that incorporates morbidity and mortality. Test track simulations under realistic circumstances with a realistic surrogate bicyclist target are conducted. Empirical models are developed for system performance and potential benefits for injury and fatality reduction. These models identify three key variables in the analysis: vehicle speed, cyclist speed and cyclist age as key determinants of potential co-benefits. We find that the evaluated system offers only limited benefits for any but the oldest bicycle riders for our tested scenario. Details of these studies are in Section 2.4.

2.1.4 References

[1] Bo Tang, Stanley Chien, Yaobin Chen, "Obtain a Simulation Model of a Pedestrian Collision Imminent Braking System Based on the Vehicle Testing Data", 17th IEEE International Conference on Intelligent Transportation Systems, Qingdao, China, October 8-11, 2014.

[2] Alberto López, Stanley Chien, Lingxi Li, Qiang Yi, Yaobin Chen, Rini Sherony, "Certainty and Critical Speed for Decision Making in Tests of Pedestrian Automatic Emergency Braking Systems", IEEE Transactions on Intelligent Transportation Systems, PP(99):1-13, September 2016 DOI: 10.1109/TITS.2016.2603445.

[3] Wensen Niu, "A Petri Net Based Model for AEB Systems Considering Vehicle and Pedestrian/Cyclist in a Certain Area," Master Thesis Electrical and Computer Engineering, Purdue University Indianapolis. December 2017.

[4] Wasif Javaid, Yaobin Chen, Stanley Chien, "Design and Implementation of Vehicle Automatic Emergency Pull Over Strategy Using Active Safety Systems on a Driving Simulator", Fourth International Symposium on Future Active Safety Technology Towards Zero Traffic Accidents (Fast-zero), Nara, Japan, September 18-22, 2017.

[5] Mingxin Liu, Stanley Chien, Yaobin Chen, "Improve Road Safety Using Combined V2V and Pre-Collision Systems", 24th International Technical Conference on the Enhanced Safety of Vehicles (ESV2015), Gothenburg, Sweden, June 8-11, 2015.

[6] Bo Tang, Stanley Chien, Zhi Huang, Yaobin Chen, "Pedestrian Protection Using the Integration of V2V and the Pedestrian Automatic Emergency Braking System", 19th IEEE International Conference on Intelligent Transportation Systems, Rio de Janeiro, Brazil, November 1-4, 2016.

[7] Bo Tang, "Pedestrian protection using the integration of V2V communication and pedestrian automatic emergency braking system," Master Thesis Electrical and Computer Engineering, Purdue University Indianapolis. December 2015.

[8] Shalabh Rakesh Bhatnagar, Stanley Chien, Yaobin Chen, "Reducing Delay in V2V-AEB System by Optimizing Messages in the System", 25th International Technical Conference on Enhanced Safety of Vehicles (ESV), Detroit, USA, June 5-8, 2017.

[9] Zhi Huang, "Vehicle sensor-based pedestrian position identification in V2V environment," Master Thesis Electrical and Computer Engineering, Purdue University Indianapolis. December 2016.

[10] Jie Xue, Zhi Huang, Stanley Chien, Yaobin Chien, "A Hierarchical Clustering Analysis (HCA) for Pedestrian Position Identification in Autonomous Driving with Vehicle-to-Vehicle Communication", 25th International Technical Conference on Enhanced Safety of Vehicles (ESV), Detroit, USA, June 5-8, 2017.

[11] David Good, Kerry Krutilla, Stanley Chien, Lingxi Li, Yaobin Chen, "Preliminary Benefit Analysis for Pedestrian Crash Imminent Braking Systems," 18th International IEEE Conference on Intelligent Transportation Systems, Gran Canaria, Spain, November 2015. DOI:10.1109/ITSC.2015.186

2.2 Improve the Safety of Vulnerable Road Users

This section reports the two Pedestrian AEB models developed in this project. The first is a simple model for the simulation in PreScan environment. The second is an advance model for that can be used for systematic AEB design.

2.2.1 Obtain a Simulation Model of a Pedestrian Autonomous Emergency Braking System

2.2.1.1 Introduction

Pedestrian AEB is an active safety system component that aims to avoid or mitigate the collision with pedestrians [1]. Many automotive companies have been developing pedestrian AEB systems and have started to equip pedestrian AEB in some vehicles (e.g., Lexus 460L, Mercedes S550, and Volvo XC60). The performance of different pedestrian AEB systems varies significantly. Many research groups and government agencies are actively studying the methodologies for the evaluation of pedestrian AEB systems [2]. There are two ways to gather data to study the performance of pedestrian AEB system. The first is to conduct vehicle tests to gather the actual performance data. Due to the high cost of gathering the test data, and the complexity of test setup, only a limited number of tests with simple scenarios can be conducted practically. The second approach is to use a driving simulation for evaluating the effectiveness of an AEB system [3] in complex and severe crash scenarios. The requirement of the simulation approach is that the AEB simulation model must be sufficiently close to the actual AEB system being evaluated.

There are different approaches to generate an AEB model. The first one is to develop models of all components of an AEB system and link the component models together to make a AEB model. This approach is useful for the AEB system developer who has all the required component parameters. Without the parameters of the AEB components, it is difficult for a research institution to develop an AEB model that can mimic the actual performance of a real AEB system due to the complexity of the system. The second approach is to use physics principles to generate a demonstration model of the AEB systems. However, the model generated in this approach is not sufficient to determine the performance of a specific AEB system.

In this report we describe a new approach to create a pedestrian AEB simulation model for a specific vehicle. The approach is to use the general knowledge of the AEB components, which are published by the car manufacture, and use the collected pedestrian AEB performance test data of the AEB equipped vehicle in a set of test scenarios. This approach is implemented using the PreScan software [4]. PreScan is a strong physics-based simulation platform provided by TASS International. It is used in the automotive industry for the development of Advanced Driver Assistance Systems (ADAS). PreScan is also used for designing and evaluating vehicle-to-vehicle (V2V) and vehicle-to-infrastructure (V2I) communication applications as well as autonomous driving applications.

Section 2 shows the information needed for developing a pedestrian AEB simulation model. Section 3 describes the method for designing and implementing the pedestrian AEB simulation model. Section 4 evaluates the performance of the AEB simulation model. Section 5 concludes the paper.

2.2.1.2 Data collection for developing AEB model

The development of an AEB simulation model for a vehicle is based on two types of data, (1) the testing environment data and (2) the AEB performance data. Both of them can be obtained by

researchers in a series of well-designed AEB tests. The environment data is recorded before or during each test. The pedestrian AEB performance of a vehicle may vary significantly in different test environments. According to the testing data, seven factors are considered significant to the AEB performance. Table 1 lists all the environment data and the AEB performance data that used for developing the AEB simulation model. The more data collected, the more accurate the simulation model will be.

TABLE 1: THE ENVIRONMENTAL AND PEDESTRIAN AEB PERFORMANCE DATA USED FOR DEVELOPING AEB SIMULATION MODEL

Environment Data

Pedestrian Speed (m/s)	The actual moving speed of pedestrian.
Pedestrian Direction	Left to right, right to left, along traffic, against traffic
Pedestrian Size	Adult, child.
Pedestrian Cloth Color	The color of cloths of pedestrian.
Light Condition	Daylight, dark, dark lit.
Weather Condition	Sunny, cloudy, etc.
Vehicle Speed (m/s)	The actual moving speed of vehicle.

Performance Data

Warning Starting Distance to Target (m)	The distance from vehicle to pedestrian when the AEB warning starts.
Warning Starting Time to Collision (s)	The Time to Collision (TTC) when the AEB warning starts.
Braking Starting Distance to Target (m)	The distance from vehicle to pedestrian when the AEB braking starts.
Braking Starting TTC (s)	The TTC when the AEB braking starts.
Total Braking Time (s)	The duration of the total AEB braking
Average Deceleration During Braking (m/s²)	The average deceleration during braking process.
Stopped at Distance if Collision Avoided(m)	If the collision is avoided, this value represents the distance from vehicle to the pedestrian when the vehicle stopped.
Collision Speed if Collided (m/s)	If a collision with pedestrian occurred, this value represents the collision speed.
Estimated Minimum Safe TTC (EMST) (s)	When TTC to an object drops below this value, the object is considered dangerous. Then the pedestrian detection algorithm starts to verify whether this object is a pedestrian. This value is an estimated average value derived from the average of Warning Starting TTC.
Estimated Lateral Safe Distance (m)	When the lateral distance from vehicle to pedestrian drops below this value, pedestrian classification will start. This value is an estimated average value that derived from special test.

2.2.1.3 Develop the pedestrian AEB model
A. Structure of the AEB model

PreScan provides a demo of Pedestrian Protection System (PPS), which is similar to the pedestrian AEB system. The PPS provides early warnings when a potential collision with pedestrians is detected, and brakes automatically when a collision with pedestrian is inevitable. However, since the parameters used in PPS may not match the corresponding behavior in a specific

AEB system, part of the PPS provided by PreScan is modified to match the result of the AEB tests. For simplification and compatibility, the input and output ports of our developed AEB model are made identical to PPS. The pedestrian AEB model also consists of three sub-models that are similar to PPS's Radar Detection Model, Pedestrian Identification Model, and Decision Making Model. Our pedestrian AEB model uses the same Radar Detection Model as provided in PPS. We replaced the Camera Detection Model by a Pedestrian Identification Model since no video images are provided by the test data, and rewrote the Decision Making Model based on the pedestrian AEB testing data.

The purposes of sub-models of AEB are described as follows:

- Radar Detection Model - Based on the radar characteristics, this model can detect an object and calculate the time to collision (TTC). If the TTC drops below Estimated Min Safe TTC, this object will be considered dangerous.
- Pedestrian Identification Model - If a dangerous object is detected by the Radar Detection Model, this model continues to check whether it is a pedestrian, and provides a warning if a pedestrian classified.
- Decision Making Model - If an imminent crash to a pedestrian is identified by the Pedestrian Identification Model, this model decides the warning and braking behavior of the vehicle.

B. Development of sub-models of the pedestrian AEB model

1) Radar Detection Model

Radar Detection Model simulates the radar behavior for detecting potential collisions to objects. Radar is an object-detection system that can determine the distance, motion direction and speed of objects. Based on the radar information, the absolute velocity vector of an obstacle can be calculated. Assuming that the vehicle and the obstacle are moving in straight lines, absolute velocity vectors may intersect at a point where the collision will take place. Then the TTC is calculated.

Our Radar Detection Model was developed based on the same model in PreScan's PPS model, but some output parameters of the original model unrelated to AEB model were eliminated. Only two output parameters, TTC and Radar Detection Flag are reserved. Radar Detection Flag is used to indicate whether a dangerous object is detected by radar sensor. TTC is used to measure the severity of the dangerous object and relative decisions will be made based on it.

2) Pedestrian Identification Model

Usually, if an object is detected by radar sensor and considered to cause a potential crash, the pedestrian detection algorithm based on the camera sensor is engaged in order to determine whether the detected object is a pedestrian. However, it is hard for the researchers to know what technique and image-processing algorithms are used in the AEB system. Hence, it is not proper for the AEB simulation model to use any specific image-processing algorithm for pedestrian classification. As a result, our study only focuses on the behavior of the pedestrian AEB system and does not care what image processing technique and algorithms that the AEB use. Specifically, our pedestrian AEB simulation model concentrates on determining the conditions that whether a pedestrian could be detected by the AEB system and how long the AEB would take to classify the pedestrian. It is a testing data based classification algorithm. Usually, the efficiency and accuracy of image processing based pedestrian detection algorithms vary significantly in different test

environments. Our classification algorithm considers all these environmental factors to mimic the performance of real image processing algorithms. The input and output parameters of our algorithm are shown in Table 2.

TABLE 2: INPUT AND OUTPUT PARAMETERS OF WARNING DECISION MODEL

Input Parameters

V_{car}[m/s]	The actual moving speed of vehicle.
Radar Detection Flag	A flag indicating whether a pedestrian has been detected by radar sensor.
V_{ped} [m/s]	The Moving speed of the pedestrian.
S_{ped}	The size of the pedestrian. (e.g. child, fit adult, overweight adult)
C_{ped}	The cloth color of the pedestrian. (e.g. white, black, green, red)
D_{ped}	The moving direction of the pedestrian.
Light Condition	The light condition. (e.g. day, night)
Weather Condition	The weather condition. (e.g. sunny, cloudy, snow, rain, fog)

Output Parameters

Pedestrian Detection Flag	The flag to indicate whether a pedestrian is detected.

The single output parameter is a timed Pedestrian Detection Flag used to indicate if a pedestrian can be identified by the AEB, and when it would be identified. According to the testing data, the performance of AEB system can vary significantly under different test conditions. Higher vehicle speed, higher pedestrian speed, smaller pedestrian size, or poor visibility due to lighting condition and weather may cause longer pedestrian recognition time or even fail to recognize a pedestrian. A longer recognition time may mean a shorter time-period for AEB warning and braking, and may increase the probability of a crash. The testing data shows there are two circumstances that the vehicle collides with the pedestrian, (1) The vehicle fails to classify the pedestrian, and it hits the pedestrian directly without taking any action to avoid this collision (2) It takes too much time for the vehicle to classify this pedestrian successfully. Although automatic braking applied, the collision is still not avoided completely.

Within our pedestrian classification algorithm, the calculation of this Pedestrian Detection Flag is transformed to the calculation of Total Recognition Time. Since several parameters can affect the recognition time, the calculation process of the total recognition time is divided into several sub-problems. The recognition time relative to each parameter was calculated individually. Then these times are summed up to make a Total Recognition Time. However, we do not exactly know how much each of the parameters affects the image processing performance. Our approach to solve this problem is to manipulate the weights to match the testing data of a specific pedestrian AEB for each vehicle.

For example, the testing data of an AEB system shows that once the vehicle speed is higher than 45 mph, it always fails to warn and brake. During 0 to 45 mph, the vehicle speed is divided into several intervals. In this paper, the granularity of the intervals is assigned to be 5 mph. If a

higher accuracy required, the granularity can be set smaller. The recognition time for each speed interval is denoted as $T_{VS}[x < v \leq y]$ (x is the start of the speed interval, and y is the end of the speed interval). Within each vehicle speed interval, the recognition time is considered to be the same as the higher value, so that $T_{VS}[x < v \leq y] = T_{VS}[v = y]$. In order to get the recognition time for each speed interval ($T_{VS}[y]$, $y = 5, 10, 15 \ldots 40, 45$), a set of vehicle tests and calculations are needed. For each speed interval, the tests are repeated five times and then the average value of the obtained Warning TTC (denotes as TTC $[x < v \leq y]$ is obtained. Therefore, the different Warning TTC for different vehicle speed intervals can be obtained (the difference of recognition time between different speed intervals can also be calculated). Then the recognition time can be calculated as follows:

$$T_{VS}[x < v \leq y] = T_{VS}[0 < v \leq 5] + (TTC[0 < v \leq 5] - TTC[x < v \leq y]),$$

$$\text{(for } x = 0, 5, 10, 15, \ldots 35, 40, 45, y = x + 5)$$

(1)

$$T_{VS}[x < v \leq y] = \infty, \text{for } x > 45 \; mph$$

In equation 1, $T_{VS}[0 < v \leq 5]$ is a base value, and $(TTC[0 < v \leq 5] - TTC[x < v \leq y])$ is a difference value between $T_{VS}[x < v \leq y]$ and $T_{VS}[0 < v \leq 5]$. Since Warning TTC decreases with the increasing of vehicle speed, $TTC[0 < v \leq 5] - TTC[x < v \leq y] > 0$, when $x > 0$, the recognition time for each speed interval can be calculated based on the base value and the difference value between them. However, the value of base value $T_{VS}[0 < v \leq 5]$ is unknown. The only way to find the base value is to make a good guess and assign an initial value to it. After building the AEB simulation model, the correctness of the base value can be verified through simulations using the AEB test data. The base value can be adjusted to a more precise value by minimizing the difference of Warning TTC between the simulation data and AEB test data.

Table 3 is the recognition time with respect to the vehicle speed for an AEB being tested. T_{VS} is the recognition time delay caused by the vehicle speed factor. The recognition time for each speed interval was calculated based on the AEB test data. For example, $T_{VS}[5 < v \leq 10]$ was set as 0.1 s initially. Run the simulation with the AEB test scenario, TTC[0< v ≤5] is 2.31 s, and TTC[5< v ≤10] is 2.26 s. The difference value between them is 0.05 s. Then $T_{VS}[5 < v \leq 10]$ is reassigned as 0.1 + 0.05 = 0.15 s.

TABLE 3: VEHICLE SPEED AND RELATIVE TIME COST

Vehicle Speed (mph)	$T_{VS}(s)$
0-5	0.1
5-10	0.15
10-15	0.2
15-20	0.25
20-25	0.3
25-30	0.5
30-35	0.75
35-40	0.90

40-45	0.95
Others	∞

Table 4 – 7 present the recognition times caused by Pedestrian Speed, Pedestrian Type, Contrast and Pedestrian Direction. All of them are obtained in the same way as T_{VS}. Table 4 depicts the recognition time relative to pedestrian speed. T_{PS} is the pedestrian recognition time caused by the pedestrian speed.

$$T_{PS}[x < v \leq y] = T_{PS}[v = 0] + (TTC[v = 0] - TTC[x < v \leq y])$$

(2)

$$when(x, y = 0, 1.0, 1.5, 2.2, 2.5\ 3.0)$$
$$T_{PS}[x < v \leq y] = \infty, when\ (x > 3.0)$$

TABLE 4: PEDESTRIAN SPEED AND RELATIVE TIME COST

Pedestrian Speed (m/s)	T_{PS} (s)
0.0	0.1
0.0-1.0	0.1
1.0-1.5	0.1
1.5-2.2	0.5
2.2-2.5	0.8
2.5-3.0	0.95
Others	∞

Table 5 depicts the recognition time relative to pedestrian size. T_{PT} is the time of recognition caused by pedestrian type.

TABLE 5: PEDESTRIAN TYPE (SIZE) AND RELATIVE TIME COST

Pedestrian Type	T_{PT}(s)
Child	0.3
Fit Adult	0.1
Obese Adult	0.3

Table 6 represents the recognition time relative to the contrast of the pedestrian to the background. T_C is the recognition time caused by the contrast between the pedestrian and the back ground. The type of contrast is intuitively specified based on the Light Condition, Weather Condition, and the Cloth Color of Pedestrian. The principle is that, the easier to classify a pedestrian from the background, the higher the contrast is.

TABLE 6: CONTRAST AND RELATIVE TIME COST

13

Contrast	T_C(s)
High Contrast	0.2
Medium Contrast	0.4
Low Contrast	0.7
Super Low Contrast	∞

Table 7 describes the recognition time relative to pedestrian direction. In this paper, the pedestrian is assumed to be moving straight forward. So five basic directions for pedestrian are defined and discussed. The calculation method of the recognition time is also based on base value and difference value.

TABLE 7: PEDESTRIAN DIRECTION AND RELATIVE TIME COST

Pedestrian Direction	T_{PD} (s)
Stand (Face to the vehicle)	0.1
L2R	0.2
R2L	0.2
Along Traffic	0.3
Against Traffic	0.3
Others	N/A

Based on the weights and time costs that described in Tables 3 to 7, the total recognition time was calculated.

$$T_R = T_{VS} + T_{PT} + T_{PS} + T_C + T_{PD}$$

(3)

Additionally, Warning Starting TTC (WST) can be calculated based on T_R. If T_R is *greater than EMST* (Estimated Minimum Safe TTC), it means that the Pedestrian Identification Model fails to classify the pedestrian, then the *Pedestrian Detection Flag* will not be triggered. Otherwise, if TTC drops below WST, *Pedestrian Detection Flag* will be triggered.

$$WST = 0, when\ T_R \geq EMST$$

$$WST \approx EMST - T_R, when\ T_R < EMST$$

(4)

3) Decision Making Model

In the AEB Simulation model, the Decision Making sub-model is the last step to determine the behavior of the vehicle. It is a modification of the Actuation Model provided by PreScan. In the original Actuation Model in PreScan, the Warning Flag is set if a pedestrian has been classified and TTC drops below 1.6 s, and the Braking Flag is set if the TTC drops below 0.6 s. Furthermore,

the Braking Pressure is a preset value. Although the thresholds of Warning TTC, Braking TTC, and Braking Pressure can be modified in the original PreScan model, they are still not able to reflect the behavior of a pedestrian AEB system in a real vehicle. According to the AEB test data, the Warning TTC, Braking TTC, and Braking Pressure vary significantly in different test conditions. The threshold of Warning TTC has been described in the section describing the Camera Detection Model. In this section, the methods for calculating the thresholds of Braking TTC and Braking Pressure are discussed. Table 8 describes the input and output parameters of Decision Making Model. The output parameters are used by the action model and the display model provided by PreScan. If the Warning Flag is set, the action model will turn on the warning lights and beeps. If the Braking Flag is assigned, the action model will apply a specified braking pressure to the vehicle. All the actions and relative results will be displayed by the display model.

The Decision Making Model keeps examining the input parameters, Radar Detection Flag and Pedestrian Detection Flag. Once both Radar Detection Flag and Pedestrian Detection Flag are raised, the Decision Making Model triggers the Warning Flag immediately. Otherwise, the Warning Flag is not assigned.

TABLE 8: INPUT AND OUTPUT PARAMETERS OF DECISION MAKING MODEL

Input Parameters

V_{car} [m/s]	The actual moving speed of vehicle.
TTC	The time to collision.
Radar Detection Flag	The output parameter of the Radar Detection Model.
Pedestrian Detection Flag	The output parameter of the Pedestrian Identification Model
Output Parameters	
Warning Flag	A flag to indicate whether a warning should be triggered.
Braking Flag	A flag to indicate whether the brake should start.
Braking Pressure [bar]	The pressure applied to brake. It can be used to calculate the vehicle deceleration.

According to the testing data, the threshold of Brake Starting TTC (BST) can be modeled as a linear function of vehicle speed. When a pedestrian is detected as a collision object and TTC drops below the threshold of BST, the Braking Flag is assigned. Then desired Braking Pressure (BP) will be applied until the vehicle stops.

Figure 1 shows the modeling result of BST based on the testing data of a 2013 model year sedan. The x-axis is the speed of vehicle in mph. The y-axis is the BST in seconds. 325 tests are shown in this figure. Using the polyfit function provided by MATLAB, a straight line representing BST is plotted. To make it more realistic, a random offset, is generated and added to the sum. The range of the offset is from –x to x. 2x is the range of the BST in the AEB test data under each vehicle speed. Then the BST can be calculated as follows.

$$BST = 0.0647 * V_{car} + 0.2225 + offset$$

(5)
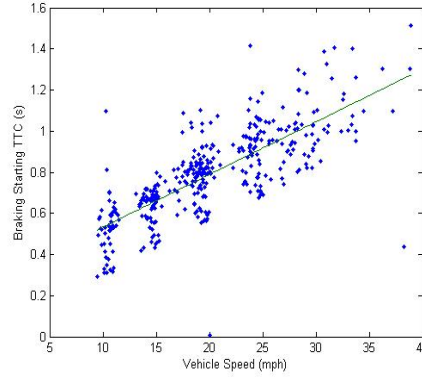
Figure 1. BST versus vehicle speeds.

In this study, the Braking Pressure was calculated based on the Average Deceleration in AEB braking. Figure 2 shows the desired deceleration under a specific vehicle speed of a 2013 model year sedan. The x-axis is the speed of the vehicle in mph. The y-axis is the Average Deceleration in AEB braking. To make it more similar to actual vehicle testing, a random offset is generated and added to the sum. The range of the offset is form –x to x. 2x is the maximum differences of the Average Deceleration in the AEB test data under each vehicle speed. The following is the calculation method of desired Deceleration.

$$Deceleration = 0.0912 * V_{car} + 6.5953 + offset$$

(6)

Once the desired average deceleration is calculated, the brake pressure, BP, can be calculated based on this desired deceleration. In the original PreScan Actuation Model, the default Braking Pressure is Max Brake Pressure (MBP). Under MBP, the deceleration of the vehicle is exactly 1g (9.81 m/s2). If the desired deceleration is known, the portion of the desired deceleration versus 1G can be calculated. Furthermore, multiply the Max Brake Pressure by this portion, then the desired BP is obtained. Once the full braking is applied, the Braking Pressure will remain a constant until the vehicle halt. The following formula shows the method for calculating desired Braking Pressure.

$$BP = MBP * (Deceleration / 9.81)$$

(7)
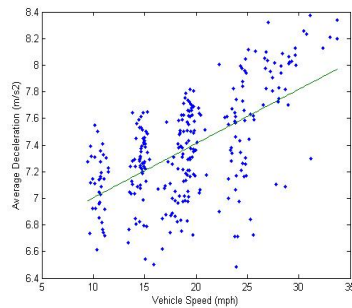
Figure 2. Average Deceleration versus vehicle speeds.

2.2.1.4 Simulation and results

Two different 2013 model year sedans with pedestrian AEB capability were tested. 400 test runs were for vehicle A, and 350 for vehicle B. 20% of the testing data were used to test our AEB simulation model (75 simulations were engaged for vehicle A and 63 for vehicle B). The average error of simulation results are shown in Table 9. Since the Stop at Distance is usually a small value (85% of them are less than 1 meter), so it is quite sensitive to the error of Warning Starting TTC, Braking Starting TTC and the Average Deceleration.

TABLE 9. AVERAGE ERROR OF SIMULATION DATA FOR VEHICLE A AND VEHICLE B

|	Error for A	Error for B
Warning Starting TTC (s)	12.1%	16.7%
Braking Starting TTC (s)	6.3%	8.2%
Average Deceleration (m/s^2)	4.7%	5.6%
Collision Speed (m/s)	7.8%	8.6%
Stop at Distance (m)	31.1%	39.7%

2.2.1.5 Conclusions and future work

This paper described a systematic methodology to develop a simulation model based on the pedestrian AEB using vehicle test data. This vehicle model is developed in Simulink, so it has good maintainability and extendibility. Test results of the proposed vehicle model match closely to the actual vehicle test results. Currently, the vehicle model can only support straight road segment, so one future direction is to optimize it to support curved road and vehicle turning scenarios.

2.2.1.6 References

[1] C. A. M. Partnership, "Crash Imminent Braking (AEB) First Annual Report," N. H. T. S. A., U.S. Department of Transportation, ed., June 2010.
[2] Stanley Chien, Lingxi Li, and Yaobin Chen, "A Novel Evaluation Methodology for Combined Performance of Warning and Braking in Crash Imminent Braking Systems," IEEE Intelligent Transportation Systems Magazine, pp.62-72, winter 2013.
[3] Jianhong Guan, Hanwu He, WenxuanZhai, Yanfei Liang, "Research on Real-time Collision Detection for Vehicle Driving in the Virtual Environment," Information and Automation, ICIA 2008, pp. 1834-1839, 2008.
[4] Qiang Miao, Xiaodong Tang, Dazhi Wang, Martijn TIDEMAN, Jiaqi Li, "The Application of PRESCAN in the Concept Development of Active Safety System," Digital Manufacturing and Automation (ICDMA), 2012 Third International Conference, pp. 884-886, 2012.
[5] Kusano K.D, Gabler H.C, "Safety Benefits of Forward Collision Warning, Braking Assist, and Autonomous Braking Systems in Rear-End Collisions," IEEE Transactions Intelligent Transportation Systems, pp. 1546-1555, 2012.
[6] Adam Berthelot, Andreas Tamke, Thao Dang, Gabi Breuel, "A novel approach for the probabilistic computation of Time-To-Collision," 2012 IEEE Intelligent Vehicles Symposium (IV), pp. 1173-1178, June 2012.
[7] F. Hendriks, M. Tideman, R. Pelders et al., "Development tools for active safety systems: Prescan and VeHIL," 2010 IEEE International Conference on Vehicular Electronics and Safety, pp. 54-58, June 2010.
[8] Coelingh E, Eidehall A, Bengtsson M, "Collision Warning with Full Auto Brake and Pedestrian Detection – a practical example of Automatic Emergency Braking," Intelligent Transportation Systems (ITSC), 2010 13th IEEE conference, pp. 155-160, Sept 2010.

[9] Yuanlin Chen, Kunyuan Shen, Shunchung Wang, "Forward collision warning system considering both time-to-collision and safety braking distance," Industrial Electronics and Applications (ICIEA), 2013 8th IEEE Conference, pp. 972-977, June 2013.

[10] Martijn Tideman, Martijn van Noort, "A Simulation Tool Suite for Developing Connected Vehicle Systems," 2013 IEEE Intelligent Vehicles Symposium (IV), pp. 713-718, June 2013.

2.2.2 Certainty and Critical Speed for Decision Making from Test Data

2.2.2.1 Introduction

The Transportation Active Safety Institute (TASI) of Indiana University-Purdue University Indianapolis carried out a large set of tests for pedestrian AEB from a previous Toyota sponsored project. Three different sizes of mannequins and their carrier were developed. These mannequins (child, fit and obese) have been designed and tested with two cars in near 1000 tests during a two-year periods. Two main types of tests were carried out, activation tests to assess the true positive situations and non-activation tests to assess the false positive situations in which the mannequins were close to but did not enter the crash zone. The tests were performed at both day light and at nighttime. The mannequin movement pattern include standing, moving left to right, right to left and also along and against traffic. The mannequin speeds were 0, 1.2, 1.5 and 2.2 m/s. The vehicles' speeds were ranged from 4.46 m/s (10 mph) to 22.3 m/s (50 mph) in intervals of 2.23 m/s (5 mph). A set of sensors, differential GPS, video recording and data acquisition systems were installed to measure all the relevant variables. Fig. 1 shows a scheme of the test setting.
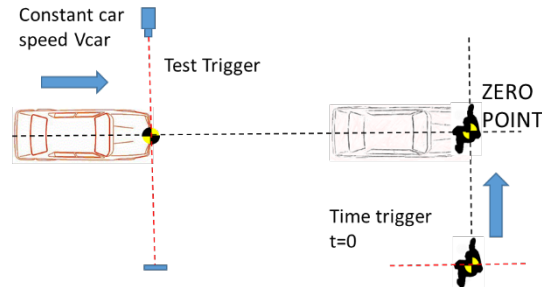
Fig. 1. Pedestrian AEB test setting.

This paper presents the modelling of decision making and braking phases of the AEB under these tests, analyzing the influencing variables related to the test design and procedure. The goal is to gain a better understanding of the AEB systems under those tests and the improvement of the test procedure accuracy and efficiency. The models presented in this paper can also be used in the design of those systems as they are accurate and simple to run in real time. Many of the test results shown here can be useful themselves for the community of active safety researchers as they are difficult to gather in real car-pedestrian crashes. The structure of the paper is the following: First a literature review is presented. Then the analytic vehicle model is presented for evaluating the braking phase. The model has been optimized and validated wih test results. The variation of its main input parameters and output variables, the friction coefficient, the transient response and the low levels of final effective deceleration, are analyzed. Using the model, three decision making indicators, based on the Active Safety Margin are defined and tested. Finally the decision making phase is described by introducing the concepts of Certainty and Critical Speed for Decision Making (CSDM). Both concepts are calculated and their results are compared with real decision timing recorded in tests. Ranges, maximum and minimum values of numerical data, and statistical distribution of the main factors are presented.

The main scientific contribution of this paper is the new concept and complete analytical modelling of CSDM, the speed beyond which the impact cannot be avoided, based on a novel

approach of series expansions of vehicle dynamics equations. The main significant results for the industry are the following:

- The proposal of a new simple and effective scale of Certainty in this kind of tests.
- The analytical expressions applied to the vehicle dynamics model that could be used in real time controllers in real cars.
- The models presented here allow the definition of more accurate test scenarios and test methods for pedestrian AEB systems, including the Certainty among the test variables.
- The background of 1000 tests supporting the conclussions.

2.2.2.2 Literature review

Pedestrian automatic emergency braking has been a subject of intense research and industrial activities in recent years. Good surveys of the research work of such systems can be found in [1-3], [4], and, [5] that provided the analysis of pedestrian crash avoidance by steering and braking. The pedestrian detection technologies were reviewed in [6-12] among others. The view of the industrial applications in real cars can be found in [13, 14]. In [13] Hitoshi stated that the major factor affecting the pedestrian lateral appearance position was whether the driver's view of the pedestrian was blocked by a parked vehicle or other objects. This visual influence was low in the case of crashes involving elderly pedestrians, but important in half of crashes involving children aged 12 or less. According to [14], the vehicle speeds involved in pedestrian crashes were 40 km/h or less.

The assessment of the risk in instants prior to the crash has been the object of several analysis, proposals and metrics. In [15] and [16], the authors defined the Time to Collision (TTC) as the simple quotient between the distance to the obstacle and the relative speed of that obstacle with respect to the vehicle, provided that any action is made by the driver to avoid the impact. In [16], the concept of Predicted Minimum Distance (PMD) was defined as the minimum distance between a vehicle and a potential obstacle predicted in real time, assuming constant values in the main variables of vehicle dynamics: turn rate, longitudinal and lateral acceleration. In [16], the authors used the idea of the Required Deceleration (RD) to stop the car in the measured distance of the pedestrian position, and used a first-order braking model of the system response obtained from tests. Several concepts assessing the risk in terms of Time-to-X were presented in [17, 18]. Time to Braking (TTB) was the remaining time until an emergency braking at maximum deceleration must be applied in order to avoid a crash by braking; the authors considered a constant deceleration in braking action. This same idea was extended in [18] to combine steering and braking actions in terms of Time to React (TTR). This is the same idea of Time to Brake (TTB) but applied to four avoidance maneuvers: maximum braking, maximum acceleration, minimum radius steering to the left, and minimum radius steering to the right; the authors defined consequently reaction Time to Brake (TTB), Time to Kickdown (TTK) and Time to Steer (TTS), all of them were particular cases of TTR. Additionally, they also defined Time to Enter (TTE) and Time to Disappear (TTD) that analyze when a car would enter or exits the path of the ego vehicle. [19] presented the concept of Time Difference To Collision (TDTC) which was defined as the time difference for a pedestrian and a vehicle to travel to the potential conflict point if its speed keeps constant. The authors in [20] defined the Post Encroachment Time (PET) as the time differential between when the leading vehicle occupied his location and the trailing vehicle arrived. [21] gave the definition of

Deceleration to Safety Time (DTS); it was the necessary deceleration to reach the last calculable PET0 (i.e. when PET=0), it referred to the position of the first road user, when leaving the conflict area. The second road user may reach this point no early than the first road user leaves it. An interesting metric found in [22] defined the Pedestrian Risk Index (PRI) that evaluated the potential severity in both time duration and danger. They use the classical definition of TTC and the Time to stopping t_s; the difference between them (ΔT) is used to evaluate the reduction in time for making a safe emergency brake. To assess the severity, they estimated the speed at the impact V_i and the PRI which is defined as the summation of the product $V_i^2.\Delta T_i$ during the time of potential conflict between the pedestrian and the vehicle.

In the process of decision-making, prior to triggering an emergency braking action, it will be required to calculate the level of certainty/uncertainty about the possible pedestrian entry in the crash zone. For that reason, the kinematics of the pedestrian's movement and its behavior has to be assessed. Indeed, [23-25] provided several analyses of the driver and pedestrian reaction times in pedestrian crashes. In [26-28] the authors analyzed the difference of pedestrian walking speeds at sidewalks and signalized crosswalks. The effects of season, age and gender of pedestrians were discussed. It was concluded that pedestrian walking speeds at crosswalks were significantly different from those on sidewalks at a 95% confidence level. In general, pedestrians walk faster at crosswalk compared to on sidewalk and walkway. [29 and 30] demonstrated that the average pedestrian deceleration was about $1.5 m/s^2$ and it did not depend much on the walking speed, with a maximum value of $2.5 m/s^2$. The stride frequency is about 0.9Hz according to [31]. Very similar results (1Hz) were published in [32].

Pedestrian behavior models can be found in [33], where C. Walkim developed a Markov chain model proposing a statistical representation of the pedestrian behavior based in four states (standing still, walking, jogging, and running) with transitions among them. From the former pedestrian state, the model of Walkim calculated the current state. Then, the pedestrian speed vector was split up into the norm and the angle from the available information on the statistical distribution of these quantities. Their values follow from the present pedestrian discrete state. The model generates statistically significant pedestrian trajectories and predicts potential car-to-pedestrian impacts. That Markovian model has been applied to Renault vehicles. Researchers from the Daimler group published a model of braking and steering system for pedestrian crash avoidance including the strategies for decision-making [5]. The approach of Toyota in this field can be found in [14].

The decision-making algorithms could use the calculated severity and risk of fatality of the crash if the speed is too high. The severity, as a function of the impact speed, has been analyzed in [34], where the authors collected a study of 492 pedestrian crashes with passenger cars in Germany resulting in 36 fatalities. They proposed the following mathematical expression to estimate the risk of death as a function of the impact speed v (km/h) and the age of the pedestrian. (It is a probability among 0 and 1). $P(v, age) = 1/(1+\exp(9.1-0.095 \cdot v - 0.04 \cdot age))$.

Finally, the effort in the development of standards for these pedestrian protection systems, common tests procedures, mannequin development, measurement techniques etc., can be seen in [35-42]. Among the works of the Transportation Active Safety Institute (TASI), [35] and [39]

provided a detailed explanation of the test procedure, which is modelled in this paper, being this test model the essential new approach of this paper. [37-38] and [40] gave the details of the mannequin development.

2.2.2.3 Vehicle dynamics model
A. Test data set
The selected tests to be analyzed in this paper were the following:

- Only AEB activation tests.
- The mannequin movements were only, crossing road from left to right (L/R) or right to left (R/L).
- Three mannequin sizes (adult fit, adult obese, and child).
- Daylight, dark, and dark but lighted conditions.
- The tests were carried out always in dry asphalt and flat surface.

This leads to a set of 426 tests for car A (84 % were successful, the car stopped before hitting the mannequin) and 35 tests for car B (65.7 % successful). Initial speeds (V_0) were ranged from 4.46 m/s (10 mph) to 22.3 m/s (50 mph). For activated AEB cases, stopping time ranged from 0.6 s to 2.3 s. Stopping distances ranged from 1.5 m to 18.5 m. The 2nd degree polynomial that fits the stopping distances (426 tests, car A) is as follows:

$$x_s = -1.52 + 0.58V_0 + 0.0378V_0^2$$

The distance from car A to the potential crash point, when the car starts braking (x_{s0}), was very well correlated with the initial speed, $x_{s0} = -2.9 + 1.2V_0$ (m/s). Final positions to the potential crash point once stopped showed an average value of 1.17 m. The standard deviation was 1.44 m.

B. Equations
To analyze the braking behavior of the car in the tests, following model is developed from the forces equilibrium presented in Fig.2 leading to the equation (1). Table I describes notations:
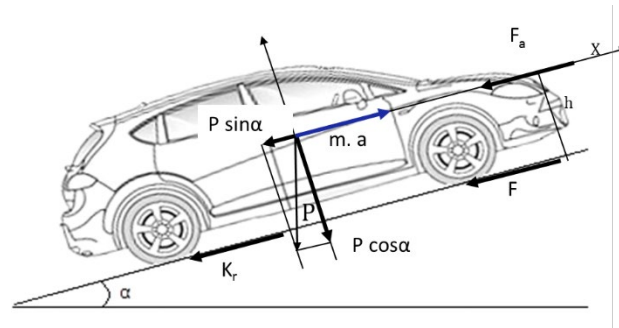

Fig.2. Vehicle dynamics model

$$m \cdot \left(\frac{d^2x}{dt^2} \right) + K_a \cdot \left(\frac{dx}{dt} \right)^2 + K_1 x + K_0 + K_r + F = 0$$

(1)

TABLE I. Terms in the vehicle dynamics model.

m	Vehicle mass equivalent, including the rotating masses effect
a	Vehicle longitudinal acceleration
x	Longitudinal displacement
P	Vehicle weight
F_a	Aerodynamic Force $= K_a \cdot \left(dx \middle/ dt \right)^2$
$K_a = \dfrac{1}{2} \cdot C_x \cdot A_f \cdot \rho$	Longitudinal aerodynamic drag
C_x	Longitudinal aerodynamic resistance coefficient
A_f	Frontal area of the vehicle
ρ	Air density
$K_r = m \cdot g \cdot f_r$	Rolling resistance force
f_r	Rolling resistance coefficient
$P \cdot \sin(\alpha) \approx P \cdot \tan(\alpha)$ $= P \dfrac{dy}{dx} = K_1 \cdot x + K_0$	Gravitational force, assuming a road with parabolic profile. In this case, it is zero. All tests were carried out in a flat surface.
$F = C_{f3} \cdot t^3 + C_{f2} \cdot t^2 + C_{f1} \cdot t + C_{f0}$	Braking force input , as a cubic spline
C_{fi}	Coefficients of the braking spline

The values of m, C_x and A_f are taken from the technical data sheets of both cars. Equation (1) can be solved numerically, but as the braking time is short, power series expansion can generate very accurate analytical solutions, see [43] and [44]. Assuming the existence of a solution for the displacement as the following:

$$x(t) = \sum_{n=0}^{\infty} c_n t^n$$

(2)

Where, t is time and c_n are the series expansion coefficients.
Taking derivatives, the speed and acceleration series can be obtained and the equation (1) becomes:

$$m \cdot \left(\sum_{n=0}^{\infty} (n+1) \cdot (n+2) \cdot c_{n+2} t^n \right) +$$

$$K_a \cdot \left(\sum_{n=0}^{n=\infty} \left[\sum_{i=0}^{n} (i+1) \cdot (n+1-i) \cdot c_{i+1} \cdot c_{n+1-i} \right] \cdot t^n \right) + $$

(3)

$$+ K_1 \cdot \sum_{n=0}^{\infty} c_n t^n + K_0 + K_r + C_{f3} \ t^3 + C_{f2} t^2 + C_{f1} t + C_{f0} = 0$$

23

with initial conditions:

$$x(t_0) = x_0; \ \dot{x}(t_0) = V_0$$

Collecting (3) in powers of t and equating coefficients to 0, a linear system of equations is obtained, from which the series coefficients can be obtained too (expanding until n=5):

$$c_0 = x_0; \ c_1 = V_0 \ ; \ c_2 = \frac{-K_a \cdot V_0^2 - K_r - C_{f0}}{2 \cdot m}; \ c_3 = \frac{-K_a \cdot 4 \cdot V_0 \cdot c_2 - C_{f1}}{6 \cdot m}$$

$$c_4 = \frac{-K_a \cdot \left(6 \cdot c_1 \cdot c_3 + 4 \cdot c_2^2\right) - C_{f2}}{12 \cdot m}; \ c_5 = \frac{-K_a \cdot \left(8 \cdot c_1 \cdot c_4 + 12 \cdot c_2 \cdot c_3\right) - C_{f3}}{20 \cdot m}$$

$$x(t) \approx c_0 + c_1 t + c_2 t^2 + c_3 t^3 + c_4 t^4 + c_5 t^5 \tag{4}$$

This model solution is of closed form, not numerical, and that can help to analyze trends, or the influence of every single factor. Additionally, as it is a simple polynomial of degree 5, its computation is very fast and can be applied for real time simulation.

C. Braking input

The braking force (F) can be expressed as a cubic spline (see Fig.3) in terms of initial and final slope (F'$_0$ and F'$_f$) and maximum values of time (t_0+d) and braking force (F_0+h):
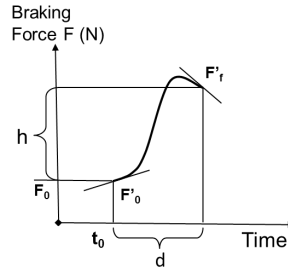
Fig. 3. Braking force spline

$$C_{f3} = \frac{(F_0' + F_f') \cdot d - 2 \cdot h}{d^3}; \quad C_{f2} = \frac{1}{2}\left(\frac{(F_f' + F_0')}{d} - 3Cf_3 \cdot (2.t_0 + d)\right)$$

$$C_{f1} = F_0' - 2.Cf_2.t_0 - 3Cf_2.t_0^2; \quad C_{f0} = F_0 - (Cf_1.t_0 + Cf_2.t_0^2 + Cf_3.t_0^3) \tag{5}$$

The braking action can be split in two stretches, the transient one (we will call it stretch T) during the settling time until t_f and the second one at constant maximum braking force, we will call it stationary stretch S, (see Fig 4).

Fig. 4. Two braking stretches

In the first stretch, $F'_f=F_0 = t_0=0$ so equation (5) becomes:
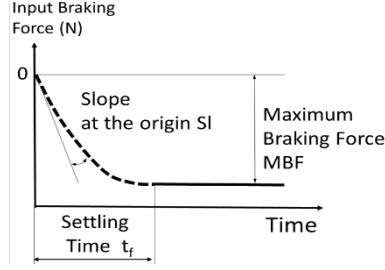
$$C_{f3} = \frac{F_0' \cdot d - 2 \cdot h}{d^3}; \ C_{f2} = \frac{1}{2}(\frac{F_0'}{d} - 3Cf_3.d) \ ; \ C_{f1} = F_0'; \ C_{f0} = 0$$

$$(6)$$

As $x_0=0$; the speed in function of time in the first stretch becomes:

$$v_T(t) \approx V_0 + 2c_{2T}t + 3c_{3T}t^2 + 4c_{4T}t^3 + 5c_{5T}t^4 \quad (7)$$

The second sub-index of c_{iT} refers to stretch T. In stretch S, $C_{f3} = C_{f2} = C_{f1} = 0$; $C_{f0} = h$. As the response in stretch S is quite flat, we can use a degree 3 displacement so the speed in the second stretch (V_S) becomes:

$$v_S(t) \approx v_f + 2c_{2S}t' + 3c_{3S}t'^2 \quad (8)$$

where, $t'=t - t_f$; $v_f = v_T(t_f)$ and $x_f = x_T(t_f)$.

The stopping time t_s, can be calculated from the root of the equation (8) t'_{sS}, being $t_s = t'_{sS}+t_f$. The lower case sub index s means stopping. The stopping distance is:

$$x_s \approx x_f + v_f t'_{sS} + c_{2S}t'^2_{sS} + c_{3S}t'^3_{sS} \quad (9)$$

The simulated crash time (t_c) will happen when $x_S(t) = x_p$, being x_p the measured distance to the potential crash point when the car starts braking. The simulated crash speed is $v_c = v_S(t_c)$.

D. Optimization and data fit

To fit the outputs of the model to real data, an optimization process was carried out. The *fminsearch* function in MATLAB, implementing the Nelder-Mead method, was applied. The optimal values of parameters to be found in the optimization were the slope at the origin in the braking force spline, *Sl*, (see Fig. 5), the settling time t_f and the Maximum Braking Force (*MBF*). The optimization criterion was the minimum deviation summation in the deceleration signal. The optimal values of initial slope *Sl* and settling time t_f were dependent on the vehicle speed. The MBF

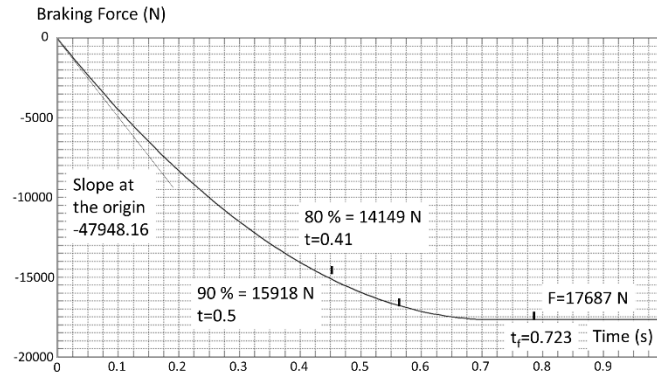was not a function of the speed. Fig. 5 shows the average braking spline for car A (mean of 426 tests).

Fig. 5. Average braking force spline for car A.

The average slope at the origin was Sl = -47,948 N/s. The braking force reached its maximum at t_f=0.72 s, which points out the importance of the transient phase. The length of the final constant braking stretch depends on the initial vehicle speed. Constant braking continues until the car stops. The average maximum value of that braking force was 17,687 N. At that point, the car starts to slip and the ABS acts keeping the maximum braking force approximately constant. Entering this average braking action as input to the model with the initial speed, we could get the output values of stopping distance and time, simulated speed and decelerations.

E. Accuracy of the model.

The output values of the model show a very good fit with values measured in AEB testing. Fig. 6 shows the distributions of relative errors in the stopping time when the optimal values for every test are applied. Similar values of relative error can be found in the stopping distances. Results with car B are also accurate. Obviously, if the average braking action is applied, the results are also an average, but they are very good as a general model.
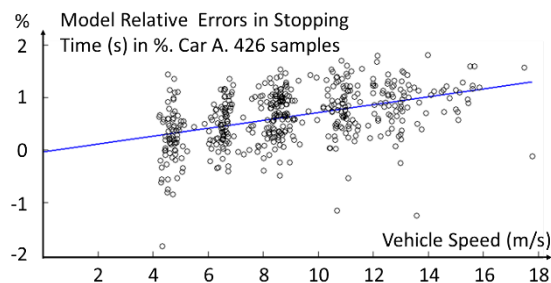
Fig. 6. Relative error in stopping time between real data and simulation.

F. Friction coefficient

The ABS action limits the braking force. The capacity to brake depends on the available friction potential in the tire-road contact patch. This can change the result of the test by reducing or extending the stopping distance, and so will do in the real performance of the AEB.

From the values of MBF derived from testing data, we can obtain an approximation of the effective friction coefficient. The average value is 0.89 and the standard deviation 0.046 (426 tests

with car A). The test track was an unused airport runway, the asphalt surface was clean and the average friction is slightly higher than the normal value in open roads (0.8). In series of tests in different tracks, with the same vehicle, this factor could add uncertainty to the results.

G. Importance of the transient phase

The average value of settling time was 0.72s and the range of stopping times in this low range of speeds was from 0.6 s to 2.3s, which means that the percentage of braking time during the transient phase spans between 35% and 100%. On an average, at least 50% of the braking time was transient. For that reason, the average effective deceleration was quite low, and far from the maximum possible, according to the friction potential (see next sub-section H).

H. Low levels of effective deceleration

The Full Effective Deceleration (FED) obtained in the simulation is the effective final value of deceleration that would stop the car at the same stopping distance in real braking. FED= $-V_0^2/(2x_s)$, where x_S is the braking distance calculated with model (9). Obviously, the distribution of FED is dependent on the vehicle speed, due to the transient time. The regression line is FED= -4.4 - 0.18V_0 for car A in a Normal distribution (-5.96, 0.6)(m/s^2). FED=-3.8-0.25V_0 for car B. The average values of FED (-5.96m/s^2 for car A and -5.57m/s^2 for car B) are much lower than that the average values of maximum point decelerations (-10.11m/s^2 for car A and -9.14m/s^2 for car B). Therefore, the average effective deceleration that can be expected in good dry asphalt with a state of the art passenger car, with excellent ABS braking, is only about 6m/s^2 in this range of low speeds used for pedestrian crash avoidance tests. At higher speeds, the pedestrian is usually run over.

2.2.2.4 Indicators for decision-making

To build a complete model of the pedestrian anti-crash system, some indicators are required to establish the decision-making strategy in real time if the braking action needs to be triggered. Starting from the analytical model presented in III, we will define some indicators and use them to predict the occurrence of a crash with the mannequin (pedestrian).

A. Impact speed

Assuming that the vehicle knows the distance to the mannequin (measured with the radar) and the vehicle speed, the model presented in III can calculate in advance the impact speed. As depicted in Fig. 7, the predicted impact speeds show a very low error compared with the real measured impact speeds for car A.
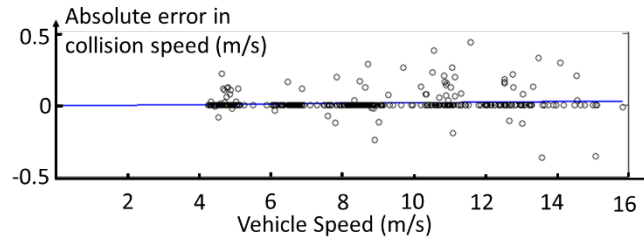

Fig. 7. Absolute error in the impact speed, Car A.

B. Active safety margin

The Active Safety Margin (*ASM*) can be defined in terms of deceleration, time, or distance, denoted as *ASM_A, ASM_T* and *ASM-D,* respectively.

$$ASM\_A = FED - Astop \text{ (10)}$$

FED describes how much the car can brake in a given time and *Astop* shows how much acceleration is needed to stop the car before hit the mannequin. *FED* is calculated with the model presented in section III.

$Astop = V_0^2/(2DTP)$ is a function of the current initial speed V_0 and the Distance to the Pedestrian (DTP) when braking starts. As the solution to the model is analytical and a simple polynomial (see equation (4)), it can be calculated easily in real time. The unit of the *ASM_A* is m/s^2.

When the car is running at speed V_0 and the pedestrian is detected at a distance *DTP*, if *ASM_A* > 0 the car would be able to stop before crashing to the pedestrian (Avoidance), the braking action could wait longer. If *ASM_A* < 0, the crash will happen for sure, but with reduced speed and hence with reduced severity of injuries (Mitigation), which is very important.

As the friction coefficient in every test is not known a priori, an average braking action like the one shown in Fig. 5 can be used; Fig. 8 shows the real test impact speed versus calculated *ASM_A*. In every real test case, a point depicts the calculated *ASM_A* and the real impact speed. If the result is avoidance, the points have 0 crash speed. All tests with avoidance' results are points covered with an arc in the *ASM_A* axis around 0 and 2.
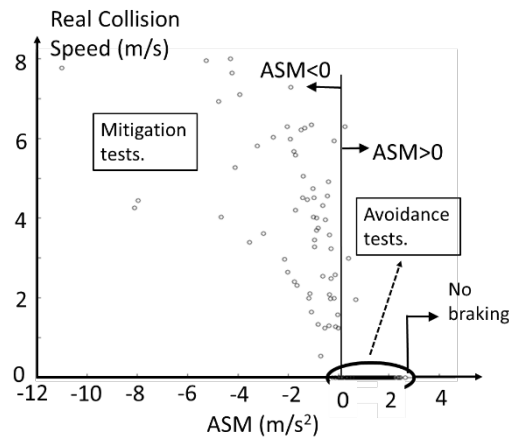
Fig. 8. Active Safety Margin in terms of deceleration. Car A.

In the area of *ASM_A*≥0, all test results are supposed to be avoidance and that is true in 352 out of 357 (true avoidances), so the prediction of this indicator is correct in 98.6% of the avoidance tests.

The prediction of avoidance tests is wrong (false avoidances) in 5 out of 357 (1.4 %). In the area of *ASM*<0, all test results are supposed to be mitigation or full speed crash and that is true in 66 out of 69, so the prediction of this indicator is correct in 95.7% of the mitigation tests (true mitigations). The prediction of the mitigation tests is wrong in 3 out of 69 (4.3%) (False

mitigations). An interesting remark is that there are no braking actions beyond $ASM\_A>2.6m/s^2$, this gives a first indication of the decision-making strategy. This indicator is accurate to predict the likelihood of the crash with the pedestrian.

C. Active safety margin in terms of distance and time

The Active Safety margin can also be expressed in terms of distance (ASM_D) and it can be defined as the difference between the distance to the pedestrian (DTP) and the required distance to stop (DTStop) calculated using the model presented in this paper. The unit of ASM_D is meter. Fig. 9 shows the concepts of ASM_D and ASM_T.

$$ASM\_D = DTP - DTStop$$

The *ASM_T* indicates how much time the car can continue at the current constant speed without start braking before the crash will be unavoidable. The unit of *ASM_T* is second.

$$ASM\_T = ASM\_D/V_0 \quad (11)$$
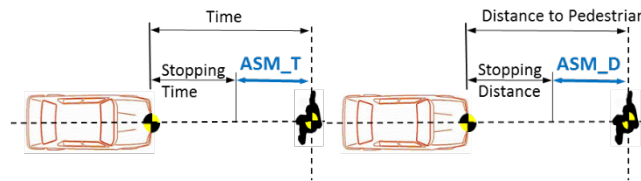
Fig. 9. Active Safety Margin in terms of distance and time.

Fig. 10 shows the test results of vehicle A with respect to *ASM-T*. It can be seen in this series of real tests, 73% of crashes can be avoided if the car could started braking only 0.2 s earlier. This underlines the importance of an early recognition and the subtle equilibrium between avoiding impacts and preventing false positive triggers of the system at the same time.
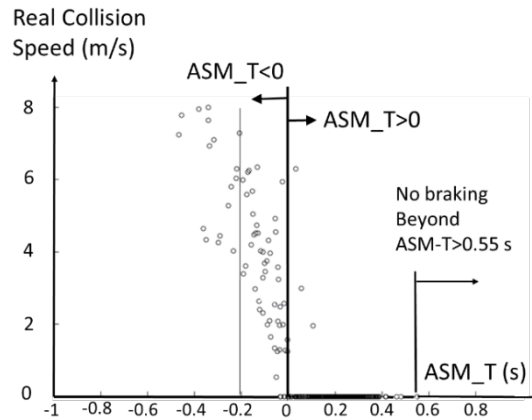
Fig. 10. Active Safety Margin of car A in terms of time.

The concept of *ASM_T* presented in this paper is also known as Time to Risk, which not the same as the Time to Collision (TTC) is presented in crash avoidance and active safety literature. The test results also showed that there were no braking actions beyond *ASM_D*>4.8m or ASM-T>0.55s. This gives another indication of the decision-making strategy. *ASM_A, ASM-T* and *ASM-*

D calculated according to the analytical model presented here, are excellent predictors of the crash and they are simple enough to be used in real time. The *ASM_A* measured in terms of deceleration has two additional advantages:

- Its value does not depend on the speed.
- It can be used in combined braking/steering actions in terms of lateral active safety margin combined with this longitudinal *ASM_A*.

The results shown in Fig. 10 have been obtained based on braking with the average Maximum Braking Force (*MBF*) by using the average effective friction coefficient (*AEFC*) equals 0.89. The value of the *AEFC* was known after testing the car. In general, some hypothesis of the value of the AEFC has to be made for real time prediction. If value=0.8 is accepted as normal in dry conditions in open roads, the same method of computing the *ASM_A* can be used with that value, just adjusting the variable *h* in equation (5).

2.2.2.5 Lateral behavior and decision-making.

The decision of triggering an emergency braking in a general driving situation has been analyzed in the models presented in [44], [5] and [14], among others. Those models are well adapted to general driving situations. In the case of a more controlled environment as it happens in performance tests, some simplifications can be assumed. As the motion direction of the pedestrian is always perpendicular to vehicle's trajectory, the braking decision can be split based on two independent indicators. First, the longitudinal active safety margin (*ASM*) has to reach a certain threshold value, close to 0. In addition, once that value is reached, the probability of the pedestrian to be in the impact zone (IZ) when the car gets the zero point should be as high as possible to avoid false positive situation. It is assumed that the width of the impact zone (IZ) is *b* that equals the total width of the car plus two segments of 30 cm (due to the thickness of pedestrian's body and the position of the feet/legs), one before the Center of Gravity of the pedestrian enters the IZ and the second one after exiting the IZ (see Fig. 11).

A. Model of certainty
To evaluate the probability of a pedestrian being in an impact zone (IZ), following are assumed:

- The normal gait frequency of a pedestrian is 2 steps/sec according to [31, 32], the step length is $v_p/2$ m, where v_p is pedestrian's speed in m/s.
- The average pedestrian's deceleration is about 1.5 m/s^2 according to [29, 30].
- If the pedestrian notices the vehicle prior to enter the IZ, the pedestrian will try to stop with a constant deceleration. Otherwise, it is assumed that the pedestrian will enter the IZ at the same constant speed. Only these two normal pedestrian behaviors are considered. Turnarounds after exiting the IZ or accelerating for passing the IZ are excluded.

According to assumptions above, we propose the scheme shown in Fig. 11 to analyze pedestrian's movement before entering the IZ. When *ASM* =0 (t=0 in Fig 11), the time for the vehicle to reach the zero point equals the time to stop (t_s). The lateral distance of the pedestrian to the IZ (y_1), pedestrian's speed (v_p) and the longitudinal distance of the vehicle to crash point, is measured continuously by the vehicle.

If the pedestrian starts above position y_s, the pedestrian cannot reach the IZ in a normal behavior at the time t_s with a constant speed, the pedestrian can at most be at point $(t_s, 0)$ at the time t_s. If the pedestrian is at positions between y_s and y_1, the probability of being inside the impact zone at time t_s (for example in y_1) is the same as the distance ratio (OB/AB) assuming a constant density distribution of the probability in the pedestrian deceleration value. We will call the probability of being inside IZ at the time t_s as "certainty" C in this paper, C= OB/AB.
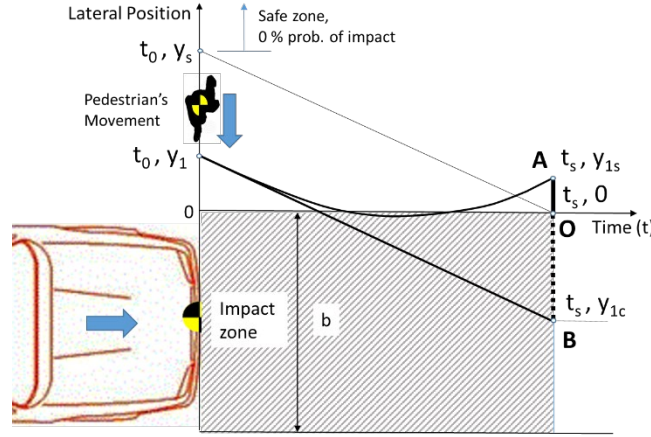

Fig. 11. Analysis of the uncertainty in the pedestrian behavior.

With those hypothesis, Fig. 12 shows the value of the lateral position y_1 as a function of C and the vehicle speed V_0 in increments of 2.26 m/s (5 mph), being v_p=1.5 m/s and the value of pedestrian deceleration A_{ped}= 1.5 m/s^2. An analytical expression of C, as shown in (12), can easily be obtained.

$$AO=y_{1s}=y_1-(v_p \cdot t_s- (1/2)A_{ped} \cdot t_s^2);\ (12)$$

$$y_{1c}=y_1-v_p t_s;\ AB=y_{1s}-y_{1c};\ C=OB/AB= -y_{1c}/(y_{1s}-y_{1c})$$

Fig. 12 has been obtained using the Monte Carlo method. We have selected the value of A_{ped}=1.5 m/s^2 in a constant distribution to fit best the results shown in Fig. 12 corresponding to a pedestrian speed of 1.2 m/s and those corresponding to v_p=1.5 m/s. Other density functions were tried, such as normal distributions of the value of A_{ped} and truncated distributions of that value, the results are different in the final figures of certainty C. However, there is an important lack of published data about real behavior of pedestrians in the pre-crash time in real crashes for obvious reasons. A more sophisticated model of statistical distribution of these pedestrian's actions or behavior in that situation, could fall in the field of speculation. Additionally, the results would be lower or a higher value of C for a given lateral position of the pedestrian at t_0, but the decision has to be made from a certain threshold of C anyway. The numeric value of that threshold would change if the pedestrian behavior model is different but the concept would be the same, I.E.: decision making from values, longitudinal ASM and lateral C as we will see at point D. This model can be used with different types of moving objects (cyclists, animals, etc.) using their own kinematic properties and statistical distribution of accelerations. If A_{ped} is not a constant, but a

statistical variable, the Monte Carlo method should be applied. The results shown in Fig. 12 can change significantly depending on the value of A_{ped}, and the statistical distribution, according to the supposed pedestrian's behavior.
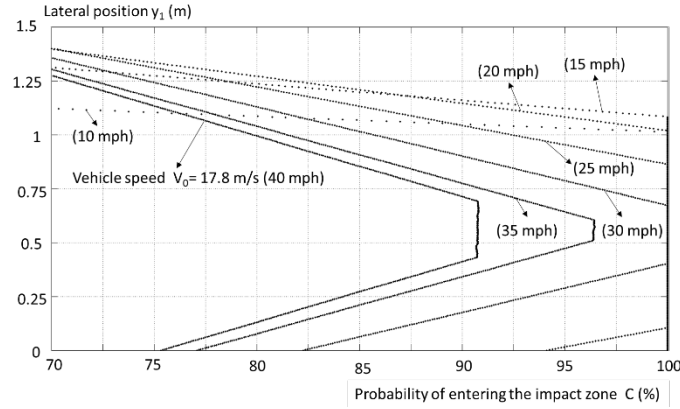

Fig. 12. Analysis of the Certainty in the pedestrian movement.

B. Critical speed for decision making (CSDM)

Fig. 12 relates lateral position of the pedestrian when the car should start braking to avoid the impact, with the probability of the pedestrian to be within the IZ when they meet at the end of the braking in a general case. The kinematic relation between pedestrian and car movement forced by the test setting is not considered in this figure. Therefore, when the car should start braking, the pedestrian could initially be anywhere.

From Fig. 11 and equation (12), we can easily obtain the following relation between y_1, C and t_s:

$$y_{1=} v_p{\cdot}t_s - C{\cdot}(1/2){\cdot}A_{ped}{\cdot}t_s^2 \text{ (13)}$$

If V_0 is constant, t_s is constant too so the set of straight lines shown in Fig. 12 is obtained for different values of initial speed of the vehicle. In Fig. 12 it can be observed that there is a limit in the vehicle speed to any specified level of probability that the pedestrian to be in IZ. Above that speed, the specified probability level will not hold and hence the decision of braking cannot be made for that specified level of probability. For example, when a braking decision is made at C=95%, the vehicle can avoid crash when the vehicle speed is less than 16.26 m/s = 36.5 mph =58.5 km/h. C=95% cannot be true when vehicle speed is greater than 36.5 mph.

The emergency braking maneuver cannot be triggered with a high probability of a false positive action. Thus in high speeds the car needs time to brake but cannot make braking decision (even though it can recognize the pedestrian early) until too late for avoiding crash. In high vehicle speed situations, only mitigation strategies are possible because the decision simply cannot be made. The vehicle speed for separating the complete crash avoidance and crash mitigation at a given certainty level is defined as the Critical Speed for Decision Making (CSDM).

32

If the road is wet, the time to stop is longer and the CSDM value is lower. Obviously, for the driver it is strongly recommended to reduce the speed if there are pedestrians close to the road. The critical speed condition is at $y_{lc}=-b$, (see Fig. 11) since C cannot be higher when $y_{lc}>-b$. From equation (12), we can easily conclude that the time to stop at the CSDM (we call it Critical Stopping Time for Decision Making, CSTDM) is:

$$CSTDM = \sqrt{\frac{2.b}{A_{Ped}.C}} \quad (14)$$

With $0 \leq C \leq 100\%$. The initial speed corresponding to that value of CSTDM can be obtained using the model in equations (8) and (9).

The CSTDM and CSDM do not depend on the pedestrian speed but they change very fast with its deceleration (A_{ped}). Fig. 13 shows the values of CSDM versus Certainty (in %) at different pedestrian deceleration values. It can be seen that if the system wants to avoid false positive situations, (accepting only high values of Certainty, C>95 %), the maximum initial speed of the car (CSDM) must be low, otherwise the decision of emergency braking must be delayed assuming only a final result of mitigation.

All pedestrian AEB tests carried out by the TASI (almost 1000 tests) have been made on dry asphalt. The maximum vehicle speed resulting in a complete avoidance was 15.74m/s= 35.3mph=56.67 km/h. In return, all the 136 non-activation tests were negative; both test cars were completely effective in preventing false positive actions. It means that indeed the selected levels of Certainty were very high.

In equation (13), If C is constant, the initial speed and every corresponding t_s are variable obtaining the family of constant certainty curves (see the parabolic curves in Figures 14 and 15).
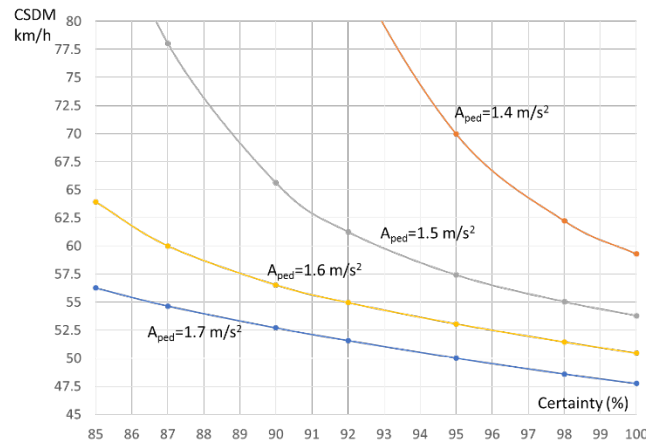

Fig. 13. Critical Speed for Decision Making versus Certainty at different levels of pedestrian deceleration (a).

When the car moves to the longitudinal position of ASM=0, it is the last opportunity to start braking with full crash avoidance at the speed V_0 in a braking time t_s. At this moment, the decision

has to be made, but can only be made with a level of certainty C or higher, to avoid the crash, if the distance of the pedestrian to the IZ (y_1) is equal to or smaller than the value of y_1 according to (13), and the speed is lower than the CSDM value.

C. Uncoupled decision making model

The braking decision-making can be decoupled when the path of the pedestrian is perpendicular to the vehicle path. For every initial speed of the car, there are two associated values of stopping time t_s and stopping distance x_s according to (9) when ASM=0.

In the designed setting for this real test, the lateral position of the pedestrian is related with the longitudinal position of the car stopping distance x_s.

$$y_1 = v_p \cdot x_s/V_0 - b/2 \quad (15)$$

The shorter pedestrian lateral position means the shorter longitudinal distance between the car and the pedestrian if they move at constant speed and do crash.
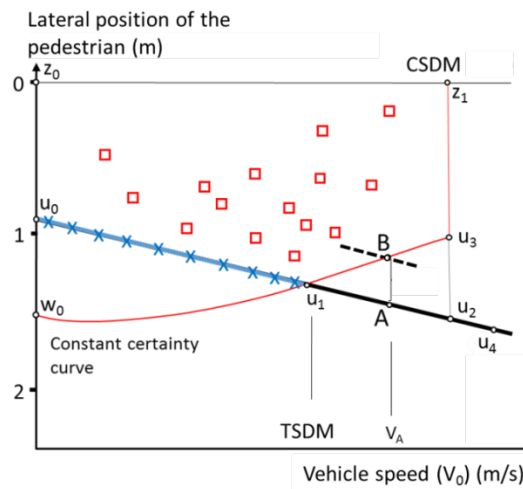
Fig. 14. Regions in the decision making model

Thus, in Fig. 14, the line u_0-u_4 defines the true lateral positions of the pedestrian in the real test as it is designed for different vehicle initial speeds when the car should start braking for full avoidance. Above the line u_0-u_4, the pedestrian is closer to the vehicle, meaning that the ASM-T < 0 when the car starts braking; in that case the best braking result can only be mitigation (e.g., shown by square markers). Below the line u_0-u_4, ASM-T >0 and the braking decision can "wait" since there is still time for condition changes. The parabola w_0-u_1-u_3, is the constant certainty relation for a given level of certainty C_i. It depicts the lateral positions where the pedestrian should be at every speed when ASM_T=0, to have a certainty C_i of being in the IZ. Lower constant certainty values lead to lower curves (see the family of parabolic curves in Fig 15.

In this ideal theoretical model, if the pedestrian is recognized early, the decisions of braking with result of full avoidance (x markers) should be made on the ASM=0 segment u_0-u_1. If the recognition was late, the decision points would be found above line u_0-u_4 resulting in mitigation (square marks). The car speed corresponding to u_1 is the highest speed to avoid crash with certainty

C_i, we will call it Test Speed for Decision Making (TSDM). In the speed range corresponding to the range of u_0 and u_1, the car can fully avoid the crash with a level of certainty C_i (or higher). If C_i curve is the lowest threshold value of Certainty acceptable to avoid false positive actions, all tests beyond TSDM will end only in mitigation although the recognition is early since the decision of triggering the automatic braking cannot be made because C is below desired certainty level C_i.

In order to find the limit stopping time t_{slim} at the TSDM, the intersection between equation (14) and line u_0-u_4 should be found. Introducing the value $y_{1=} v_p \cdot t_s - C \cdot (1/2) \cdot A_{ped} \cdot t_s^2$ on the left side of equation (14) the value of t_{slim} and consequently the TSDM can be obtained. Unlike the CSDM, the TSDM depends on the pedestrian speed v_p.

If the recognition is late, the decision is not made on time, the car continues some time t_c at a constant speed and the resulting position of the pedestrian is closer when the Certainty threshold is reached and braking starts (see point B), but the result will only be mitigation.

D. Test results

Fig. 15 shows the results of 116 tests carried out with car A. Mannequin's speed was 1.2 m/s. The results of 35 of them were mitigation and 81 were fully avoided. The dashed line (almost hidden under the black circular points) shows the regression of the lateral position of the mannequin (x marker points) when the car started braking in avoidance tests for every speed. There is a variation compared with the ideal model of Fig. 14, because the real car speed was not always exactly the same (it was controlled by the driver) and the mannequin was a little closer or further than expected from its theoretical lateral position. The deviation of vehicle speed with respect to the desired speed showed a Normal distribution $(\mu, \sigma) = (0.291, 0.549)$ in m/s (426 tests, Car A). The real vehicle speed was slightly lower (0.291 m/s) than the desired speed. Additionally, some statistical variation can be expected as usual in real tests. Circular markers depict the predicted position of the mannequin when the car should trigger the braking to avoid crash based on the *ASM_T* criterion. Cross markers depict the position of the mannequin when the car triggered the braking to avoid crash in real tests. Rectangular markers show the positions of the mannequin when the car triggered the braking and resulted in mitigation in real test. We can see that for 10, 20 and up to 25 mph, the decision is made approximately based on the pure longitudinal *ASM_T* within the region of C≥95%. So the model fits very well the test results, but from 25 mph until 30 mph the decision starts to be delayed in some tests, the *ASM_T=0* criterion is no longer satisfied and the last avoidance test is found about V_0=12.5 m/s (27.95 mph). The figure presents the different limit curves of C, the value C≥95% seems to be the limit used in this car if this model of certainty is used.
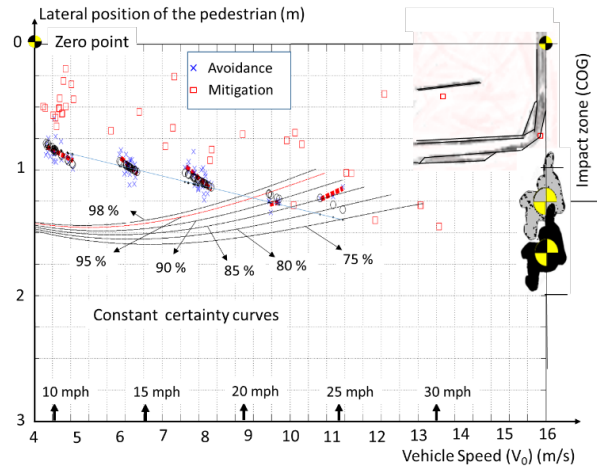
Fig. 15. Lateral position of the pedestrian when the car starts braking.

Some mitigation tests observed in the high speed area (about 15 m/s) could have been decided with a lower level of certainty, taking into account the high severity of the impact at higher speed; the injuries can be reduced if the final crash speed is reduced, see [45]. Fig. 15 also shows pedestrian lateral positions indicating how close from the side of the car (situated at 938 mm from zero) they are. Figures 16 and 17 show the lateral positions of the pedestrian when the braking action starts (lower line) and when it finishes (upper line), in two sets of car A tests at high and low speeds, respectively.
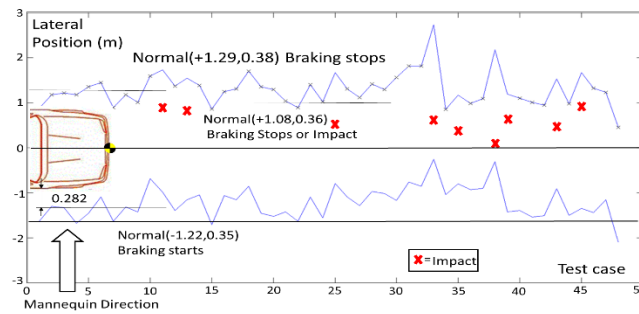
Fig. 16. Lateral mannequin position during braking maneuver in high speed, 40.2 and 48.3 km/h (25 and 30 mph). Car A.
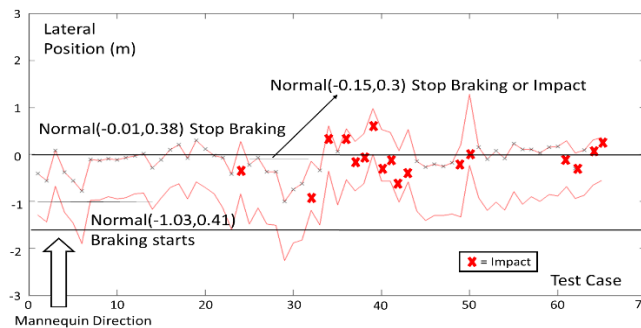
Fig. 17. Lateral mannequin position during braking maneuver in low speed, 16 km/h (10 mph). Car A.

Table II summarizes the numeric results of previous Figs. 16 and 17.

TABLE II. Pedestrian distance to zero point (m).

When the car...	...starts braking		... stops braking	
	Low speed (16 km/h)	High Speed (48.3 km/h)	Low speed (16 km/h)	High Speed (48.3 km/h)
Average μ	-1.03	-1.22	0.01	1.08
Std. deviation σ	0.41	0.35	0.38	0.36

E. Influence of the zero point position in the test results

Fig 16 shows that as test vehicle's speed is not constant due to the braking action, the car arrives late to the designed zero point (DZP) located in the middle of the bumper, the pedestrian has already passed and the real zero point (RZP) is beyond the DZP. At low speeds (see Fig. 16), this effect is reduced because both, FED and stopping time are much lower.

If the test had been designed with closer lateral positions of the pedestrian for every value of x_s, assuming for example (see Fig 11):

$$y_{1=} \; v_p \cdot x_s/V_0 - b/2 - H \;(16)$$

H being a positive value, the line u_0-u_4 in Fig. 14 would have moved upwards and the TSDM would have been higher; the number of full avoidance tests results would then be bigger. However, if the TSDM reaches the CSDM, the certainty cannot grow anymore, because if the pedestrian is too close of the IZ when the car is at x_s, the pedestrian could escape just keeping at constant speed, or even running, (see Fig. 11).

All the TASI tests have been designed with the DZP located at the mid-point of the car (Point B in Fig. 18), but in order to consider the behavior of the system in different levels of Certainty, the DZP should have been varied too. Variations in the DZP lead to changes in the decision-making, in the RZP and in the test results.

For standardization purposes, a scale of Certainty variation in this kind of tests (see Fig. 18) can be proposed based on the DZP position assuming a standard round value of b=2 m (which includes not only the car's width, but part of the pedestrian step), valid for a wide range of passenger cars.

The lateral distance of the DZP from the mid-point B in cm can be used, when designing the test, as an indicator of the certainty level in which the decision has to be made. Associated with that distance, it can be defined a Standard Certainty Factor (SCF) which varies among 0 and 100 in every range of b (valid for different values of b in wider vehicles) and of course it can be defined a symmetric Standard Uncertainty Factor (SUF=100-SCF). See Fig. 18 for a more clear understanding.
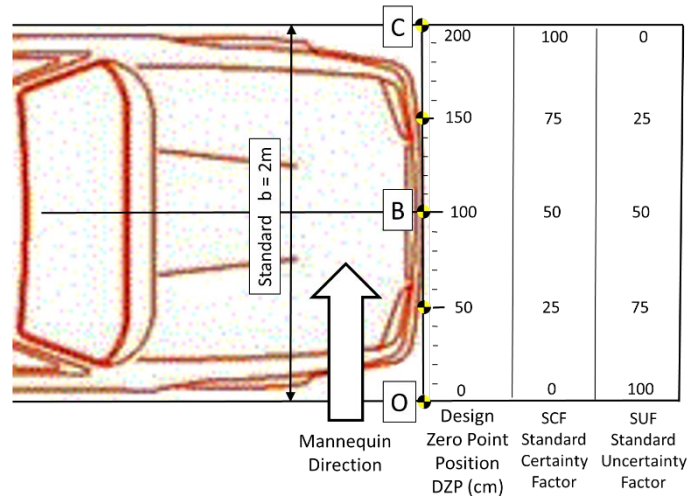
Fig. 18. Proposed Scale of Certainty in Pedestrian AEB tests.

The DZP or SCF values are not exactly the value of C in equation (12) but they are directly related, actually looking at Fig 15, for speeds among 20 and 30 mph, variations of the lateral position of the mannequin of 10 cm correspond, in a rough approximation, to variations of C about 5%. This is approximately the same variation of the SCF when DZP changes in Fig. 18.

All tests made by the TASI team and presented in this paper have been carried out with SCF=50. The tests to assess the performance of pedestrian AEB systems can be carried out with different values of designed SCF in every speed, leading to a more accurate assessment of the system. Thus, very conservative strategies, triggering the system only with very high values of C, braking to the full, will get good results when testing with high values of SCF. In return, systems starting a soft braking with lower levels of C will get good results in tests with low values of SCF. Values of SCF<0 can also be possible in non-activation tests. Values of SCF>100 can also make sense for assessment, testing or research.

2.2.2.6 Conclusions and future work
The TASI team has carried out a complete set of tests with two cars equipped with pedestrian AEB systems. In this paper the models of braking and decision making phases for this kind of tests have been presented. The influence of the friction coefficient that can modify the results depending on the track where the tests were carried out and the importance of the transient phase in those low values of initial speed, that lead to moderate levels of final effective decelerations, are two important conditions for these tests. An accurate and standard definition of what is exactly an impact, as the Center of Gravity of the mannequin is retarded or advanced with respect to the feet should be adviseable.

The model presented here, can calculate the Active Safety Margin to trigger the tests as an accurate indicator. But the decision making is also dependent on the lateral position of the pedestrian. The importance of an accurate measurement of the lateral position of the mannequin (not only the car position) in this kind of tests, is also identified. The concepts of Certainty and Critical Speed for Decision Making have been modeled. They help to clarify the reasons for the only mitigation results in higher speeds. Although the certainty model presented at section V.B

includes a simple kinematic and statistical description on the pedestrian behaviour, it is valid to outline the importance of this concept of Certainty and its influence in the tests results. There is a lack of published data about real behaviour of pedestrians in the pre-crash conditions. More testing and research is required in this area, perhaps with the help of driving simulators.

All the tests have been designed to meet both car and mannequin at the zero point assuming no braking action, but some tests with more varied lateral positions of the zero point are required to get a better contrast of the decision making behavior, completing the points in the Fig. 15 leading to a better understanding of this kind of systems in those tests. A scale of certainty variation in the pedestrian AEB tests has been proposed.

When AEB pedestrian protection systems evolve, tests scenarios could include in the future, more complex and challenging situations, for example, random longitudinal and lateral combined movement, or partial pedestrians occlusion testing. In that case, the car will continue being subjected to the physics and vehicle dynamics, but the pedestrian model and its related mathematical expressions should be different. The concepts of Certainty and CSDM presented here, could be a valid basis to analyze these situations, in order to compare and improve these AEB systems. A careful step by step approach should be considered, analyzing these more complex scenarios from a well-stablished basis of models and tests obtained in more simple cases.

2.2.2.7 References

[1] Gerónimo D., López A.M., Sappa A.D., and Graf T., "Survey on pedestrian detection for advanced driver assistance systems". *IEEE Trans. Pattern Anal. Mach. Intell.* , vol. 32, no. 7, pp. 1239–1258, Jul. 2010.

[2] Enzweiler M. and Gavrila D.M., "Monocular pedestrian detection: Survey and experiments". *IEEE Trans. Pattern Anal. Mach. Intell.* , vol. 31, no. 12, pp. 2179–2195, Dec. 2009.

[3] Gandhi T. and Trivedi M.M., "Pedestrian protection systems: Issues, survey, and challenges". *IEEE Trans. Intell. Transp. Syst.* , vol. 8, no. 3, pp. 413–430, Sep. 2007.

[4] Llorca D., Milanés V., Parra I., Gavilán M., García I., et al. "Autonomous Pedestrian Collision Avoidance Using a Fuzzy Steering Controller". *IEEE Transactions on Intelligent Transportation Systems*, Vol.12, No 2, pp 390-401. June 2011.

[5] Keller, C.G., Thao Dang, Fritz, H., Joos, A. more authors. "Active Pedestrian Safety by Automatic Braking and Evasive Steering". *IEEE Transactions on Intelligent Transportation Systems*, Vol. 12, No. 4, pp. 1292-1304. December 2011.

[6] Llorca D., Sotelo M.A., Parra I, Naranjo J.E., Gavilán M., and Álvarez S. "An experimental study on pitch compensation in pedestrian-protection systems for collision avoidance and mitigation"..*IEEE Transactions on Intelligent Transportation Systems*, Vol. 10, No. 3pp. 469-474, September 2009.

[7] Fuerstenberg K.C., "Pedestrian protection using laser scanners." *Proc. IEEE Intell. Transp. Syst.".* Vienna (Austria).pp. 437–442. 2005.

[8] Parra I., Llorca D., Sotelo M.A., Bergasa L.M, Revenga P., Nuevo J., Ocaña M, and García-Garrido M.A., "Combination of feature extraction methods for SVM pedestrian detection," *IEEE Trans. Intell. Transp. Syst.*, vol. 8, no. 2, pp. 292–307, Jun. 2007.

[9] Broggi A., Bertozzi M., Fascioli A., and Sechi M., "Shape-based pedestrian detection," *Proc. IEEE Intell. Vehicle Symp.*, Dearborn (MI), USA. pp. 328–333, October-2000.

[10] Llorca D, Parra I., Sotelo M.A., Revenga P., Álvarez S., and Gavilán M., "3d candidate selection method for pedestrian detection on non-planar roads," in *Proc. IEEE Intell. Vehicle Symp.*, Istanbul, Turkey, pp. 1162–1167. June 2007.

[11] Suganuma N. and Fujiwara N., "An obstacle extraction method using virtual disparity image," *Proc. IEEE Intell. Vehicle Symp.*, Istanbul, Turkey, pp. 456–461, June 2007.

[12] Gavrila D.M. and Munder S., "Multi-cue pedestrian detection and tracking from a moving vehicle," *Int. J. Comput. Vis.*, vol. 73, no. 1, pp. 41–59, Jun. 2007.

[13] Hitoshi Y., Masashi N., Tsutomu M., Naoyuki Y., Makoto N.,"Research into Evaluation Method for Pedestrian Pre-collision System". Proceedings of the 23rd International Technical Conference on the Enhanced safety of Vehicles Seoul, Republic of Korea,. (ESV). Paper Number 13-0110. May 27-30, 2013.

[14] Hayashi H., Inomata R., Fujishiro R. , Ouchi Y., Suzuki K., Nanami T. "Development of pre-crash safety system with pedestrian collision avoidance assist". Proceedings of the 23rd International Technical Conference on the Enhanced safety of Vehicles Seoul, Republic of Korea, (ESV), Paper Number 13-0271. May 27-30, 2013.

[15] Labayrade R., Royere C., and Aubert D., "A collision mitigation system using laser scanner and stereovision fusion and its assessment," Proc. IEEE Intell.Veh.Symp., Las Vegas (Nevada), USA, pp. 441–446. 2005.

[16] Polychronopoulos A., Tsogas M., Amditis A., Scheunert U., Andreone L. and Tango F., "Dynamic situation and threat assessment for collision warning systems: The EUCLIDE approach," in *Proc. IEEE Intell. Veh. Symp.*, Parma, Italy, pp. 636–641. 2004.

[17] Hillenbrand J., Schmid V., and Kroschel K., "Situation assessment algorithm for a collision prevention assistant," *Proc. IEEE Intell. Veh. Symp.* , Las Vegas (Nevada), USA, pp. 459–4652005.

[18] Hillenbrand J., Spieker A., and Kroschel K. "A multilevel collision mitigation approach," *IEEE Trans. Intell. Transp. Syst.*, vol. 7, no. 4, pp. 528– 540, Dec. 2006.

[19] Zhang Y., Danya D., Qiu T.Z., Peng L. and Zhang Yi, " Pedestrian Safety Analysis in Mixed Traffic Conditions Using Video Data," *IEEE Transactions on Intelligent Transportation Systems*, 13(4) , pp. 1832 – 1844. 2012.

[20] Gettman D., Pu L., Sayed T., and Shelby S., "Surrogate safety assessment model and validation: Final report," Fed. Highway Admin., McLean, VA, FHWA-HRT-08-051, 2008.

[21] Hupfer, C. "Deceleration to Safety Time (DST) - a Useful Figure to Evaluate. Traffic Safety". *ICTCT Conference Proceedings of Seminar 3*, Department of Traffic Planning and Engineering, Lund University, Lund. 1997.

[22] Salvatore C., Garcia A., Rosario C., Rojas, M.,"Pedestrian Crossing Safety Improvements: Before and After Study using Traffic Conflict Techniques". *Proceedings of 4th International Symposium on Highway Geometric Design*, Valencia, Spain. June 2-5, 2010,

[23] Staczyk T.L., Jurecki R., Jakiewicz M., S., Walczak, R. and Janczur. "Researches on the reaction of a pedestrian stepping into the road from the right side from behind and an obstacle realized on the track". *Journal of KONES Powertrain and Transport*, Vol. 18, No. 1, 2011.

[24] Staczyk, T. L., Lozia, Z., Jurecki, R., Pieniek, W., Zeszyty "Studies of reactions of drivers in simulated accident situations", *Naukowe Instytutu Pojazdów Politechniki Warszawskiej.* Nr 1(77)/2010, s. 27-52,Warszawa 2010.

[25] Staczyk, T. L., Jurecki, R., Pieniek, W., Jakiewicz, M., Karenda, M.P., Wolak, S. "Studies on reactions of drivers to the vehicle approaching from the right side, carried on a car track". *Zeszyty Naukowe Instytutu Pojazdów Politechniki Warszawskiej,* Nr 1(77)/2010, s. 307-319,Warszawa 2010.

[26] Zhang X., Chen P., Nakamura H., Asano M., "Modelling Pedestrian Walking Speed at Signalized Crosswalks Considering Crosswalk Length and Signal Timing". *Proceedings of the Eastern Asia Society for Transportation Studies*, Vol. 9, 2013.

[27] Chandra S. , Rastogi R. , Das V.R., Ilango T. "Pedestrian behaviour under varied traffic and spatial conditions". *European Transport*. Issue 56, Paper no. 5, ISSN 1825-3997. (2014)

[28] Montufar, M., Arango, J., Porter, M. and Nakagawa, S., "Pedestrians' normal walking speed and speed when crossing a street", *Transportation Research Record* , TRB, National Research Council, Washington D C, USA, pp. 90-97. 2002.

[29] Fransen M. ; Heussler J. ; Margiotta E.; Edmonds J. "Quantitative gait analysis comparison of rheumatoid arthritic and non-arthritic subjects". *Australian Journal of Phisiotherapy*. Volume 40, Issue 3, pp. 191–199. 1994.

[30] Miff S.C., Childress D.S., Gard S.A., Meier M.R., Hansen A.H, Brown J., "Temporal symmetries during gait initiation and termination in nondisabled ambulators and in people with unilateral transtibial limb loss". *Journal of Rehabilitation Research and Development*. Volume 42 Number 2, March/April Pages 175 – 182. 2005.

[31] Kohler S., Goldhammer M., Bauer S., Doll K., Brunsmann U., Dietmayer K. "Early Detection of the Pedestrian's Intention to Cross the Street". *15th International IEEE Conference on ITS*. Anchorage, Alaska, USA, September 16-19, 2012.

[32] Hoogendoorn S.P., Bovy P.H.L, "Simulation of Pedestrian Flows by Optimal Control and Differential Games". *Optimal control applications methods,* 24, pp. 153-172. 2003.

[33] Wakim C., Capperon S., and Oksman J., "A Markovian model of pedestrian behavior," *Proc. IEEE Int. Conf. Syst., Man, Cybern.* , pp. 4028–4033. Oct. 2004.

[34] Rosén, E., Sander U., "Pedestrian fatality risk as a function of car impact speed," *Accident Analysis and Prevention*, 41, pp 536-542.2009.

[35] Chien S., Yi Q., Chen Y., Gholigafari A., Sherony R., "Method of Selecting Test Scenarios for Pedestrian Forward Looking Pre-Collision System Evaluation," *SAE World Congress & Exhibition*, paper number 14AC-0125, Detroit, Michigan, USA, April 2014.

[36] Yanagisawa M., Swanson E., Najm W.G., "Target crashes and safety benefits estimation methodology for pedestrian crash avoidance/mitigation systems," Washington, DC: National Highway Traffic Safety Administration, 2014.

[37] Chien S., Dong L., Yi Q., Chen Y., Sherony R., and Takahashi H., "Joint Motion Pattern of Limb Moving Mannequins for Active Safety Vehicle Tests," *23rd ESV Conference*, Seoul, Korea, May 27-30, 2013.

[38] Yi Q., Chien, S., Brink, J., Chen Y., Li L., Chen C. , Good, D., Sherony R., "Mannequin Development for Pedestrian Pre-collision System evaluation". *IEEE 17th International Conference on Intelligent Transportation Systems (ITSC).* Qingdao. China, 2014.

[39] Tang B., Chien, S., Chen, Y. "Obtain a simulation model of a pedestrian collision imminent braking system based on the vehicle testing data" . *IEEE 17th International Conference on Intelligent Transportation Systems (ITSC)*. Qingdao. China, 2014.

[40] Chien S., Dong L., Yi Q., Chen Y., Sherony R., and Takahashi H., "Joint Motion Pattern of Limb Moving Mannequins for Active Safety Vechicle Tests," *23rd ESV Conference*, Seoul, Korea, May 27-30, 2013.

[41] López A., Sheroni R., Chien S., Li L., Yi Q., Chen Y. "Analysis of the braking behaviour in Pedestrian Automatic Emergency Braking". *IEEE 18th International Conference on Intelligent Transportation Systems*, Las Palmas de Gran Canaria. Spain; September, 2015.

[42] Good D., Chien S., Li L., Chen Y. "Preliminary benefit analysis for pedestrian crash imminent braking systems". *IEEE 18th International Conference on Intelligent Transportation Systems*, Las Palmas de Gran Canaria. Spain; September, 2015.

[43] López, A., Vélez P., Moriano C.: "Método de procesamiento rápido de las ecuaciones de la dinámica vehicular mediante polinomios de Chebyshev". *Encuentro Int. de Algebra Computacional*. EACA. Sevilla, Spain (2006).

[44] López,A. Moriano C., Olazagoitia J.L., Páez F.J., "Fast Computing on Vehicle Dynamics"**.** *IEEE-ASME Transactions on Mechatronics*., Issue 99. February 2015.

2.3 Integrate the Active Safety Sensing Information in the V2V Environment

2.3.1 Improve Road Safety Using Combined V2V and Pre-Collision Systems

2.3.1.1 Introduction

Based on statistics from the 2005-2008 National Automotive Sampling System (NASS) General Estimates System (GES) crash databases, V2V-based safety applications would potentially address about 4,336,000 police-reported light-vehicle crashes annually, with the 95 percent confidence interval between 3,691,000 and 4,981,000 [1]. The advancement in computation power and communication capability enables the practical implementation of vehicle to vehicle communication (V2V) systems. The advantage of V2V systems has been well discussed in many literatures. Pilot V2V implementation programs are conducted in several countries [2, 3]. The fundamental advantage of V2V is its capability of exchanging vehicle information that enables the intelligent decisions regarding road safety and efficiency. V2V-based safety applications predominantly apply to crashes that involve multi-vehicle pre-crash scenarios. This analysis is conducted with support from the Intelligent Transportation System's program for safety and mobility applications based on V2V and vehicle-to-infrastructure (V2I) communications [4]. To improve the intelligence of V2V systems, there are studies for incorporating information from traffic lights and road sensors through vehicle to infrastructure (V2I) systems, vehicle to pedestrian (V2P) systems into V2X systems. However, the current development of V2X systems is based on the concept that each participant provides its own operating information to the V2X system. There will be a long time-period that V2V capable and non-V2V vehicles coexist on roads. The current design of the V2X systems does not benefit non-V2X equipped objects (vehicle and pedestrians) since the information of these objects cannot be entered into the V2X systems. To solve this problem, there should be a way to gather the information of non-V2V enabled objects on the road, transmit this information the V2X system, and use the information to improve the safety of all objects on the road.

PCS system is an active safety component in many commercially available vehicles. A PCS has sensors (video camera, radar, lidar, etc.) to detect vehicles, pedestrians and bicyclist. The sensor information is presently used for collision imminent warning, automatic braking and maneuvering. If the PCS sensor information of a vehicle can be broadcast to a V2V network, other V2V enabled vehicles may use the information to improve the safety of the sensed objects. This paper discusses the future technology development in combining V2V and PCS together to enable a V2V vehicle to broadcast its PCS detected information and use recieved information to make better crash avoidance decisions. The combined V2V-PCS can effectively extend the information gathering range of V2V vehicles and enables all V2V vehicles to get information of non-V2V enabled objects.

This paper describes a systematic process to investigate all V2V-PCS scenarios that potentially benefit the pedestrians with the adoption of the combined V2V-PCS systems. First the variables and their values relevant to V2V-PCS scenarios are identified. Then all scenarios generated from the combination of the variable values are examined to determine if they can improve pedestrian

safety. The computation method for determining if the V2V-PCS improves the pedestrian safety for each scenario is described. The calculation of the first appearance location of the pedestrian to the vehicle and time to collision due to the location of the obscure object is described. The result of this study serves three purposes, (1) it provides a baseline to describe the usefulness of a V2V-PCS system, (2) it provides all pedestrian V2V-PCS simulation scenarios and crash calculation for future study and demonstration, and (3) it supports the establishment of testing scenarios for the performance evaluation of the V2V-PCS enabled vehicles.

2.3.1.2 Environment description and scenario categorization

It is assumed that there are three types of vehicles on the road: vehicles without V2V capability, vehicles with V2V capability but no PCS capability, vehicles with both and V2V and PCS capabilities. Each vehicle can be either moving or stationary. It is also assumed that pedestrians and stationary objects on the road do not have V2V capability. To describe V2V-PCS scenarios for pedestrian safety, the objects in the scenarios include pedestrians, vehicle potentially crashes the pedestrians (crashing vehicle), and V2V-PCS enabled vehicle that broadcast the pedestrian information and objects that obscure the view of the crashing vehicle. To describe the scenarios that a V2V-PCS system could show pedestrian safety advantage, following variables are identified:

Crash Location – The crash location variable has four relevant values: not-at-intersection, before-intersection in-intersection, after intersection.

a) Crashing Vehicle Motion Direction: possible values are straightforward, turn left, turn right, merge left, and merge right. In not-at-intersection scenarios, crashing vehicles cannot turn left or right so there are only three possible values: straight forward, merge left, and merge right; in intersection related scenarios, merging while turning is equivalent to turning with a different radius, so there are only three possible values: straight forward, turn left, and turn right.
b) Pedestrian motion direction relative to the crashing vehicle: Four possible values are Left to Right, Right to Left, Along Traffic, and Against Traffic.
c) Obscure object: There are seven interested values for this variable: no obscure object, stationary/moving obscure objects on left/front/right. The presence of obscure objects blocks the view of the crashing vehicle and shortens the reaction time to a potential collision.

For the convenience of describing the V2V-PCS scenarios, the notations for these variables and their values are defined in Table 1.

Table 1. Variables and values relevant for describing V2V-PCS scenarios

Crash location	Crashing vehicle direction	Pedestrian direction respect to crashing vehicle	Obscure object- location with respect to crashing vehicle (M=motion, S=Stationary)
IB – before intersection	VLT – left tern	PLR – left to right	OS/M – obscure obj.
IA - after intersection	VRT – right turn	PRL – right to left	OS/M – obscure obj.
II – in intersection	VST - straight	PAL – along traffic	OS/M – obscure obj.
IN – not in intersection	VLM – left merge	PAG –against traffic	ON – no object

VRM –right merge

VLC – left curve

VRC –right curve

168 different scenarios can be identified based on the combination of all possible values of environment variables as described in Table 1. In which 108 are intersection related and 60 are non-intersection related. 108 intersection related cases are calculated as 1(intersection)*3(Before, In, or After intersection)*3(Turn left, Turn right, Straight Forward)*4(Left to Right, Right to Left, Along Traffic, Against Traffic)*3(moving obscure objects, stationary obscure objects, no obscure object) . 60 non-intersection scenarios are calculated as 1(non-intersection)*5(Curve left, Curve right, Straight Forward, Merge left, Merge right) *4(Left to Right, Right to Left, Along Traffic, Against Traffic)*3(moving obscure objects, stationary obscure objects, no obscure object).

Each of these 168 scenarios was studied to determine if it could benefit from the use of V2V-PCS systems. The basic idea is to check if the crashing vehicle can get potential crash information earlier when a V2V-PCS system is adopted. The crashing vehicle may not be able to see the pedestrian for various reasons. If there is another vehicle (the informing vehicle) that has the PCS capability to detect the pedestrian and send the information to the crashing vehicle, the crashing vehicle may able to take measures in advance to avoid the collision. Here it is assumed that pedestrians do not detect the potential danger and cannot send their location information to vehicles. According to the selection criteria described above, 96 scenarios (listed in Table 2) are able to benefit from V2V-PCS systems and 72 Scenarios will not benefit from V2V-PCS systems.

Table 2. 96 scenarios that the V2V-PCS system can improve the pedestrian safety

Location	Vehicle	Pedestrian and the Obscure object
IB	VLT	PLR_OS; PLR_OM; PLR_ON; PRL_OS; PRL_OM; PRL_ON; PAL_ON; PAG_ON
	VRT	PLR_OS; PLR_OM; PLR_ON; PRL_OS; PRL_OM; PRL_ON; PAL_ON; PAG_ON
	VST	PLR_OS; PLR_OM; PLR_ON; PRL_OS; PRL_OM; PRL_ON; PAL_ON; PAG_ON
IA	VLT	PLR_OS; PLR_OM; PLR_ON; PRL_OS; PRL_OM; PRL_ON; PAL_ON; PAG_ON
	VRT	PLR_OS; PLR_OM; PLR_ON; PRL_OS; PRL_OM; PRL_ON; PAL_ON; PAG_ON
	VST	PLR_OS; PLR_OM; PLR_ON; PRL_OS; PRL_OM; PRL_ON; PAL_ON; PAG_ON
II		None
IN	VST	PLR_OS; PLR_OM; PLR_ON; PRL_OS; PRL_OM; PRL_ON; PAL_ON; PAG_ON
	VLC	PLR_OS; PLR_OM; PLR_ON; PRL_OS; PRL_OM; PRL_ON; PAL_ON; PAG_ON
	VRC	PLR_OS; PLR_OM; PLR_ON; PRL_OS; PRL_OM; PRL_ON; PAL_ON; PAG_ON
	VLM	PLR_OS; PLR_OM; PLR_ON; PRL_OS; PRL_OM; PRL_ON;

		PAL_OS; PAL_OM; PAL_ON; PAG_OS; PAG_OM; PAG_ON
	VRM	PLR_OS; PLR_OM; PLR_ON; PRL_OS; PRL_OM; PRL_ON; PAL_OS; PAL_OM; PAL_ON; PAG_OS; PAG_OM; PAG_ON

Table 3. 72 Scenarios that the V2V-PCS cannot improve the pedestrian safety

Location	Vehicle	Pedestrian and the Obscure object
IB	VLT	PAL_OS; PAL_OM; PAG_OS; PAG_OM
	VRT	PAL_OS; PAL_OM; PAG_OS; PAG_OM
	VST	PAL_OS; PAL_OM; PAG_OS; PAG_OM
IA	VLT	PAL_OS; PAL_OM; PAG_OS; PAG_OM
	VRT	PAL_OS; PAL_OM; PAG_OS; PAG_OM
	VST	PAL_OS; PAL_OM; PAG_OS; PAG_OM
II	VLT	PLR_OS; PLR_OM; PLR_ON; PRL_OS; PRL_OM; PRL_ON; PAL_OS; PAL_OM; PAL_ON; PAG_OS; PAG_OM; PAG_ON
	VRT	PLR_OS; PLR_OM; PLR_ON; PRL_OS; PRL_OM; PRL_ON; PAL_OS; PAL_OM; PAL_ON; PAG_OS; PAG_OM; PAG_ON
	VST	PLR_OS; PLR_OM; PLR_ON; PRL_OS; PRL_OM; PRL_ON; PAL_OS; PAL_OM; PAL_ON; PAG_OS; PAG_OM; PAG_ON
IN	VST	PAL_OS; PAG_OS; PAL_OM; PAG_OM
	VLC	PAL_OS; PAG_OS; PAL_OM; PAG_OM
	VRC	PAL_OS; PAG_OS; PAL_OM; PAG_OM
	VLM	None
	VRM	None

To make the graphical description easier, following icons are used in figures:

人 The pedestrian sign represents the pedestrian without the capability to communicate with vehicles.

🚗 The red vehicle represents the crashing vehicle equipped with V2V (may have PCS capability).

🚗 The yellow vehicle represents the informing vehicle equipped with both PCS and V2V.

The blue vehicle represents the stationary vehicle equipped with both PCS and V2V

The hexagon represents the obscure object.

    Figure 1A demonstrates a situation that the use of a V2V-PCS system could improve the safety of a pedestrian. The red car (crashing vehicle) is going straightforward. The stationary blue car is waiting for the left turn signal and is obscuring the view of the red car. The pedestrian is walking across the road from left to right. The red car may not be able to stop due to the short reaction time. If the yellow car (the informing vehicle) coming from the other side or the blue car has pedestrian PCS and V2V capability, they can detect the pedestrian and send the pedestrian motion information to the red car so that the red car can take measures in advance to avoid potential crash to the pedestrian. If the red car is equipped with V2V but no PCS, it can generate warning to the driver, and or generate pre-braking command to the brake system to be ready for real brake. If the red car has both PCS and V2V capabilities, it can pay special attention to the location where the pedestrian is expected to appear and make quicker and better decisions. The V2V-PCS is useful even if the obscure blue car is not present (Figure 1B). If the pedestrian is far from the fast moving red car, the sensors in the red car may not be able to detect the pedestrian so the PCS on the red car may not be able to make effective braking decision. Since the pedestrian is much closer to yellow car, the V2V-PCS of the yellow car can provide pedestrian information before the red car can recognize the pedestrian.

(A) IB-VST-PLR-OS   *(B) IA-VST-PLR-ON*
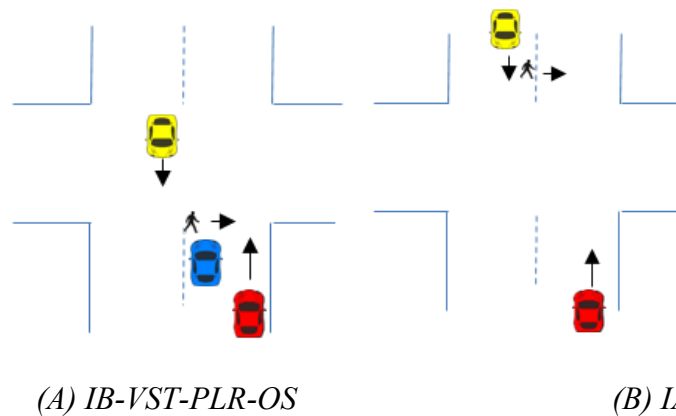
Figure 1. Example scenarios showing that the V2V-PCS system may prevent a crash to the pedestrian.

Figure 2 demonstrates a scenario that the V2V-PCS system cannot improve the safety of a pedestrian. The red car (crashing vehicle) is going straight forward. The obscure blue car is in front of the red car. The pedestrian is walking along the road. Even the pedestrian information sent by the blue car and received by the red car, there is not a situation that the red car can crash to the pedestrian.
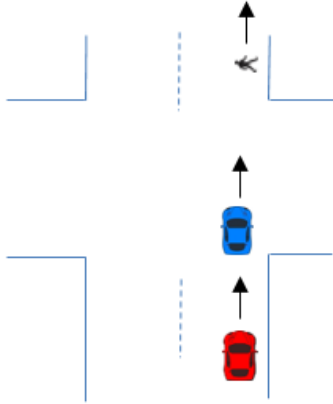
Figure 2. A scenario IA-VST-PAL-OM showing the scenarios at the V2V-PCS system does not help pedestrian safety.

2.3.1.3 Analysis of scenarios

All scenarios that V2V-PCS systems improve the safety of the pedestrians are identified in last section. The next step is to answer two practical questions quantitatively,

A. Given any scenario as described in Table 2 with detailed motion information of all objects, how do we know if there is a crash or not? The answer to this question is useful for developing a V2V-PCS warning/braking strategy.

B. Given any scenario as described in Table 2 with the positions and speeds of all objects except the initial position of the crashing vehicle, what is the initial position of the crashing vehicle so that there is a crash to the pedestrian at a specific location of the vehicle? The answer to this question is useful for setting up the test scenario for evaluating the effectiveness of the V2V-PCS systems.

To answer these questions, scenarios in Table 2 are reorganized into three categories based on the vehicle motion direction: vehicle move straight, vehicle change/merge lanes, and vehicle move in a curved lane.

2.3.1.3.1 The straight moving vehicle crashes a pedestrian crossing a street

This subsection provides a method to check if there will be a crash when a pedestrian is crossing the road and vehicle is moving straight. This method is essential for evaluating whether or not a V2V-PCS system is capable of improving a pedestrian's safety. Figure 3 depicts a situation where a straight moving vehicle crashes into a pedestrian crossing the street. The red car is moving straight forward with center at the y-axis, while a pedestrian crosses the road from left to right with an angle of Θ to x-axis. Assuming the crash location is at the origin of the coordinate system, the following equations can answer the aforementioned two questions.
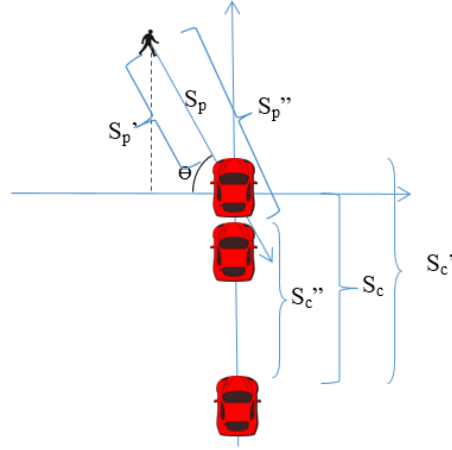
Figure 3. The straight moving vehicle crashes a pedestrian crossing a street.

Definition of notations in Figure 3:

Θ: The angle of the pedestrian's motion with respect to x axis

L_c: The length of the vehicle

W_c: The width of the vehicle

S_c: The distance between the vehicle's initial position (front center) and the potential collision point

S_c': The distance between vehicle's initial position (front left corner) and the potential collision point

$$S_c' = S_c + 0.5W_c \tan \Theta$$

S_c'': The distance between vehicle's initial position (front right corner) and the potential collision

$$S_c'' = S_c - 0.5W_c \tan \Theta$$

S_p: The distance between pedestrian's initial position (front center) and the collision point

S_p': The distance between the pedestrian's initial position and the collision point with vehicle's front left corner

$$S_p' = S_p - 0.5W_c/\cos \Theta$$

S_p'': The distance between pedestrian's initial position and the collision point with vehicle's front right corner

$$S_p'' = S_p + 0.5W_c/\cos \Theta$$

v_p: The velocity of the pedestrian (Assume the pedestrian is moving at a constant speed)

v_c: The initial velocity of the vehicle

a_c: The acceleration of the vehicle

Determine if there is a collision between the vehicle and the pedestrian

According to Figure 3, potential crash time t_c is bounded by two conditions, one where the pedestrian is struck at the left front corner of the vehicle and one where the pedestrian is struck at the right front corner of the vehicle. The time interval for the pedestrian to move between these

two points can be expressed as [t_p', t_p''], and the time interval for the vehicle to move between these two points can be shown as [t_c', t_c'']. Vc crashes to the pedestrian when [t_c', t_c''] overlaps [t_p', t_p''].

t_p' and t_p'' can be calculated as S_p'/v_p and S_p''/v_p, respectively.

t_c' and t_c'' can be calculated using Newton's laws of motion: $t = (-v_c \pm sqrt(v_c^2 + 2a_cS_c)) / a_c$,

If $a_c > 0$, If $sqrt(v_c^2 + 2 a_cS_c) \geq v_c > 0$, Then $t = (-v_c + sqrt(v_c^2 + 2a_cS_c)) / a_c$

If $v_c > sqrt(v_c^2 + 2a_cS_c') > 0$, Then no positive t, invalid for this application.

If $a_c < 0$, If $v_c \geq sqrt(v_c^2 + 2a_cS_c') > 0$, Then $t = (-v_c + sqrt(v_c^2 + 2a_cS_c')) / a_c$

If $0 < v_c < sqrt(v_c^2 + 2a_cS_c')$, Then $t = (-v_c + sqrt(v_c^2 + 2a_cS_c')) / a_c$

If $a_c = 0$, $t = S_c/v_c$

Example 3.1:

Given the situation in Figure 2 and the variable values in the following table

a_c	v_c	v_p	Θ	L_c	W_c	S_p	S_p'	S_p''	S_c	S_c'	S_c''
5m/s²	13.5m/s	1.5 m/s	60°	4.8m	1.8m	7.5m	5.7m	9.3m	55m	56.56m	53.44m

The calculation of (t_p', t_p'') is (3.8 sec, 6.2sec), and (t_c', t_c'') is (3.96 sec, 4.18 sec). Since there is an overlap time range which is [3.96 sec, 4.18 sec], it there is collision between the pedestrian and the crashing vehicle during this time interval.

Determine the initial positions of Vc and the pedestrian that guarantee a crash

According to Figure 3, the crashing vehicle is on y-axis and the crash point is at the origin, so the initial position of the vehicle is (0, -S_c) and the initial position of pedestrian is (-$S_p$cosΘ, $S_p$sinΘ). To guarantee a crash for vehicle testing, the initial position of the vehicle can be decided according to the initial position of the pedestrian and vice versa. In other word, the travel time for the pedestrian to reach origin should be the same as that for the vehicle. If the desired crash point is not at the middle front of the vehicle, the path of vehicle in the y-direction can be shifted along the-x axis accordingly.

2.3.1.3.2 The vehicle crashes a pedestrian crossing a street while change lanes

This section provides the method to check if there is a crash when a pedestrian is crossing the road and vehicle is changing lanes. Figure 4 depicts the situation that a vehicle crashes into a pedestrian crossing the street while changing lanes. The red car Vc is changing to the left lane centered at y-axis while a pedestrian crosses the road from left to right with an angle of Θ to x-axis. The definitions of the notations in Figure 4 are the same as that in Section 2.3.1.3.1. The additional notation α is the angle between y-axis and the line from the vehicles initial position to origin.

Determine if there is a crash between Vc and the pedestrian

Practically, in the vehicle changing lanes cases, the distance that the vehicle moves forward is much longer than the distance that the vehicle moves laterally (equals the width of a lane). Thus the width of the lane that the vehicle merges can be ignored so that these cases can be regarded as the vehicle moving straight forward as described in Section 3.1. So the method described in Section 3.1 can be used for these change lanes cases.
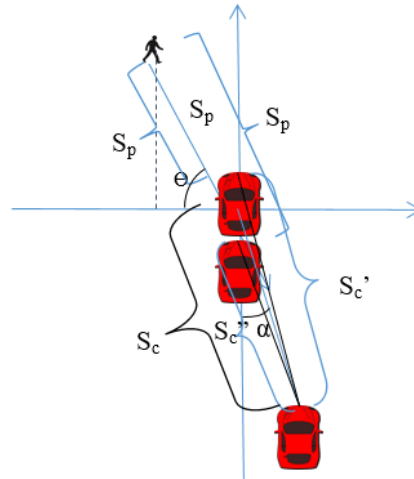
Figure 4. The vehicle changes lanes and crashes a pedestrian crossing a street.

Determine the initial positions of Vc and the pedestrian for vehicle V2V-PCS performance evaluation

According to Figure 3, the initial position of Vc is $(S_c\sin\alpha, -S_c\cos\alpha)$ and the initial position of the pedestrian is $(-S_p\cos\Theta, S_p\sin\Theta)$. To guarantee a crash in V2V-PCS evaluation, the initial position of the vehicle needs to be decided according to the initial position of the pedestrian and vice versa. In other words, the travel time for the pedestrian to reach origin should be the same as that for the vehicle. If the desired crash point is not at the middle front of the vehicle, the path of vehicle in the y-direction can be shifted along the-x axis accordingly.

2.3.1.3.2 The vehicle crashes the pedestrian while following a curved road

This subsection provides the method to check if there will be a crash when a pedestrian is crossing the road and vehicle is moving along a curved road (depicted in Figure 5). The red car is curving with center at y-axis while a pedestrian crosses the road from left to right with an angle of Ɵ to x-axis. It is assumed that the crash location will be at the origin of the coordinate. The curved lane in a non-intersection location can be considered as a straight lane in terms of traveling distance and time. Therefore, the method described in section 3.1 for determining if there is a collision between the vehicle and the pedestrian can be directly applied is this case. The method described in Section 3.2 for determining the initial positions of Vc and the pedestrian that guarantee a crash also can be directly applied is this case.
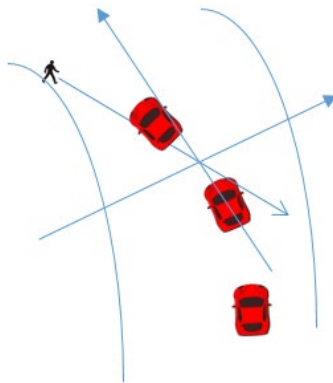
Figure 5. The vehicle crashes a pedestrian crossing a street while curving.

2.3.1.4 Add obscuring objects to the scenarios

The presence of obscuring objects does not change the collision time. However, they would delay a vehicles ability to recognize the pedestrian, which leads to less time for the vehicle to react to imminent crash to the pedestrian. To analyze the effect of the obscuring objects, the following question needs to be answered:

Given the path of the pedestrian and the location of the obscuring objects, how could the locations of the obscuring objects be determined so that the object obscures the vehicles view of the pedestrian?

By answering this question, the time between the first appearance point of the pedestrian and a collision, or time to collision (TTC), can be calculated. If PCS systems are obscured then vehicles must rely more on V2V systems. Figure 6 will be used to describe the effect of the location of obscuring objects on potential crashes. For the simplicity of explanation, it is assumed that the camera is located at the front center of each vehicle. Notations in Figure 6 are defined as follows:

Lvs & Wvs: The length and width of the blocking vehicle Vs.

Pp: The coordinates of the pedestrian.

Pvc: The front center position of Vc.

Pvc'& Pvc":   The initial position and the final position that Vc is blocked by Vs.

Pvs-fr: The coordinates of the front right corner of Vs
Pvs-rl: The coordinates of the rear left corner of Vs
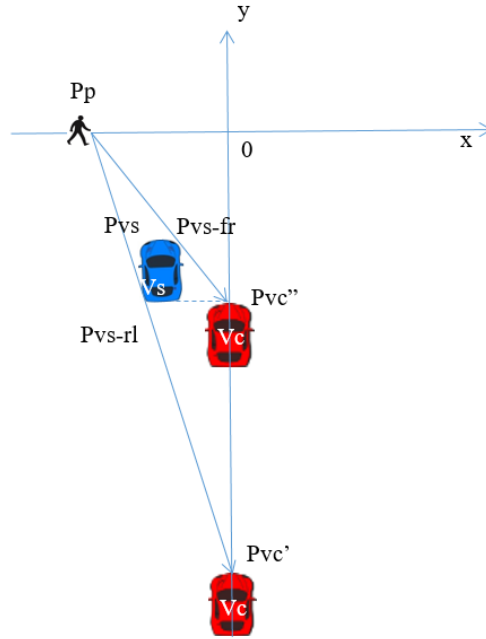
Figure 6. Add obscure vehicle Vs to scenarios

According to Figure 6, the range of positions that the blocking vehicle Vs blocks the crashing vehicle Vc's view of the pedestrian is from Pvc' to Pvc". For a given Pvs, Lvs and Wvs, Pvs-fr and vs-rl can be calculated. If Pp is given, Pvc' can be calculated as the point on y-axis and on the line of PpPvs-rl, and Pvc" can be calculated as the point on y-axis and on the line of PpPvs-fr. If Pvc is between Pvc'and Pvc", Vc cannot see the pedestrian.

2.3.1.5 Conclusion
This paper used an exhaustive analysis method to identify the scenarios that a combined PCS and V2V system can improve the pedestrian safety theoretically. 96 out of 168 pedestrian related scenarios can benefit from V2V-PCS system. The method for determining if there is a potential crash for all 96 cases for given vehicle and pedestrian motion parameters is described. The method for creating a crash condition for V2V-PCS system evaluation is also described. The calculation of the first appearance location of the pedestrian to the vehicle and time to collision due to the location of the obscure object is described. These results lay a good foundation for further V2V-PCS system studies.

2.3.1.6 References
[1] Najm, W.G., Koopmann, J., Smith, J.D. and J. Brewer. 2010. "Frequency of Target Crashes for IntelliDrive Safety Systems." DOT HS 811 381, U.S. Department of Transportation, National Highway Traffic Safety Administration, Washington, DC.

[2] Harding, J., Powell, G., R., Yoon, R., Fikentscher, J., Doyle, C., Sade, D., Lukuc, M., Simons, J., & Wang, J. (2014, August). Vehicle-to-vehicle communications: Readiness of V2V technology for application. (Report No. DOT HS 812 014). Washington, DC: National Highway Traffic Safety Administration.

[3] Frost & Sullivan, http://www.frost.com/prod/servlet/press-release.pag?docid=289374477, Daimler and Volvo Take Lead in Implementation of V2V Communication Systems in Europe.

[4] Najm, W.G., Ranganathan, R., Srinivasan, G., Smith, J.D., Toma, S., Swanson, E. and A. Burgett. 2010. "Description of Light Vehicle Pre-Crash Scenarios for Safety Applications Najm 10 Based on Vehicle-to-Vehicle Communications." To be published, U.S. Department of Transportation, National Highway Traffic Safety Administration, Washington, DC.

2.3.2 Pedestrian Protection Using V2V and the Pedestrian Automatic Emergency Braking System

2.3.2.1 Introduction

Due to the fast advancement of wireless communication technology and computation speed, Vehicle-to-Vehicle (V2V) communication becomes practical and being implemented in many research studies. The information exchange through V2V enabled vehicles to make better decisions in driving control and safety [1]. Meanwhile, Pedestrian Automatic Emergency Braking (PAEB) systems use various types of onboard sensors (such as radar, mono/stereo camera, infrared etc.) to detect the potential collision with pedestrians. The PAEB alerts the driver if there is an imminent collision and supports collision avoidance by applying the brake automatically if the driver does not take braking action [2]. Due to the range limitations of PAEB sensors and speed limitations of sensory data processing, PAEB systems often cannot detect or do not have sufficient time to respond to a potential crash. To improve the pedestrian safety, the idea of integrating the complimentary capabilities of V2V and PAEB (V2V-PAEB) together to allow the information of pedestrians sensed by PAEB of one vehicle to be shared in the V2V network is proposed. The information broadcasted through V2V network can be used by the PAEB of other vehicles.

A set of 96 scenarios that the pedestrian safety can benefit from the proposed V2V-PAEB feature has been identified [3]. Based on the V2V-PAEB features discussed in [3], this paper standardizes the V2V-PAEB functions and features, where it also provides some convincible demonstrations. These scenarios proved the potential use of the V2V-PAEB and that the simulation environment could be used for evaluating V2V-PAEB systems. These simulated scenarios can also illustrate the feasibility in the real world. However, successful V2V-PAEB actions are highly depending on the number of vehicles with the V2V-PAEB hardware.

Based on the state-of-the-art V2V, V2P (Vehicle-to-Pedestrian) communication standards [1], this paper concentrates on the detailed feasibility and experimental analysis. This paper presents a Matlab/Simulink based computer simulation architecture specially designed for the further development of V2V-PAEB system and its simulation model. This simulation architecture is organized according to the information processing steps and the problems need to be solved in a V2V-PAEB system. It is called architecture since it captures all necessary parts of a V2V-PAEB for it to be functional and allows the flexibility of future improvement of any individual subsystem. Goals for developing this simulation model architecture include: (1) present the problems and challenges in developing the V2V-PAEB system; (2) decompose the problem into a set of well-defined sub-problems; (3) present the architecture and the information processing flow for solving all sub-problems; (4) provide a simple implementation of the simulation model to demonstrate the usefulness of the model for studying the V2V-PAEB integration problems and (5) providing a foundation for quick verification of new V2V-PAEB algorithms. With the predefined architecture and function blocks described in this paper, new V2V-PAEB information processing algorithms can be quickly evaluated. The V2V-PAEB simulation model has been tested in the PreScan environment. Some pedestrian safety related V2V-PAEB experiments described in [3] were implemented by incorporating V2V-PAEB algorithms to demonstrate the usefulness of this model.

2.3.2.2 Description of V2V-PAEB Simulation Model

The V2V-PAEB simulation model connected with its required supporting upstream/downstream models in a vehicle model is shown in Figure 1. The block in the center is the V2V-PAEB simulation model, and blocks on both sides are peripheral upstream/downstream models. The V2V-PAEB model uses information from upstream models to detect potential collisions with pedestrians and make proper safety decisions. Then these decisions are sent to downstream models to trigger proper actions to avoid or mitigate the potential collisions. Various types and numbers of sensors can be used in V2V-PAEB system. The output of the sensors models provides the position, velocity, and acceleration of the detected objects. Sensors can be added to or removed from the V2V-PAEB simulation model. Current implementation of the V2V-PAEB simulation model supports two basic sensor models (radar and camera).
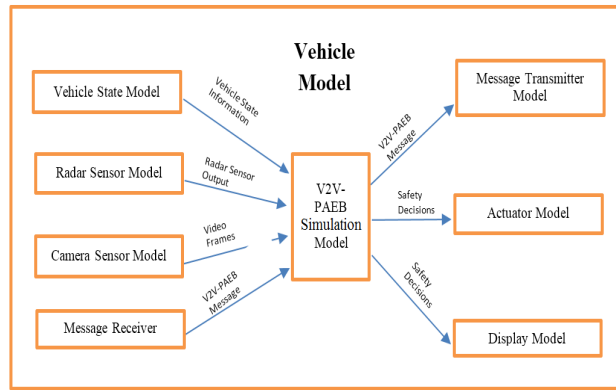

Figure 1. V2V-PAEB model in a vehicle model.

The V2V-PAEB simulation model provides the ability of message passing (transmitting and receiving) with well-defined message protocol. V2V-PAEB Message is a subtype of V2V communication message. It contains the information of pedestrians detected by their V2V-PAEB systems. TABLE 1 shows the required input of V2V-PAEB simulation model. The format of the V2V-PAEB Message is defined in TABLE 2. The detailed information of the output data of the V2V-PAEB simulation model is shown in TABLE 3.

TABLE 1. The Input Data of V2V-PAEB Model

Item	Description
X,Y,Z [m]	vehicle coordinates in global coordinate system
GPS [deg/min/sec]	The GPS Latitude, Longitude, and Altitude of the host vehicle
Rotation about X,Y,Z [deg]	X, Y, and Z -rotations of the vehicle in global coordinate system.
Yaw Rate [deg/s]	The Yaw (Turning) rate of the vehicle.
Velocity [m/s]	The moving velocity of the vehicle.
Heading Direction [deg]	The moving direction of the vehicle. North is 0o (range between 0-360 in clockwise direction).
Acceleration [m/s2]	The acceleration of vehicle.
Throttle State [%]	Throttle state of vehicle. Range between 0-100.
Brake State [%]	Brake state of vehicle. Range between 0-100.

Steering Angle [deg]	The steering Angle of vehicle.

Radar model

Beam ID [-]	The radar sensor can be configured with a number of beams with different angle coverages. This Beam ID indicates which beam is active in the current simulation time step.
Range (R) [m]	The distance between the radar sensor and the detected objects.
Doppler Velocity [m/s]	Velocity of target point, relative to the sensor, along the line of-sight between sensor and target.
Theta Θ [deg]	Azimuth angle in the sensor coordinate system
Phi Φ[deg]	Elevation angle in the sensor coordinate system
Target ID [-]	Numerical ID of the detected target.
Energy Loss [dB]	Ratio received power / transmitted power.
Alpha α [deg]	Azimuthal incidence sensor angle on the target.
Beta β[deg]	Elevation incidence sensor angle on the target.
TIS Data [-]	Communication bus signal contains sensor's output.
Doppler Velocity X/Y/Z [m/s]	Velocity of target point decomposed into X, Y, Z of the sensor's coordinate system.
Target Type ID	Radar may identify the type of detected objects. The Type ID specifies the detected object type.

Camera Model

Video Frame rate and format	The camera sensor model should be able to generate video frames at a proper frame rate.

Message Receiver Model

Message	Used for vehicles to share the sensory information. Table 2 shows the message format.

TABLE 2. THE FORMATION OF V2V-PAEB MESSAGE

Item	Description
Header	
Destination	The destination of the message if unicast is supported.
Source	The sender of this message.
Type of message	Type of message (e.g., V2V-PAEB type).
Subtype of message	The subtype of the message. In case for expanding this message in the future.
Priority of message	The priority of the message.
Event time	The event time stamp of the message.
Total packs	Total packages of the message.
Packet id	The pack id of current message.
Length of payload	The length of the payload of this message.
Payload	
Vehicle ID	Host vehicle's unique ID in the V2V network.
Vehicle type	To indicate the type of the host vehicle
Vehicle color	Host vehicle's color.
Vehicle GPS location	Host vehicle's latitude, longitude and altitude [deg].
Vehicle speed	Host vehicle's moving velocity [m/s].
Vehicle heading	Host vehicle's heading direction. North is 0 degree range between 0-360o clockwise.
Vehicle acceleration	The acceleration of the host vehicle.
Vehicle GPS accuracy	The accuracy of host vehicle's GPS device.
Number of pedestrians	To indicate how many pedestrians' information are included in this message
Pedestrian ID	The ID of the first pedestrian
Confidence	The confidence level of this Ped information
Pedestrian size	The size of the first pedestrian
Pedestrian color	The color of the first pedestrian

Pedestrian GPS location	The latitude, longitude and altitude of the first pedestrian
Pedestrian velocity	The velocity of the first pedestrian [m/s]
Pedestrian heading	first pedestrian's heading direction [deg]
Ped. acceleration	The acceleration of the first pedestrian[m/s2]
Pedestrian ID	The ID of the second pedestrian. Second pedestrian's information stars here.
……	……
……	…… the information for the third, fourth, and rest of detected objects.

TABLE 3. Information of the Output Data of the V2V-PAEB Simulation Model

Object Type ID	Description
Pedestrian Detection Flag [Y/N]	This flag is used to indicate whether any pedestrians have been detected. If so, this parameter will be set to Y. Otherwise, it will be set to N.
Driver Warning Flag [Y/N]	This flag is used to indicate if the driver warning should be triggered. If this parameter is set to Y, then a driver warning will be triggered immediately. Otherwise, if this parameter is set to N, then the vehicle will do nothing.
Automatic Braking Flag [Y/N]	This flag is used to indicate if the automatic braking should be started. If it is set to Y, then the automatic braking will be started immediately. Otherwise, if this parameter is set to N, then the vehicle will do nothing.
Brake Pressure [bar]	This value is used to control the deceleration of the vehicle when the automatic braking is started. Once the Automatic Braking Flag is set to Y, then the Brake Pressure should be assigned a value between zero and the Max Braking pressure. Otherwise, if the Automatic Braking Flag is set to N, then this parameter should be zero.
Automatic Steering Flag [Y/N]	This flag is used to indicate if the automatic steering control should be started. If it is set to Y, then the automatic steering will be started immediately. Otherwise, if this parameter is set to N, then the vehicle will do nothing.
Automatic Steering Angle [deg]	This value is used to specify the steering wheel status. A positive value means turning right, and minus value means turning left. Once the Automatic Steering Flag is set to Y, then this parameter should be assigned with a meaningful value. Otherwise, it should be zero.
Time To Collision [s]	Time to Collision represents for how much time left before the collision occurs. If many pedestrians are detected at the same time, and each one has its TTC. Then this parameter will be set to the smallest of them.
V2V-PAEB Message [array]	The V2V-PAEB Message that contains the pedestrians that detected by PAEB system on vehicle. Vehicles use this message to share the pedestrian information through V2V communication.

There are two types of output data generated by the V2V-PAEB simulation model: the V2V-PAEB Message and safety decisions (see Figure 2). The V2V-PAEB Message usually goes to the Message Transmitter Model and then being sent out to the nearby vehicles. The safety decisions are sent to both the Actuator Models for triggering proper actions and the Display Model for displaying the simulation process and results. Figure 2 shows the architecture and information processing blocks of the V2V-PAEB model. Information processing is organized in four groups.

- The gray shaded block group describes the environment, vehicle and sensor setup for simulation.

- The non-shaded group is responsible for the on-vehicle sensor based pedestrian detection and V2V-PAEB message generation.

- The yellow shaded group is responsible for receiving V2V-PAEB messages and extracting the pedestrian information from messages.

- The blue shaded group is responsible for merging the pedestrian information from onboard sensors and received messages, and making car braking decisions.

Blocks for environment, vehicle and sensor setup (gray shaded blocks):

- Vehicle Kinematic Model block describes the locations and moving directions of the sensors on the vehicle, which need to be considered in calculating the collision distance and time.

- Sensor Model block describes the characteristics of sensors, such as range, field of view, error model, etc.

- Driving Scenario Model block describes the number of vehicles and objects involved in the simulation and their relative positions and motion trajectory.

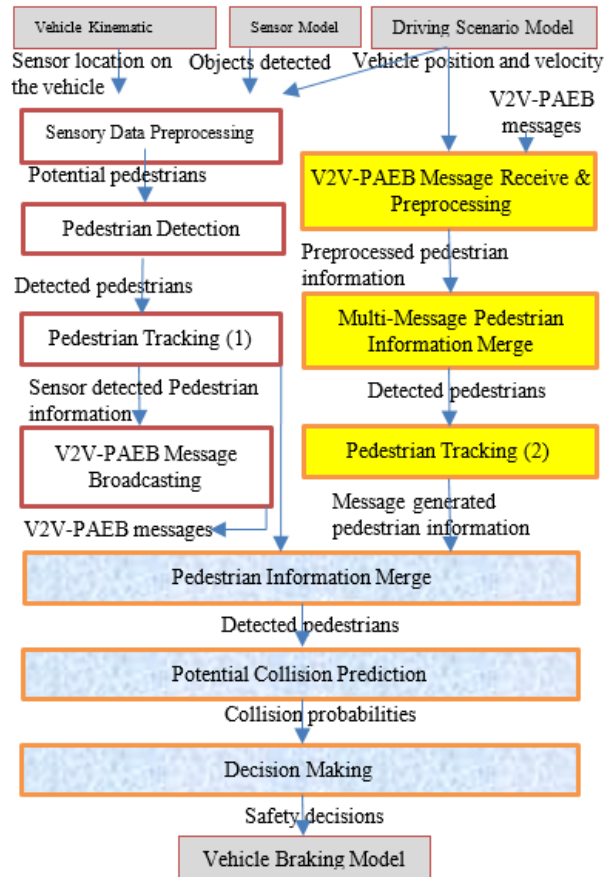- Vehicle Braking Model block describes the vehicle behavior for various braking commands.

Figure 2. Information processing flow of V2V-PAEB simulation model.

Blocks for vehicle sensor based pedestrian detection and V2V-PAEB message generation (non-shaded blocks):

Sensory Data Preprocessing block processes raw sensory data using simple cues and fast algorithms to identify potential pedestrian candidates. This stage needs to have high detection speed even at the expense of allowing false alarms.

Pedestrian Detection block applies more complex algorithms to the candidate object from the Sensory Data Preprocessing block in order to separate genuine pedestrians from false alarms.

Pedestrian Tracking (1) block tracks detected pedestrians overtime to get their trajectories.

V2V-PAEB Message Broadcasting block constructs and broadcasts V2V-PAEB Messages.

Blocks for V2V-PAEB messages receiving and pedestrian information extraction (yellow shaded blocks):

- V2V-PAEB Message Receive & Preprocessing block periodically processes received messages to obtain the motion and state information of pedestrians contained in these messages.

- Multi-Message Pedestrian Information Merge block merges all the pedestrians extracted from different messages together to obtain a whole set of pedestrians that detected by other vehicles.

- Pedestrian Tracking (2) block tracks message extracted pedestrians overtime to get their trajectories.

Blocks for pedestrian information merging from onboard sensor and received messages, and making braking decisions (blue shaded blocks):

- Pedestrian Information Merge block merges the two set of pedestrians information (one onboard sensor detected pedestrians and the other from received V2V-PAEB messages) together to obtain a complete set of detected pedestrians surrounding the host vehicle.

- Potential Collision Prediction block predicts the probability of collision between the host vehicle and pedestrians.

- Decision Making block generates warning to the driver if there is potential collision and generates braking commands if a collision is imminent [4].

The V2V-PAEB simulation model describes the information flow and processing for achieving pedestrian safety. To use it in simulation, it should be placed in a vehicle model. To reduce the complexity of developing this model, some third party simulation software (Such as PreScan, LabView and CarSim) can be used to provide complete or partial functions in some blocks. For example, PreScan software is used to provide blocks for environment, vehicle and sensor setup, and simulation display in this study. PreScan software also provided partial function support for message passing. Other blocks are developed either in Simulink or Matlab environment.

2.3.2.3 Simulation Testing

The proposed V2V-PAEB simulation architecture has been implemented and tested in PreScan environment [12]. PreScan provides several modules that the V2V-PAEB simulation needs. The intuitive graphical user interface (GUI) allows the construction of the experiment scenario and model the desired radar and camera sensors, while the Matlab/Simulink interface enables the

integration of the V2V-PAEB simulation model. Following subsections describe the development and testing of the V2V-PAEB simulation using PreScan.

Figure 3 is a scenario chosen from paper [3] for testing the V2V-PAEB simulation architecture. In this scenario, five vehicles and one pedestrian are at an intersection. The traffic light changes from green to red when the pedestrian is still crossing the street. At the same time, vehicle 5 is approaching this intersection at a speed of 6.67 m/s (24km/h). The driver does not change the speed and keeps driving through this intersection. Both the pedestrian and vehicle 5 cannot see each other for their views are obscured by vehicle 2. However, vehicle 1 and vehicle 2 can see this pedestrian. For this experiment scenario, two cases are run separately to check if the combined V2V-PAEB system works better than the PAEB only system. Combined V2V-PAEB system means information that detected by multiple vehicles will share their data in real-time through V2V network. The PAEB only system represents a scenario where vehicles detect objects individually without any communication.

Case 1: No vehicle has V2V capability and vehicle 5 is equipped with PAEB system. Since the sight of on-board sensors of vehicle 5 is blocked by vehicle 2, vehicle 5 cannot see the pedestrian until very late.

Case 2: Vehicles 1, 2 and 5 are equipped with V2V-PAEB systems. Vehicle 1 and 2 can detect the pedestrian early and broadcast this pedestrian information to vehicle 5 through V2V-PAEB messages.
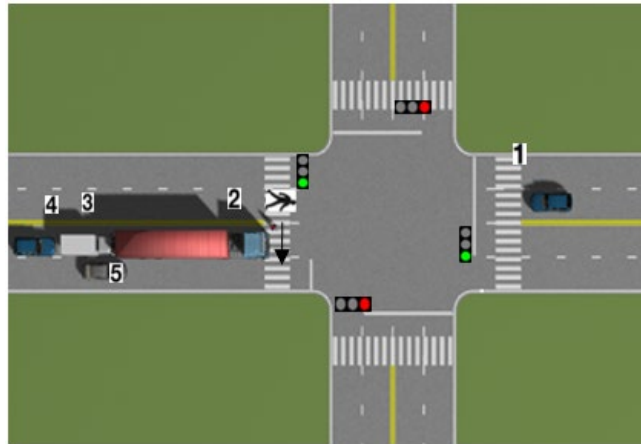

Figure 3. Simulation scenario used for testing the V2V-PAEB simulation model.

A.   Build Experiment Scenario

This experiment can be easily built in PreScan's GUI by using drag and drop actions to the library elements of road sections, infrastructure components (trees, buildings, traffic signs), actors (cars, trucks, bikes, and pedestrians), sensors (radar, camera, LiDAR, etc.), weather conditions (such as rain, snow, and fog) and light sources (such as the sun, headlights, and lampposts).

B.   Add the V2V-PAEB Model to the Vehicle Model

The V2V-PAEB simulation model described above is inserted to the vehicle in the simulation. The Vehicle State Model, Radar Sensor Model, Camera Sensor Model and DSRC Receiver Model are connected to (or implemented in) the V2V-PAEB Simulation Model. The output of V2V-PAEB simulation model is connected to the DSRC transmitter model and actuator models.

C. Simulation Result

Two cases as described earlier are simulated. Table 4 compares the simulation results of case 1 and case 2. The simulation result of vehicle 5 for case 1 shows that there was a collision between vehicle 5 and the pedestrian with collision speed 0.67m/s. The pedestrian was detected by the PAEB system when TTC was 0.39 seconds. Since it was too late and the PAEB system does not have enough time to react, the collision was not avoided but mitigated.

TABLE 4. The Comparison of the Simulation Results for Case 1 and Case 2

Items	Case 1	Case 2
Initial vehicle speed (m/s)	6.7	6.7
Pedestrian detected time (s) (TTC)	0.39	1.50
Full Braking generated time (s) (TTC)	0.39	0.58
Collision Avoided [Yes/No]	No	Yes
Collision Speed (m/s)	0.19	No collision

The simulation result of vehicle 5 for case 2 shows that the potential collision between vehicle 5 and the pedestrian was avoided successfully. The pedestrian was detected when TTC equaled to 1.50 seconds and the PAEB waited until TTC=0.58 seconds to start full braking and the collision is avoided. It can be seen in TABLE 4 that the V2V-PAEB system on vehicle 5 in case 2 can detect pedestrians much earlier than that in case 1 so that the V2V-PAEB system can have more reaction time and has a better performance than PAEB system alone. If there is 0.4 seconds delay from generating the braking command to the actual start of mechanical braking due to communication and mechanical engagement, case 1 will have no mitigation and case 2 still avoid the collision. This is a demonstration that the V2V-PAEB system can compensate the limitations of the PAEB only system, and can improve pedestrian safety significantly.

D. Other Simulation Cases

Many scenarios have been identified that V2V-PAEB can be used to improve the pedestrian safety [3]. Figure 4 shows a 2-lane road example where pedestrian is crossing the road. The cars on the right lane are waiting to move, car 4 on the left lane moves fast. While the Pedestrian 7 is obscured by car 2, car 4 is about to crash pedestrian 7. In the simulation with V2V-PAEB support, car 4 can prevent the crash by getting pedestrian information from car 2 a few seconds earlier. Whether this scenario has collision or not depends on the initial vehicle speed and TTC, however, TTC will be increased when V2V-PAEB is applied on all vehicles. Details of this simulation are not included in this paper, but the idea of the V2V-PAEB can be shown in Figure 4 clearly.

2.3.2.4 Discussion

This study sets up the architecture of the V2V-PAEB system and establishes a simulation tool to support further study. Simple algorithms are implemented to demonstrate the operation of the V2V-PAEB system. Various issues of V2V-PAEB need to be further addressed. These issues include the effect of time delay in information transmission and processing to the performance of the system, the effect of sensor error to the performance of the system, and the communication jam caused by large amount messages sent by many vehicles.
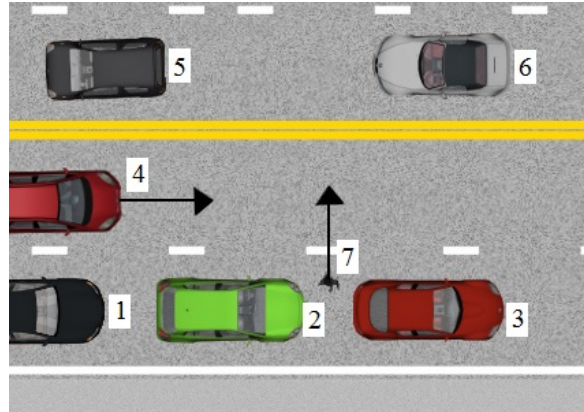
Figure 4. Simulation of V2V-PAEB – pedestrian dart out.

2.3.2.5 Conclusion

This study described the idea of using the V2V-PAEB system to compensate the limitations of PAEB system that has short detection range and unable to detect obscured objects. The approach integrates the capabilities of V2V and PAEB to allow the information of pedestrians detected by PAEB system to be shared in the V2V network. Theoretically, the V2V-PAEB system should have better performance than PAEB system because other vehicles can report the pedestrians that one vehicle's PAEB system failed to detect. Architecture for V2V-PAEB system is described. It decomposes various tasks associated to the V2V-PAEB system into smaller specific problems. The input and output parameters of the V2V-PAEB system as well as its each block are also defined. The simulation has shown that the proposed V2V-PAEB has definite advantage over the PAEB alone system. The simulation provides a good foundation and tool for further V2V-PAEB study.

2.3.2.6 References

[1] J. Harding, G. Powell, R. Yoon, J. Fikentscher, C. Doyle, D. Sade, M. Lukuc, J. Simons, and J. Wang, "Vehicle-to-Vehicle communications: Readiness of V2V technology for application," Washington, DC: National Highway Traffic Safety Administration. DOT HS 812 014, Sep 16 2014, http://www.nhtsa.gov/stat...for-Application-812014.pdf

[2] E. Coelingh, A. Eidehall and M. Bengtsson, "Collision Warning with Full Auto Brake and Pedestrian Detection – a practical example of Automatic Emergency Braking," *2010 13th International conference on Intelligent Transportation Systems (ITSC)*, Sept 19-22, 2010, pp. 155-160.

[3] M. Liu, S. Chien, Y. Chen, "Improve Road Safety Using Combined V2V and Pre-Collision Systems," *The 24th International Technical Conference on the Enhanced Safety of Vehicles (ESV2015)*, Gothenburg, Sweden on June 8-11, 2015. Paper Number 15-0431.

[4] T. Gandhi, M. Trivedi, "Pedestrian Protection Systems: Issues, Survey, and Challenges," *IEEE Transactions on Intelligent Transportation Systems*, Sept. 2007, pp. 413-430.

[5] Bartsch, A., F. Fitzek, and R. H. Rasshofer. "Pedestrian recognition using automotive radar sensors." Advances in Radio Science 10.4 (2012): 45-55.

[6] A. Bhawiyuga, H. Nguyen. H. Jeong, "An Accurate Vehicle Positioning Algorithm Based on Vehicle-to-Vehicle (V2V) Communications," *2012 IEEE International Conference on Vehicular Electronics and Safety (ICVES)*, 24-27 July. 2012.

[7] L. Bowen, Y. Danya. "Calculation of Vehicle Real-time Position Overcoming the GPS Positioning Latency with MEMS INS," *IEEE International Conference on Service Operations, Logistics, and Informatics (SOLI)*, 8-10 Oct. 2014.

[8] B. Tang, S. Chien, and Y. Chen, "Obtain a Simulation Model of a Pedestrian Collision Imminent Braking System Based on the Vehicle Testing Data," *17th IEEE Int.Conf. on Intelligent Transportation Systems*, Oct 8-11, 2014, Qingdao, China.

[9] O. Trullols-Cruces, M. Fiore, J.M. Barcelo-Ordinas, "Understanding, modeling and taming mobile malware epidemics in a largescale vehicular network," World of Wireless, *2013 IEEE 14th International Symposium and Workshops on Mobile and Multimedia Networks (WoWMoM)*, June 4-7, 2013.

[10] Y. Chen, K. Shen, S. Wang, "Forward Collision Warning System Considering Both Time-to-Collision and Safety Braking Distance, *2013 8th IEEE Conference on Industrial Electronics and Applications (ICIEA)*. June 19-21, 2013.

[11] M. Heesen, M. Dziennus, T. Hesse, A. Schieben, "Interaction design of automatic steering for collision avoidance: challenges and potentials of driver decoupling," *Intelligent Transport Systems, IET*. 22 Jan. 2015.

[12]   M. Tideman, M. Noort, "A Simulation Tool Suite for Developing Connected Vehicle Systems," *2013 IEEE Intelligent Vehicles Symposium (IV)*, June 23-26, 2013.

2.3.3 A Hierarchical Clustering Analysis (HCA) for Pedestrian Position Identification

2.3.3.1 Introduction

As many automobile companies have announced the incorporation of Autonomous Emergency Braking (AEB) into their automobiles, pedestrian recognition systems based on onboard vehicle sensors, such as radar, camera, LiDAR, etc., have been installed on more vehicles. If a vehicle can send its sensor detected pedestrian information to nearby vehicles through the Vehicle-to-Vehicle (V2V) communication network, receiving vehicles may be able to use this information as early pedestrian detection and the chance of crashes will be reduced.

The V2V communication based on DSRC (Discrete Short Range Communication) technology has been studied extensively [1,3]. Many efforts have been made to use this technology to improve the road safety. Meanwhile, there also have been developments in Pedestrian Autonomous Emergency Braking (PAEB) technology, which can provide autonomous braking when there is an eminent frontal crash to a vehicle, pedestrian, or bicyclist if the driver fails to apply braking or applies insufficient braking [2,3]. The PAEB system uses radar, camera, and LiDAR sensors individually or in conjunction with one another to detect the presence and the location of the object in front of the vehicle [4,5]. For example, Premebida et al. [4] proposed a LiDAR and vision-based approach for pedestrian detection and tracking.

The performance of PAEB system has been improved significantly in recent years and been offered as standard equipment or an option on many vehicles. It is certain that all vehicles will be equipped with V2V communication capability and PAEB features in the future. There will also be a long period of time during which vehicles with and without the PAEB and V2V technology will coexist on the road.

If V2V works in conjunction with PAEB, this system is referred to V2V-PAEB system. One of the problems for this system is that when a subject vehicle receives many pedestrian position information messages from other vehicles, it does not know if each pedestrian reported by one vehicle is the same pedestrian reported by other vehicles. Therefore, it is necessary to create a method in order to accurately determine the actual amount of pedestrians. The main goal of this paper is to develop an efficient method for accurately identifying the exact positions and the amount of pedestrians from data provided by multiple vehicles equipped with PAEB systems in the V2V communication network environment.

There are significant safety benefits when the PAEB system is integrated into V2V communication systems. The benefits can be achieved by empowering every V2V enabled vehicle to make PAEB decisions based on the PAEB sensory data from other nearby vehicles. Figure 1 shows a scenario to demonstrate the usefulness of an integrated V2V and PAEB (V2V-PAEB) system. When the black car on the right lane is moving forward, a pedestrian is crossing the street. The pedestrian and the black car cannot see each other since their views are obscured by the truck in the middle lane. It is possible that the black car may collide with the pedestrian since it may be too late for the black car to brake after its PAEB system sees the pedestrian. In a V2V-PAEB environment, the position and the trajectory of the pedestrian can be detected by the truck and the car on the left lane. Then the pedestrian information can be transmitted through the V2V network

to the black car on the right lane long before the black car can see the pedestrian. This enables the black car to use the received pedestrian information to make safety decisions earlier.
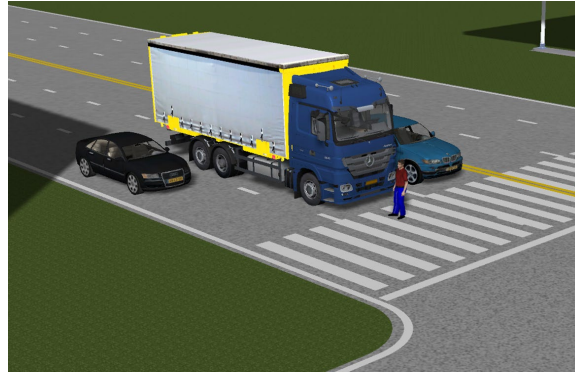

Figure 1. The truck obscures the right car and the pedestrian.

Figure 2 shows an example of V2V-PAEB environment in a busy intersection. Curved lines connecting cars represent the V2V communication.

The key for the successful operation of the collaborated V2V-PAEB includes (1) each vehicle broadcasts its own PAEB detected pedestrians' information and receives pedestrian information from nearby vehicles through the V2V network, and (2) be able to extract location and trajectory information of pedestrians accurately from the V2V messages from many different sources.
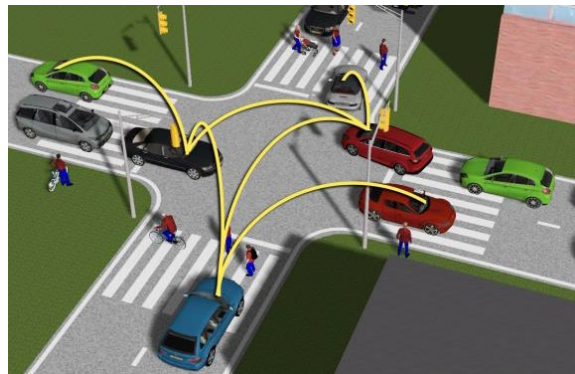

Figure 2. V2V-PAEB environment in a busy intersection.

Figure 3 shows an information extraction process of the V2V-PAEB system. The goal of the pedestrian identification is to develop an algorithm that enables each V2V enabled vehicle to construct pedestrians' locations and trajectory information accurately from the pedestrian information sent from several nearby V2V-PAEB enabled vehicles.
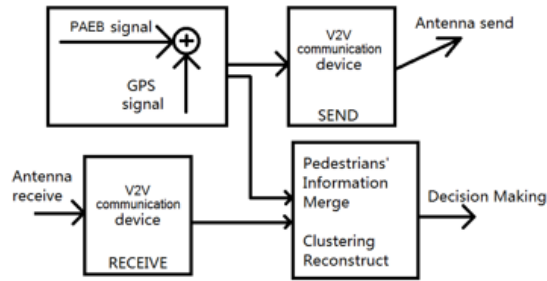
Figure 3. V2V-PAEB pedestrian safety decision-making process.

The work described in this paper is built on the prior V2V-PAEB research effort described in [6]. Figure 4 shows the architecture of the V2V-PAEB system described in [6]. The architecture assumes that V2V enabled vehicles can broadcast their PAEB system detected pedestrian position information as a V2V message, and can receive pedestrian position V2V messages broadcasted from other nearby vehicles. Each vehicle makes safety decisions (warning/braking) by predicting potential collisions based on the pedestrians' locations obtained from its own PAEB system and received V2V messages.

The flowchart in Figure 4 shows the necessary subtasks to make the V2V-PAEB system work. Each block in Figure 4 represents a specific problem that needs to be addressed in order to make the V2V-PAEB system function properly. One specific block,
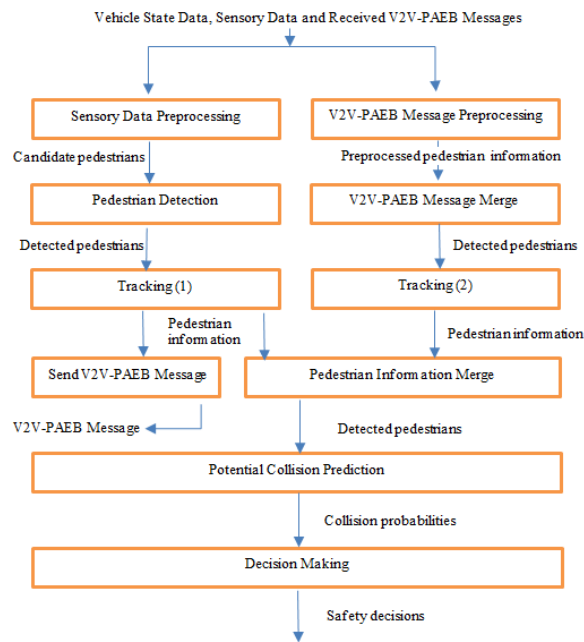

Figure 4. V2V-PAEB system proposed in [6].

"Pedestrian Information Merge", presents an interesting problem. When n pedestrians and m vehicles are in a small area, each vehicle can potentially see 0 to n pedestrians and can broadcast detected pedestrian positions through the V2V network. Due to the errors introduced by the inaccuracy of a vehicle's GPS and PAEB sensors, different vehicles may generate different pedestrian locations for the same pedestrian. There is a high possibility that $n \times m$ pedestrian positions are broadcasted in the V2V network. Assuming that each pedestrian is seen by at least one vehicle, and each vehicle does not necessarily see all pedestrians, how to determine the location of n pedestrians from V2V messages by m vehicles is a major issue raised but not solved [6]. This paper describes a method for the block "Pedestrian Information merge". The method enables each V2V-PAEB enabled vehicle to construct pedestrians' location information accurately from the pedestrians' information received from nearby vehicles.

In order to extract real pedestrian information in a large set of PAEB messages in the V2V network, the nature of the errors in the data need to be investigated. Wang, T. et al. [7] described human tracking using Delphi ESR-Vision Fusion in complex environments. A radar-vision fusion system has been built utilizing a 77GHz 2D Delphi Electronically Scanning Radar (ESR) and a CCD camera. The radar error distribution results has been explained. A simple uniform error distribution will be taken into consideration in the experiments of this paper.

Based on our best knowledge, there is no published work on data fusion (reconstructing pedestrians from PAEB information) in a V2V network provided from multiple vehicles. This paper attempts to develop a data fusion (pedestrians' signal reconstruction /clustering) algorithm to address this problem.

This paper is organized in three parts. Section II describes the problem formulation of pedestrian position detection and broadcast between vehicles. In Section III, an algorithm is proposed to cluster pedestrian information from different vehicles, find the approximate number of pedestrians, and draw the safe region. Simulation and conclusions are given in Section IV.

2.3.3.2 Problem formulation

Figure 5 shows a scenario at a road intersection, while vehicles and pedestrians are going across the intersection at the same time. In this scenario, there exist four vehicles (A, B, C, and D) and five pedestrians (1, 2, 3, 4, and 5).
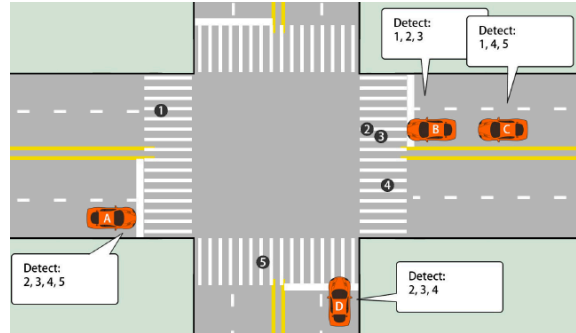
Figure 5. A road intersection scenario.

In our study, a sensor (camera, radar or Lidar) is installed in front of the vehicle. Due to the limitation of sensor's viewing angle, only the pedestrian within the detention area could be detected.

The pedestrians detection results are shown in Table 1. Pedestrian 1 is inside of the sensing area of vehicle A and B. As a result, it is detected by these two vehicles. Pedestrian 2 is detected four times by vehicles A, B, C and D. Pedestrian 3 is blocked from vehicle C's view by vehicle B. Therefore, pedestrian 3 is detected three times by vehicle A, B and D. Pedestrian 4 is outside of the sensing area of vehicle B, it can be detected three times by vehicle A, C and D. Pedestrian 5 is outside of the sensing area of vehicle B and D, it can be detected twice by vehicle A and C

Table 1. Pedestrians detected by Vehicles

Vehicle ID	Pedestrian ID
A	2 ,3 ,4 ,5
B	1 ,2 ,3
C	1 ,4 ,5
D	2, 3, 4

Because of the inevitable error of GPS and Detection sensor, the position signal for the same person varies. One pedestrian may cause multiple siginal during the detecting process. Figure 6 represents the pedestrian positions from the view of vehicle A, which means we take the position of vehicle A as the original point (0, 0). The red spot indicates the pedestrian position signal. The numbers 1 to 5 indicate the pedestrian's true position. Although there are only five pedestrians, each pedestrian is detected multiple times. As a result, there exists a total number of 13 points in Figure 6 instead of 5. The available information including the location of each signal in X and Y axis and also the vehicle ID information indicateing where the signal comes from. The signal information is presented in Table 2. Knowing the position and vehicle ID, our goal is to figure out

which signal belongs to which person and draw a safe region that is large enough to cover the person's true position.
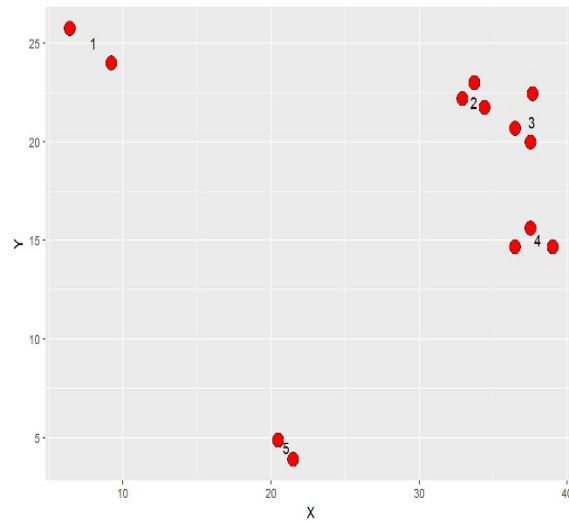
Figure 6. Pedestrian position signal.

Table 2. Pedestrian Signals

Signal ID	Vehicle ID	Position in X	Position in Y
1	A	33.719	23
2	A	36.469	20.688
3	A	37.5	15.625
4	A	20.469	4.875
5	B	6.406	25.75
6	B	32.906	22.188
7	B	37.656	22.438
8	C	9.219	24
9	C	36.469	14.688
10	C	21.469	3.906
11	D	34.406	21.75

12	D	37.5	20
13	D	39	14.688

Retrieving the pedestrian ID could be considered as clustering points into distinct groups. Finding the safe region for each group could be formulated as drawing the confidence region for each cluster. Hence, the pedestrian detection problem could be studied as a combination of clustering and confidence region.

2.3.3.3 Pedestrian detection approach

Clustering Algorithm

Cluster algorithm is an important part of unsupervised learning. It is widely applied in machine learning and data mining areas. As the algorithm is unsupervised, which means no label is assigned to the data. Clustering means the separate data into groups or clusters that the data are similar inside the group but dissimilar between each group. There are different types of clustering algorithms, including K-mean clustering algorithm, Gaussian mixture model, Latent Dirichlet allocation, and hierarchical clustering [8].

In this paper, hierarchical clustering is chosen for implementation mainly for two reasons. First of all, among other clustering algorithms, such as K-mean clustering algorithm or Gaussian mixture model, the number of clusters has to be picked beforehand. However, for our problem the true number of pedestrians is not known. In the contrast, it is the answer we would like to find out by using the signal data. Thus, these types of algorithm do not fit our problem well. The second reason is comparing with K-mean or Gaussian mixture model, the hierarchical clustering is more powerful in cope with more complex shapes. In this study, no presumption is assigned for the shape. So hierarchical could be an algorithm fit for our problem.

The hierarchical clustering algorithm is an algorithm that produces a sequence of nested clusters. There are two general ways to implement hierarchical clustering algorithms, one is the agglomerative method, and the other is the divisive method. The divisive method is a top-down approach. It starts with all data in one big group, then recursively splits until each point lies in one individual cluster or a stop criterion is met. The agglomerative method, on the other hand, is a bottom-up approach. In this approach, each data point is initialized in its own cluster, and then clusters are merged until all points fall into one large cluster .

The key step of the either divisive approach or the agglomerative approach is how to calculate the proximity between two clusters. The most common way of defining proximity including the single link, complete link, average link, ward's method, and centroid method. Single link method uses the minimum of the distance between the points in the different clusters. Complete link method uses the maximum of the distance between the points in the different clusters. The average link proximity between two clusters is determined by the average of the pairwise proximities between all pairs of points. The proximity for ward's method is defined as

the increase in the squared error that results when two clusters are merged. In this paper, the ward's algorithm is chosen because the ward's proximity provides the approach of cluster analysis that focuses on the analysis of variance. For this type of proximity measurement, the agglomerative approach is applied for implementing the hierarchical clustering algorithm [9].

There are multiple approaches for measuring the distance of quantitative variables. In this paper, Euclidean distance is chosen to measure the similarity between each signal as it is the most common way to measure the physical distance in the Cartesian coordinates.

For distance between signal s_i and s_j with position (x_i, y_i) and (x_j, y_j), the Euclidean distance is calculated as

$$d_{ij} = \sqrt{(x_i - x_j)^2 + (y_i - y_j)^2} \quad (1)$$

Vehicle ID Information Implementation

Besides of the position information, we also have the vehicle ID information within the signal. The vehicle ID information tells us where the signal comes from. This type of information could be used to prevent the clustering algorithm from grouping points from same vehicle ID. For example, s_i^A and s_j^A cannot be merged as one group. Because they should be signals from different persons. However, s_i^A and s_j^B may put into the same group as they might be signals from the same person but detected by multiple vehicles. In order to avoid signals with same vehicle ID grouping together, a relative large distance is assigned so that they would be less likely to merge.

Safe Region

The concept of multivariate analysis is applied to draw the safe region. After cutting the dendrogram, points are assigned into a number of groups. Assuming in group k, we have n points $X_1, X_2, ..., X_n$. These points are considered random samples from a $N_p(\mu, \Sigma)$ population. The confidence region for the mean, μ, of a p-dimensional normal population is available from

$$\alpha = P\left[n(\bar{X} - \mu)' S^{-1}(\bar{X} - \mu) > \frac{(n-1)p}{(n-p)} F_{p,n-p}(\alpha)\right] \quad (2)$$

where

$$(3)$$

$$S = \frac{1}{n-1}\sum_{j=1}^{n}(X_j - \bar{X})(X_j - \bar{X})' \quad (4)$$

In our case, $p = 2$ as we are dealing with signal in x and y direction [10]. So the $100(1-\alpha)\%$ confidence region for the mean of a 2-dimensional normal distribution is the ellipsoid determined by all μ such that

$$n\left(\bar{X}-\mu\right)' S^{-1}\left(\bar{X}-\mu\right) \le c^2 = \frac{(n-1)p}{(n-p)} F_{p,n-p}(\alpha) \quad (5)$$

From the symmetric 2x2 matrix S, we have the eigenvalue λ_1 and λ_2 with its corresponding eigenvector e_1 and e_2. With the center of $\bar{X}$, the axis of the confidence region are

$\sqrt{\lambda_1}\sqrt{\dfrac{2(n-1)}{n(n-2)} F_{2,n-2}(\alpha)} e_1$ and $\sqrt{\lambda_2}\sqrt{\dfrac{2(n-1)}{n(n-2)} F_{2,n-2}(\alpha)} e_2$. By choosing the significant level α,

there are $100(1-\alpha)\%$ that the true mean lies in confidence region. Usually, it is chosen to be 5% [11].

2.3.3.4 Proposed pedestrian detection algorithm

The flowchart of pedestrian detection algorithm is shown in Figure 8.
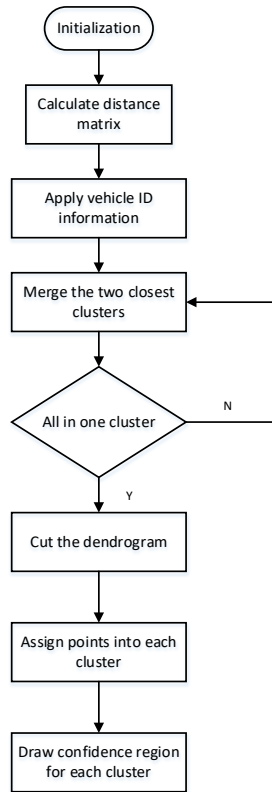

Figure 8. Flowchart of pedestrian detection algorithm.

The algorhm has 8 steps as follows:

1) Initialize each point to be its own cluster
2) Calculate Euclidean distance between each cluster

3) Assign large distance between same vehicle ID by using the maximum distance
4) Merge the two closest clusters by using ward's method
5) Repeat step 4 until all points are inside one cluster
6) Choose a distance D to cut the dendrogram
7) Group points into each cluster, by using the cutting result from step 6
8) Draw confidence region for each cluster

2.3.3.5 Simulation and discussions

One Case Simulation

In the one case simulation, we have 8 pedestrians with pedestrian ID a, b, c, d, e, f, g, h and 10 vehicles with vehicle ID A, B, C, D, E, F, G, H, I, J. The maximum spread range from the detected position to true position is set to 2.

Figure 9 shows a sample case of the simulation with pedestrian ID information. The large red spots indicate the true pedestrian position. The colored small spots indicate the Pedestrian ID. As can be seen from the plot, the shape of each point group varies for each pedestrian. Some positions may overlap with each other. For example, the position signals of pedestrian 'a' and 'e' are overlapped. This type of overlapping usually brings extra difficulty in distinguishes each group.

Figure 10 represents the same simulation case as Figure 9 but with the vehicle ID information.

Table 3. Original distance matrix

1	2	3	4	5	6	7	8	9	10	11	21	31	41	51	61	71
0.00	1.84	3.68	1.33	2.07	3.10	1.94	2.47	3.72	2.94	10.11	8.01	14.83	2.84	12.98	13.41	7.55
1.84	0.00	3.13	0.87	0.46	3.24	1.43	3.55	3.40	2.68	11.36	8.78	14.57	3.43	12.36	12.02	7.21
3.68	3.13	0.00	2.65	2.71	1.27	1.86	2.92	0.48	0.81	13.76	11.63	17.68	2.05	15.37	14.31	10.32
1.33	0.87	2.65	0.00	0.85	2.49	0.79	2.68	2.82	2.04	11.33	9.00	15.22	2.58	13.11	12.90	7.86
2.07	0.46	2.71	0.85	0.00	2.93	1.13	3.45	3.01	2.32	11.79	9.24	14.97	3.20	12.72	12.19	7.62
3.10	3.24	1.27	2.49	2.93	0.00	1.81	1.69	0.94	0.75	12.94	11.10	17.70	0.78	15.58	15.02	10.34
1.94	1.43	1.86	0.79	1.13	1.81	0.00	2.44	2.04	1.27	12.03	9.78	15.96	2.08	13.79	13.31	8.60
2.47	3.55	2.92	2.68	3.45	1.69	2.44	0.00	2.63	2.19	11.55	10.05	17.27	0.93	15.44	15.57	10.02
3.72	3.40	0.48	2.82	3.01	0.94	2.04	2.63	0.00	0.79	13.73	11.72	17.97	1.72	15.71	14.76	10.61
2.94	2.68	0.81	2.04	2.32	0.75	1.27	2.19	0.79	0.00	12.98	10.93	17.23	1.41	15.03	14.31	9.87

The large red spots still indicate the true pedestrian position. The different shapes indicate the Pedestrian ID. It is found that each pedestrian is detected 10 times by 10 vehicles.
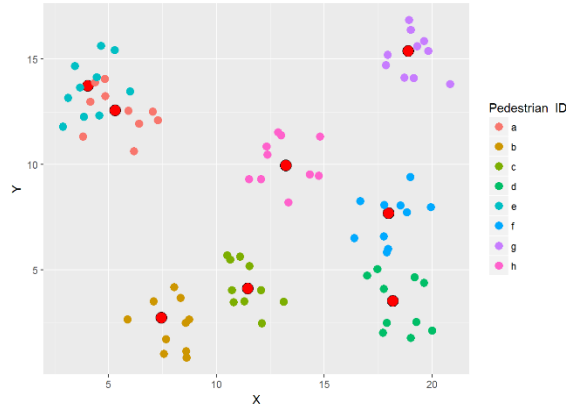
Figure 9. Pedestrian position plot with pedestrian ID.

As a result, 80 signals are obtained. By calculating the Euclidean distance between each signal, we will have an 80x80 distance matrix. Table 3 shows a part of the original distance matrix with column 1 to 10 and column 11, 21, 31, 41, 51, 61 and 71. The numbers in this table is the original computed pairwise distance.

For each vehicle, it detected all eight pedestrians. As for vehicle A, it generates eight signals from Aa to Ah. The pairwise distance between Aa and other seven signals from vehicle A matched the column 11, 21, 31, 41, 51, 61, and 71 in the distance matrix.

Vehicle ID information is used for preventing Aa of merge with signal Ab to Ah. A proportion of maximum distance is assigned to the distance from Aa to Ab, Ac, …, and Ah. The updated distance matrix is shown in Table 4. The red part is assign larger values than previous. We keep assigning large distance through the entire matrix for all ten vehicles. The proportion is decided by a block coefficient, which will be discussed in the next section.
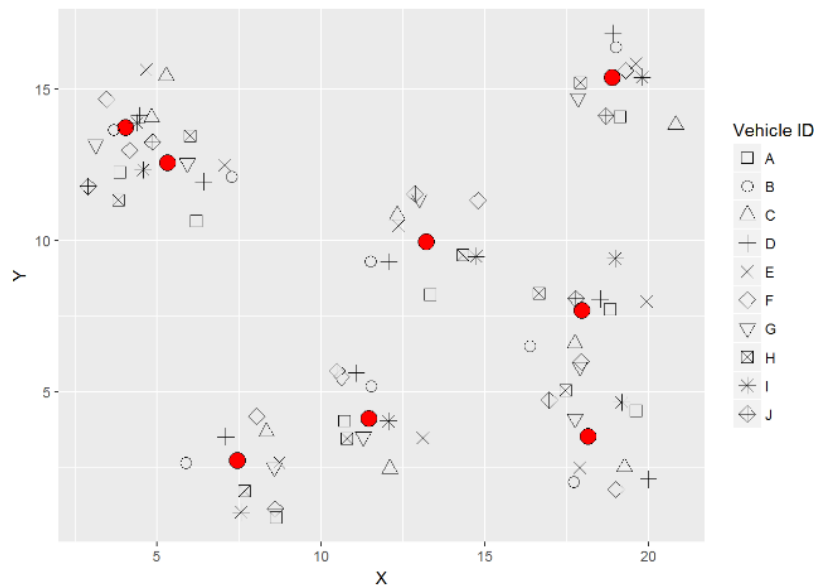

Figure 10. Pedestrian position plot with vehicle ID.

Table 4. The updated distance matrix

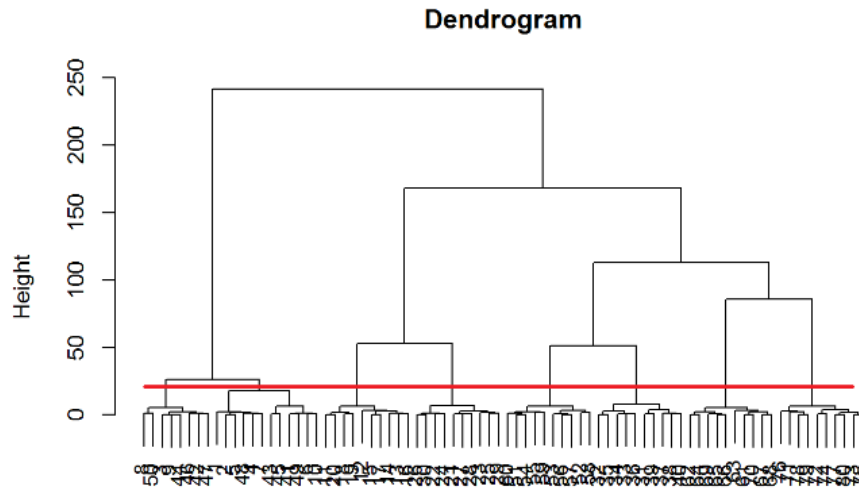By combining each point from bottom to up, a dendrogram is created as shown in Figure 11.

Figure 11. Dendrogram by hierarchal clustering.

Within the dendrogram, the X axis shows all the data points, the Y axis shows distance between each pair of clusters. After cutting the tree along the red line, we will have 8 clusters. The cut height is decided by the proportion of the maximum distance. The scale rate is given by the cut parameter. The grouping result is shown in Table 5.

From the grouping result, it is noticed that group 3 to group 8 perfectly retrieve the pedestrian signals. However, for group 1 and group 2, 2 points from pedestrian 1 are mistakenly assigned to pedestrian 2 (group 2). This type of error is tolerable, as we are more focusing on whether or not the safe region will cover the person's true position.

Updated distance matrix 1	2	3	4	5	6	7	8	9	10	11	21	31	41	51	61	71
0.00	1.84	3.68	1.33	2.07	3.10	1.94	2.47	3.72	2.94	31.18	31.18	31.18	31.18	31.18	31.18	31.18
1.84	0.00	3.13	0.87	0.46	3.24	1.43	3.55	3.40	2.68	11.36	8.78	14.57	3.43	12.36	12.02	7.21
3.68	3.13	0.00	2.65	2.71	1.27	1.86	2.92	0.48	0.81	13.76	11.63	17.68	2.05	15.37	14.31	10.32
1.33	0.87	2.65	0.00	0.85	2.49	0.79	2.68	2.82	2.04	11.33	9.00	15.22	2.58	13.11	12.90	7.86
2.07	0.46	2.71	0.85	0.00	2.93	1.13	3.45	3.01	2.32	11.79	9.24	14.97	3.20	12.72	12.19	7.62
3.10	3.24	1.27	2.49	2.93	0.00	1.81	1.69	0.94	0.75	12.94	11.10	17.70	0.78	15.58	15.02	10.34
1.94	1.43	1.86	0.79	1.13	1.81	0.00	2.44	2.04	1.27	12.03	9.78	15.96	2.08	13.79	13.31	8.60
2.47	3.55	2.92	2.68	3.45	1.69	2.44	0.00	2.63	2.19	11.55	10.05	17.27	0.93	15.44	15.57	10.02
3.72	3.40	0.48	2.82	3.01	0.94	2.04	2.63	0.00	0.79	13.73	11.72	17.97	1.72	15.71	14.76	10.61
2.94	2.68	0.81	2.04	2.32	0.75	1.27	2.19	0.79	0.00	12.98	10.93	17.23	1.41	15.03	14.31	9.87

The safe region is present in Figure 12. In the figure, it can be seen that even though group 1 and group 2 have signals miss assignment, the safe region still covers the pedestrian's true position. The centers of the group 1 and 2 are quite close to their real position. For group 3 in the left bottom, though we exactly retrieve all its signals, the group center is relative far away from the pedestrian's true position, due to the high variance of the signals. However, the confidence region is still able to cover the original position.

Table 5. Grouping result

Cluster number	1	2	3	4	5	6	7	8
Number of points	8	12	10	10	10	10	10	10
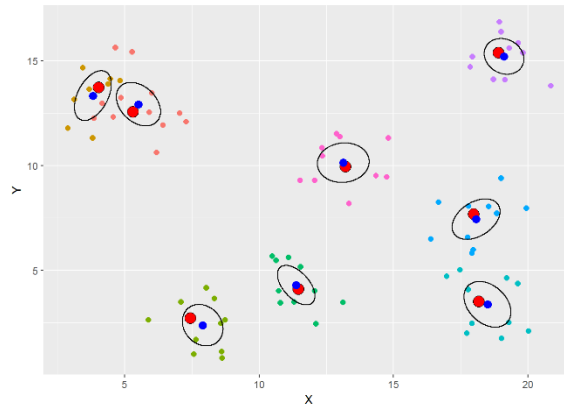
Figure 12. Safe region plot.

Multiple Cases Simulation

By choosing different proportion of block parameter and cut parameter, the clustering algorithm would have different accuracy rate. In this simulation, each case is simulated 1000 times to test the accuracy rate. True position inside the ellipsoid is considered to be passing. If true position lies out of the safe region, the case is considered a failure. The simulation results with different parameters are presented in Figure 13. The best average accuracy we get within all 441 cases 1000 simulation is 99.4%.

Figure 13. Three-dimensional plot Accuracy Rate.

Figure 14 provides the contour plot of the accuracy rate with the combination of cut coefficient and block coefficient. It pro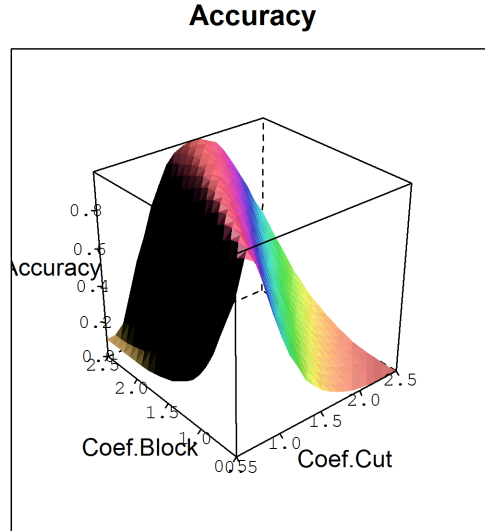jects the 3 dimensional information of Figure 13 into a 2 dimensional space. The brighter color represents the high accuracy. The white part covers the accuracy beyond 95%. The green color represents relative low accuracy. Low accuracy region is in the up-left corner and lower-right corner of the Figure 14. From Figure 14, it is also found that the pedestrian detection algorithm is able to achieve a high accuracy above 95 % (the white part) by choosing a proper block coefficient. As we can see, the white region becomes wider as block coefficient grows. We conclude that larger block coefficient leads to higher likelihood of accuracy if we choose the range between 0.48 and 0.68.
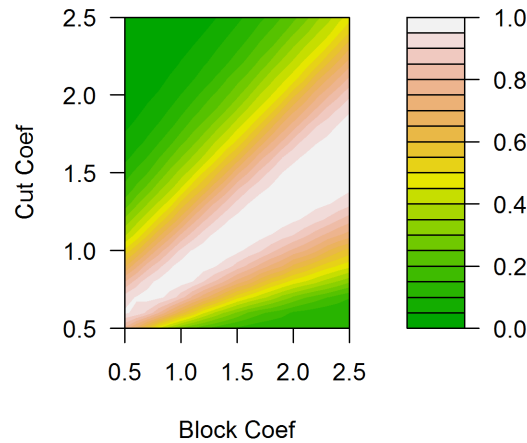

Figure 14. Contour plot Accuracy Rate.

2.3.3.6 Conclusions

As PAEB and V2V technologies are becoming mature, sending PAEB detected pedestrian information to the V2V network provides a potential benefit to make safety decisions earlier and more effective. This paper has provided a solution for a specific pedestrian data fusion problem in

the V2V-PAEB system by using hierarchical clustering algorithm to provide the safe region. A hierarchical clustering algorithm is proposed by using position and vehicle ID information. This method provides an approach of cutting the dendorgram by using a proportion of the maximum Euclidean distance. The results ensure a subject vehicle to approximate the number of pedestrians and their estimated locations from a large number of pedestrian alert messages by many nearby vehicles through the V2V network and the subject vehicle itself. The simulation results have demonstrated the effectiveness and applicability of the proposed method.

This result can be useful for PAEB system to make the warning/braking decisions earlier and hence, improve its pedestrian safety performance. The same idea can be applied to other objects (such as bicyclists) on the road.

2.3.3.7 References

[1]   Xu, Qing, et al. "Vehicle-to-vehicle safety messaging in DSRC." Proceedings of the 1st ACM international workshop on Vehicular ad hoc networks. ACM, 2004.

[2]   Rosen, Erik. "Autonomous emergency braking for vulnerable road users." IRCOBI Conference. 2013.

[3]   Coelingh, Erik, Andreas Eidehall, and Mattias Bengtsson. "Collision warning with full auto brake and pedestrian detection-a practical example of automatic emergency braking." Intelligent Transportation Systems (ITSC), 2010 13th International IEEE Conference on. IEEE, 2010.

[4]   Premebida, Cristiano, et al. "A LIDAR and vision-based approach for pedestrian and vehicle detection and tracking." Intelligent Transportation Systems Conference, 2007. ITSC 2007. IEEE. IEEE, 2007.

[5]   Szarvas, Mate, Utsushi Sakai, and Jun Ogata. "Real-time pedestrian detection using LIDAR and convolutional neural networks." Intelligent Vehicles Symposium, 2006 IEEE. IEEE, 2006.

[6]   Tang, Bo. "Pedestrian Protection Using the Integration of V2V Communication and Pedestrian Automatic Emergency Braking System." Thesis. Purdue University, Indianapolis, 2015. Print.

[7]   Wang, T., R. Aggarwal, and A. K. Somani. "Human Tracking Using Delphi ESR-Vision Fusion in Complex Environments." Proceedings of the International Conference on Image Processing, Computer Vision, and Pattern Recognition (IPCV). The Steering Committee of the World Congress in Computer Science, 2015.

[8]   James, Gareth, et al. An introduction to statistical learning. Vol. 6. New York: springer, 2013.

[9]   Friedman, Jerome, Trevor Hastie, and Robert Tibshirani. The elements of statistical learning. Vol. 1. Springer, Berlin: Springer series in statistics, 2001.

[10]   Anderson, Rolph E., Ronald L. Tatham, and William C. Black. "Multivariate data analysis." (1998).

[11]   Hair, Joseph F., et al. Multivariate data analysis: A global perspective. Vol. 7. Upper Saddle River, NJ: Pearson, 2010.

2.3.4 Reducing Delay in V2V-AEB System by Optimizing Messages in the System

2.3.4.1 Introduction

According to World Health Organization, the lives of approximately 1.27 million people are cut short every year because of road traffic crashes. Half of 1.27 million people die in road traffic crashes are pedestrians, motorcyclists, and bicyclists [1]. TASI (Transportation Active Safety Institute) at IUPUI (Indiana university-Purdue University Indianapolis) focus on research to reduce the accidents and make road safer. One project is to combine V2V network with AEB system to reduce the accidents.

In V2V (vehicle-to-vehicle communication) systems, vehicles communicate with each other over a wireless network. A common protocol used for V2V wireless network is Discrete Short Range Communication (DSRC) [1]. Each vehicle in the V2V system acts as a communication node. A node exchanges data about its location, speed and movement with other nodes and make decision based on received information accordingly. Traditional V2V message protocol has some limitations. They only broadcast about the information within the system [2]. So the safety gain is limited to vehicles in the V2V network. The current V2V system does not share the information about what is happening surrounding the vehicles. Whereas AEB (Autonomous Emergency Braking) system uses its onboard sensors such as radar, LIDAR, camera, infrared, etc. to detect potential collision and alert the driver [3]. Its limitation is that it requires clear line-of-sight to detect what is in the surrounding and it only benefits the safety of AEB installed vehicles. Our idea is to integrate the complementary capabilities of V2V and AEB system to overcome their individual limitations. V2V-AEB is a part of cooperative driving research to reduce accidents in the context of autonomous driving, where the information detected by the AEB system of the car and its own speed, location and movement is shared over V2V network, so that other vehicles can use the shared AEB sensing information to prevent potential collisions.

In vehicle-to-vehicle communication-Autonomous emergency breaking system (V2V-AEB), vehicles exchange data about the objects detected by its onboard sensor and its own location, speed and movement with other nearby vehicles. The object information detected by a vehicle and the information received through V2V network is processed by every vehicle. If there is an imminent crash and if the driver does not make appropriate braking action, the AEB system alerts the driver and/or applies the brake automatically to avoid/mitigate collison.

To make the V2V-AEB system more effective certain issues need to be resolved [5]. One of the key issues is minimizing the messages shared in the V2V-AEB network. If there are *n* vehicles and *m* pedestrians in a busy road, and each vehicle is V2V-PCS enabled and is able to detect their vehicles and pedestrians, each vehicle can have at most the information of m+ (n-1) objects. If each vehicle broadcasts a messages for each detected object, each vehicle will receive (m+n-1)×(n-1) messages. As *n* and *m* increases, the number of message will be difficult to process in reasonable time. Since it is possible that many of these objects do not cause collision threat, it is important to send only messages related to the objects presenting potential collision. In this report, we present some methods to reduce the amount of messages in the system.

The order of this paper is as follows. We first describe the basic architecture of V2V-AEB system. Then we will formulate methods to reduce the messages containing information about pedestrian. The third part is to describe how to prevent jamming of network. Then we describe the method for reducing the number of messages about the information of vehicles detected by V2V-AEB.

2.3.4.2 V2V-AEB System

In V2V communication, vehicles broadcast information about their speed, location, direction of travel and make safety decision based on the received information. The AEB system uses onboard sensors to detect potential crashes, and alerts the driver or applies automatic brake if the driver does not take necessary action. The idea is to integrate the complementary capabilities of V2V and AEB system to allow the information of objects sensed by the onboard sensors to be shared in the V2V network [2].

The overview of V2V-AEB system implemented on each vehicle is described by the block diagram in Figure 1. For better understanding of the system, we divide the system in two parts: the sender side and receiver side.

Sender side: The AEB system gets the input from the camera sensor and the radar sensor, which is processed by AEB system of the car. If there is any object (vehicle, pedestrian, and bicyclist) in the system and the AEB senses the object, it sends its information to the next block where the information is converted in the global coordinates from the local coordinates of the respective vehicle. Then the information of the object is formulated in the message format along with vehicle state, these message is then broadcast over V2V network. **Receiver side:** The messages (V2V-AEB) received by a vehicle are processed. Information in different messages may be merged as different vehicles may send same object information. The vehicle then convert the merged information in its local coordinate system. Then the object information is further merged with the information of objects detected by vehicle's own AEB system. The objects are tracked in real-time and time to collision of the object with respect to the vehicle is calculated in order to make safety related action.
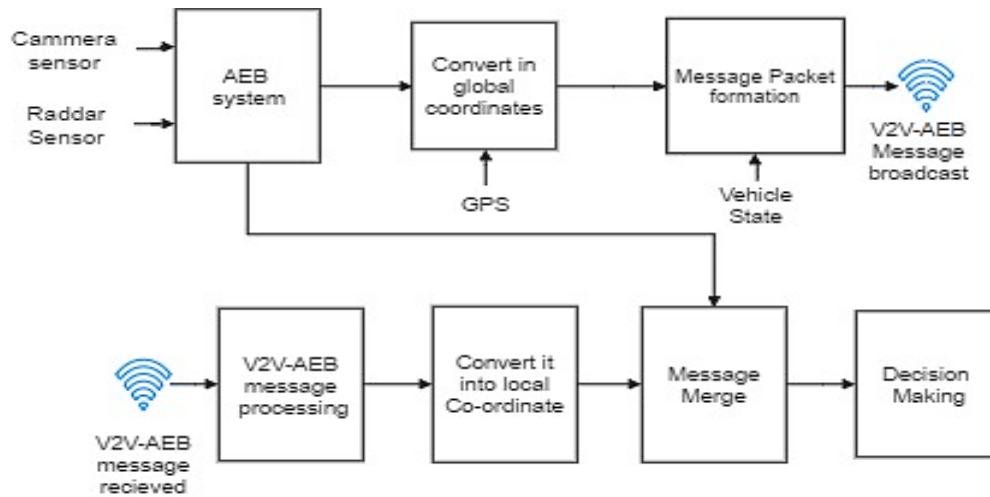

Figure 1. The architecture of the V2V-AEB system.

We have created the V2V-AEB system simulation using PreScan [4] and MATLAB Simulink. The following example simulation scenario has 3 vehicles and 2 pedestrians (See Figure 2). The speed of the vehicle is 14m/s, the maximum deceleration of the vehicle is 12m/s^2, the speed of two pedestrian are 1.2m/s and 1.5m/s, respectively.
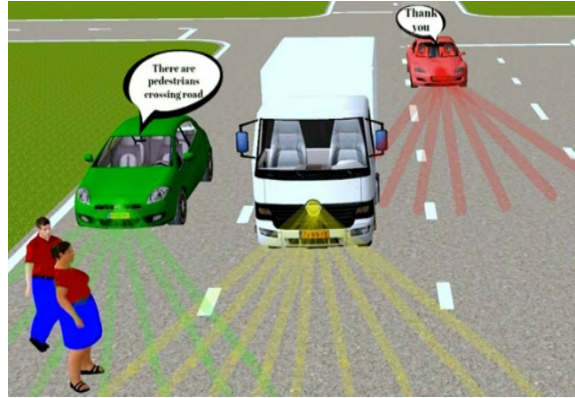
Figure 2. V2V-PAEB test scenario

2.3.4.3 Optimizing pedestrian information

The vehicle may send the information of all objects it detects. However some pedestrian are just standing and there may not be potential collision. So it's necessary to segregate the information about those pedestrian who can cause potential collision and who does not. The solution to this problem is that vehicle only sends the information about those pedestrians that can be harmed by the vehicle. So for minimizing the V2V messages about pedestrians it is necessary to decide which pedestrian information should be sent.

The pedestrian walking on the sidewalk can be removed from the V2V message, as we assume the vehicle will not go on the sidewalk. This will considerably decrease the amount of V2V messages without sabotaging the safety of pedestrian. However, if a pedestrian is moving towards the road, the vehicle should send the information about this pedestrian as it might cause safety issue.

Bifurcating the pedestrian using GPS coordinates: Assume that vehicles can get accurate GPS information and road boundary information through on board sensors, the location and boundary of a road can be found out via combining them with google maps. If the position of the pedestrian or other objects is not on the road, then the car can neglect that object. As in the near future, GPS will be more accurate to centimeter range. It can be seen from Figure 3 that Google maps can be used to determine the boundaries of roads. So this information about the road can be used to see if the pedestrian is on the road or not.
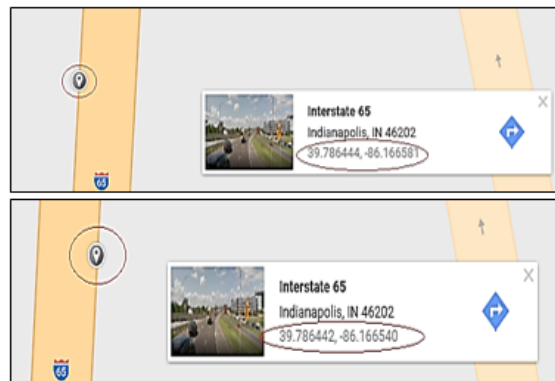

Figure 3. GPS Location of road boundary from Google map

A. Eliminating objects not likely to cause collision

If a pedestrian is behind a forward moving vehicle on a road, sending the information of the pedestrian to that vehicle does not help improving the safety (See Figure 4).
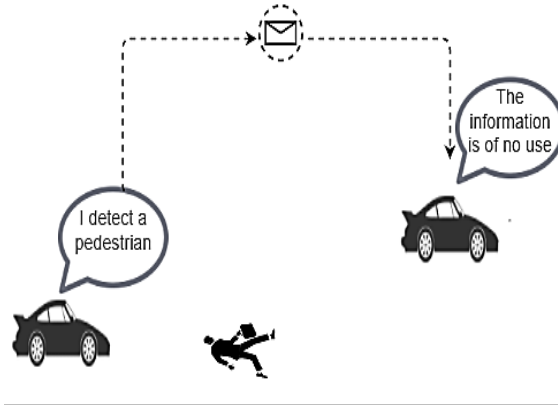

Figure 4. Sending information of pedestrian in front

Therefore, a subject vehicle can neglect sending messages of the detected objects if the objects are behind the vehicle in front and there is no vehicle behind the subject vehicle. However, the question is the definition of "no vehicle behind the subject vehicle".

B. Calculating which pedestrian information to be sent

In V2V environment, vehicles share their speeds, accelerations, positions, directions over V2V network. This information is available with vehicle to decide. If a subject vehicle that can detect a pedestrian and any vehicle in surrounding area can reach a point where pedestrians are crossing the road, should broadcast the message with the pedestrian information.

Let the pedestrian speed be V_p, the width of the road that the pedestrian has to cross be L, maximum speed of vehicle in the scenario be V_v and maximum acceleration be a_v. Assuming that the acceleration of the pedestrian is 0, the time for pedestrian to cross the road (T_p) is

$$T_p = \frac{L}{V_p} \quad (1)$$

The maximum distance, S_v, between the vehicle behind the subject vehicle and the road-crossing pedestrian detected by the subject vehicle is used to determine if the pedestrian message should be broadcast or not. S_v can be determined by distance formula considering (T_p)(Equation 1) as time required by pedestrian to cross a road and maximum vehicle speed and acceleration.

$$S_v = V_v \times \frac{L}{V_p} + \frac{a_v \times L^2}{2 \times V_p{}^2} \quad (2)$$

Where,
V_v= the speed of vehicle in behind
a_v= the acceleration speed of vehicle in behind

If a pedestrian is crossing the road, and there is a vehicle behind the subject vehicle that detected the pedestrian, and the vehicle behind is at less than a distance of S_v to the detected pedestrian (Equation 2), then the subject vehicle should send the pedestrian information to the V2V network.

However, if there are many pedestrians and vehicles in the system, the CPU time to process all the information will be large. To tackle this problem, we can select one extreme case such as the pedestrian with minimum speed, the maximum value of V_v and a_v.
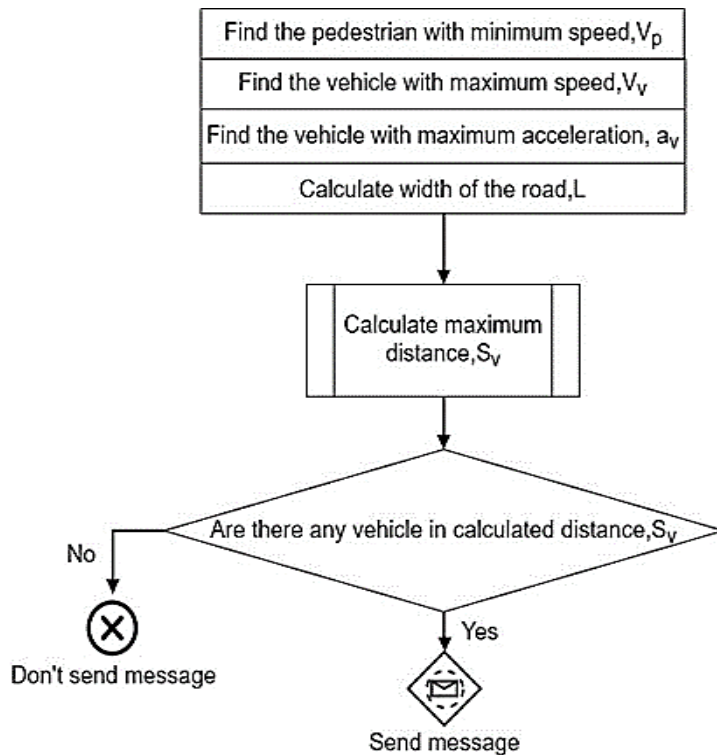
Figure 5. Flow chart to determine which pedestrian information should be sent

Example 1.
A pedestrian is crossing a 4-lane road at a speed 1.2 m/sec. The width of each lane is 3.7 m. The maximum velocity among all the vehicles behind the subject vehicle is 80km/hr (22.22 m/s) and the maximum acceleration among all the vehicles be 2m/s²

Thus, from Equation 3

$$S_v = V_v \times \frac{L}{V_p} + \frac{a_v \times L^2}{2 \times V_p{}^2}$$

$$= 3.7 \times 4 \times \frac{22.22}{1.2} + \frac{1 \times (3.7 \times 4)^2}{2 \times 1.2^2}$$

$$= 426.15\ meter$$

Therefore, if a vehicle finds any other vehicle in the range of 426.15 meter in V2V network it can broadcast the information about the pedestrian.

C. Grouping of pedestrian

In V2V-AEB, each vehicle sends the information about the pedestrians they have detected along with their own vehicle information. Consider a scenario of m V2V-AEB enabled vehicles and n pedestrians at a road intersection. If each vehicle can detect all pedestrians and broadcast them to the V2V network, then each vehicle will receive $(m-1) \times n$ messages. The receiver vehicle has to process all this messages to make a safety decision. To reduce the number of messages we propose a method to cluster the pedestrian information in groups before sending them. Thus reducing the processing time of the vehicle on receiver side and the communication delay due to packet collision in VANET.

For clustering these pedestrians, we should guarantee that safety is not compromised. Pedestrians having similar information can be grouped as one pedestrian such that all pedestrians stay in one group until the time they cross the road safely so that they can be considered as one entity.

<u>Working of the system:</u> To group the pedestrian, we use a clustering method. If the distances between two pedestrians is less than a predefined threshold a and their speed difference is less than b, they are grouped in one cluster and the pedestrian information is sent as a single pedestrian with the speed of minimum one which ensure us all the pedestrian will cross the road safely and as one entity. The value of a and b are selected such that pedestrian will remain in the same group until they cross the street safely.

When a pedestrian is detected, we calculate its distance from the detecting vehicle and thus evaluate its position in x-y plane before converting it into GPS coordinate as shown below.
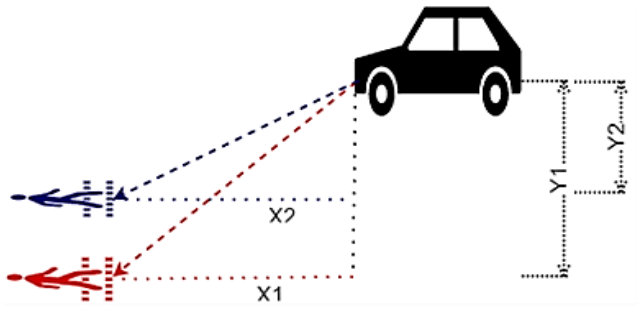
Figure 6. Pedestrian detection by the vehicle

After calculating the x, y coordinate, velocity and direction of pedestrian the information is put in matrix form.

Table1: Matrix for pedestrian information

Pedestrian	Location (x)	Location (y)	Velocity	Direction
1	x_1	y_1	v_1	D_1
2	x_2	y_2	v_2	D_2
3	x_3	y_3	v_3	D_2
4	x_4	y_4	v_4	D_1

| 5 | x5 | y5 | V5 | D2 |

To send the information of pedestrians as a group, the pedestrians are arranged in ascending order as per their positions in the y-axis. The first pedestrian is selected from the list and made as a hub. Then the pedestrians are selected and formed as a group whose distance from the hub is less than or equal to threshold a, difference between their speeds is less than the threshold b and they are moving to the same direction. Similarly, all the groups are created. The grouped pedestrian is broadcast as the single entity with the average location of the pedestrians in the hub and the lowest velocity among all the pedestrians in the hub. Before broadcasting the information, the location is converted in the form of GPS coordinates.

As the pedestrian are arranged in ascending order of their y location, when we discover the distance of a pedestrian to other pedestrian in the same hub is greater than a, a new hub is created to other pedestrians. This process iterates until all pedestrians are grouped.

Algorithm

Step1 Differentiate pedestrian as per their directions of crossing the road (here we consider 2 directions whether pedestrians are moving from left to right or from right to left with respect to the vehicle. Other pedestrians who are not in these two categories are not grouped.

Step 2 Arrange pedestrian in increasing order of their location in y axis.

Step 3 Select pedestrian 1 from the array and make it as a hub of a group. The current group number m is 1.

Step 4
For pedestrians $i=2$ to total number of pedestrians in the same moving direction of crossing the road
{Calculate the distance of pedestrian i to the hub of group m
   Calculate speed difference of pedestrian i and that of the hub if group m.

   If (distance > a or difference of speed > b)
      {j=m,
       while(j ≥1)
         {Calculate distance of pedestrian i
         to hub of group j
         Calculate the speed difference of
         Pedestrian i with hub of group j
            If ((distance<a) and (speed<b))
               exit while loop
             else
                 j=j-1
             end
        }
       If   (Already exist == 0)
       { m=m+1; make pedestrian i as a hub of group m.
       }
} //end of for loop

Repeat step 4 for the other direction

Step5: Broadcast the hub information of all groups over the V2V network

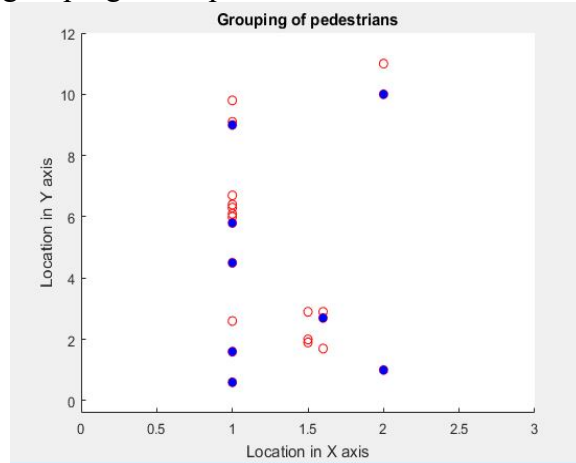Figure 9 shows the output for grouping of 24 pedestrians.

Figure. 9 Grouping of pedestrian using MATLAB (blue dots indicate the hub)

The sender side needs to process the 24 pedestrian in order to form groups and convert the location of the hub of groups to GPS coordinates. The 24 pedestrians were grouped into 8 groups by the algorithm. Suppose these 24 pedestrian and 20 cars are on the road, by using the grouping algorithm, we can reduce the number of messages from 480 to 160. Thus on the receiver side instead of processing 480 messages it just has to process this 160 messages. Each blue dot indicates one hub whose information is broadcast through the V2V network.

Example 2.

The example in Figure 7 shows how the 10 pedestrians are grouped using the proposed algorithm. Figure 7 represents the data array (dashed box) of the pedestrians. Xs represent the pedestrian by parameter (x, y, and v), where x is his location in x-axis, y in y-axis, and v is its speed. The pedestrians are arranged in ascending order, according to their locations in y-axis in an array.

After arranging the pedestrians, group is greedily selected in multiple iterations. The pedestrians whose location difference are less than or equal to 1 meter and the magnitude of difference between speed is less than equal to 0.1m/s is included in a group of the respective hub as described below. A group is defined starting from a pedestrian we call it a hub.
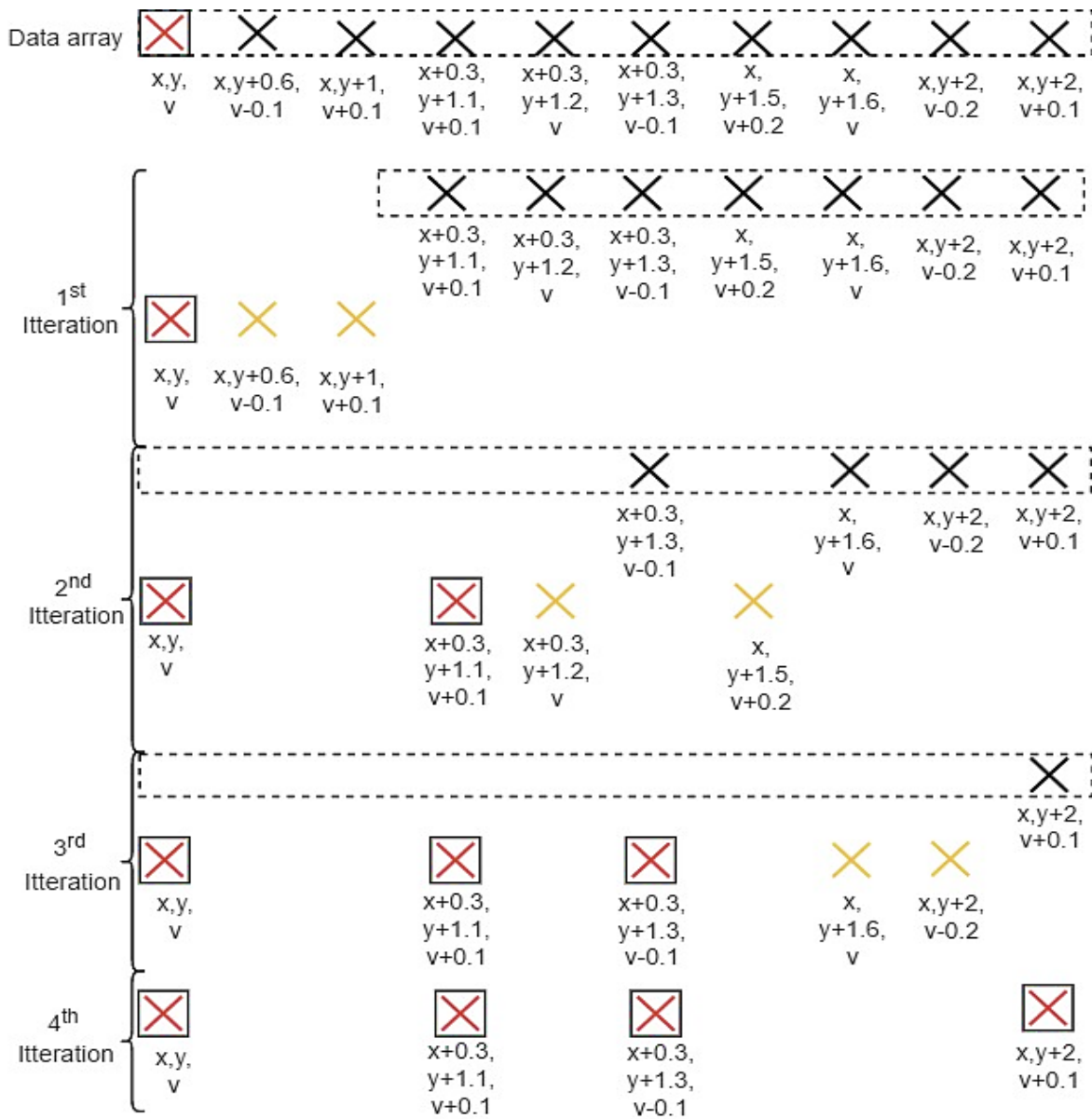
Figure.7 grouping of pedestrian example

Iteration 1: The first element of the array is created as a hub (showing in red color and in a box with solid line.) of group 1. The box with solid line represents the hub of the group 1. The pedestrians in group 1 are selected that whose distance b to the hub is less than 1 meter and difference of speed is less than or equal to 0.1m/s with respect to the hub. Yellow X denotes that 2nd and 3rd pedestrians are selected pedestrians. As we see that the distance from the 4th pedestrian from the hub is 1.14 meter which is greater than 1 meter, thus it is not included in group 1.

Iteration 2: The 4th pedestrian is selected as the hub of group 2. Pedestrians 5 and 7 are selected to form a group as explained in iteration 1. Pedestrian 6 does not belong to group 2 since its velocity difference from the hub is |0.2|m/s, which is greater than 0.1m/s limit.

Iteration 3: Pedestrian 6 is selected as the hub og group 3. Pedestrians 8 and 9 belongs to group 3 as they satisfy the group conditions as described in iteration 1.

Iteration 4: The 10th pedestrian is the hub of group 4. Since there is no other pedestrians, it forms its own group.

The iteration stops when all pedestrian are grouped. The information of all hubs are sent over V2V-AEB network.

2.3.4.4 Jamming of network
Preventing from sending messages while jamming of network

There might be cases when there are many pedestrians on the road. For example, around 14,000 pedestrian walk in one hour near west 34th street as per 2015 studies [7]. Also, according to reports [7], there were as many as 55 pedestrian fatalities. If all the information is shared over the V2V network, it will cause network overload, leading to large number of packet collision, communication delay, and message processing delay. Thus, if there are too many pedestrians in the environment, the best option will be preventing vehicle to send pedestrian messages (except in critical emergency conditions such as medical emergency condition) over V2V network, in order to prevent congestion of network.
Therefore, the question arises what is the maximum number of pedestrians detected that vehicle should stop sending pedestrian messages. However, it will not be appropriate to select based on the number of pedestrians, because it might be possible that just one vehicle is able to detect all pedestrians, whereas the pedestrians are not in the line of sight of other vehicles. In this case, information from the vehicle who can detect all the pedestrians is very important. So instead of determining by the number of pedestrian we use the time delay in the network to decide whether a vehicle should broadcast message of observed objects or not. When the network is congested and the time delay in the system is such that no safety decision can be made in time to benefit safety by using received information through V2V network, the vehicle can stop sending messages of observed objects.

That is $\quad t_d \geq Maximum\ delay, Md$

Such that, $\quad\quad ttc < ttb$
Where,

$$t_d = message\ processing\ time\ delay$$

Maximum delay (M_d): the threshold time delay above which the AEB system cannot avoid collision.

ttc = time to collision i.e. time when the car will collide with the object.
ttb = threshold time for braking, i.e. minimum time required by the vehicle to stop the car.

Therefore, the vehicle can stop sending messages when the time delay in the system is above maximum delay and will continue sending message only when delay of the system becomes lower than the maximum delay. The proposed method can be implemented as shown below (see Figure 10).
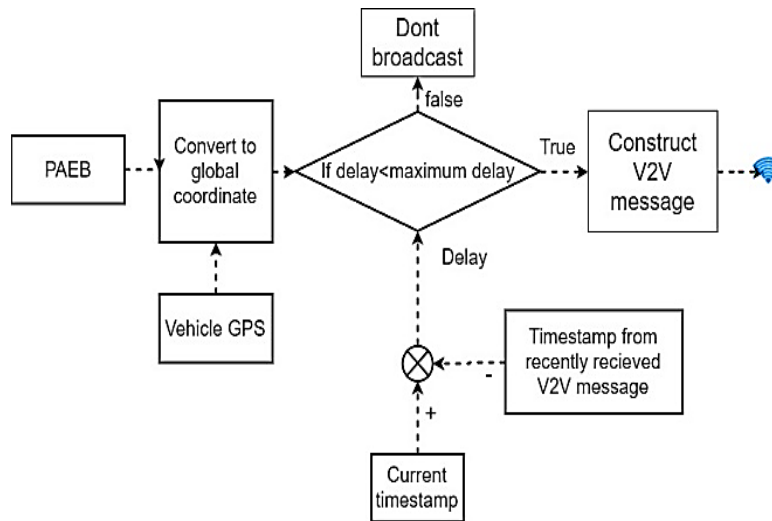
Figure 10. Sending information of pedestrian in front.

In Figure 10, the received message from V2V-AEB message has the information about when the message is generated. The time stamp from the received message is compared with the current time to calculate the delay in receiving message. If the calculated delay is found above maximum delay, the vehicle does not construct the V2V message to broadcast the object detected by its onboard sensor over V2V network. Where, maximum delay is the threshold time delay above which the AEB system cannot avoid collision i.e., when time to collision to an object is greater than threshold time for braking (i.e., minimum time required by vehicle to stop).

2.3.4.5 Optimizing vehicle information

In V2V-AEB system, the car sends the information about the pedestrian and vehicle that it detects through its onboard sensor. It is important to decide if sensed information about the vehicle should be sent. If the sensed vehicle is in the V2V network, the location and the speed of the sensed vehicle is already shared in the network. Then it is not beneficial for another vehicle to send the same but less accurate sensed vehicle information to the network again.

How to decide which vehicles are in V2V network? There can be various ways to identify if a vehicle is in the V2V network. One way is to make the car capable with V2V communication can bear some logo so that other vehicles can neglect processing those vehicles information and not sending it in the V2V network. The other way can be that vehicle can compare the information from AEB system and those received from V2V network. If the two vehicles have almost the same information, it can restrain itself from broadcasting that information in V2V network. As GPS has some error, we cannot get the exact location of the vehicle. However, we can find the similar data having similar location, speed and direction. However, in this case as the vehicles have to process the information it will take computation time.

2.3.4.6 Conclusions

The proposed system helps to reduce communication delay and processing delay in the system by reducing number of message in the V2V-AEB network. Thus, it increases the chance that V2V-AEB system makes decision on time. Using the method of elimination, information about some pedestrians are not sent if they are not on the road or there is no vehicle in the range to cause potential collision. Further, the proposed method of grouping is tested in a simulation with 24 pedestrians, which were grouped in 8 groups. We also discussed method to prevent V2V network jamming, by monitoring delay in the network.

2.3.4.7 References

[1] Betsy McKay "Traffic accidents kill 1.27 million globally, WHO says", The Wall Street journal, June 16, 2009.

[2] Tang, Bo. "Pedestrian Protection Using the Integration of V2V Communication and Pedestrian Automatic Emergency Braking System." Thesis. Purdue University, Indianapolis, 2015. Print.

[3] Hideaki Hayashi, Ryo Inomata "Development of pre-crash safety system with pedestrian collision avoidance assist," Toyota motor corporation, Japan, Paper number 13-0271.

[4] B. Tang, S. Chien, Z. Huang and Y. Chen, "Pedestrian protection using the integration of V2V and the Pedestrian Automatic Emergency Braking System," 2016 IEEE 19th International Conference on Intelligent Transportation Systems (ITSC), Rio de Janeiro, 2016, pp. 2213-2218. doi: 10.1109/ITSC.2016.7795913

[5] K. Shakyawar and S. K. Tiwari, "Throughput and packet delay analysis for improvements in VANET," 2016 International Conference on Electrical, Electronics, and Optimization Techniques (ICEEOT), Chennai, 2016, pp. 4070-4073. doi: 10.1109/ICEEOT.2016.7755479

[6] J. K. Kim *et al.*, "Experimental studies of autonomous driving of a vehicle on the road using LiDAR and DGPS," *2015 15th International Conference on Control, Automation and Systems (ICCAS)*, Busan, 2015, pp. 1366-1369.
doi: 10.1109/ICCAS.2015.736485

[7] Winnie Hu, "New York's Sidewalks Are So Packed, Pedestrians Are Taking to the Streets," The New York Times, June 30, 2016.

2.4. Analysis of Potential Co-Benefits for Bicyclist Crash Imminent Braking Systems

2.4.1 Introduction

In the US, the number of traffic fatalities has had a long term downward trend as a result of advances in the crash worthiness of vehicles. These improvements in crash worthiness do little to help protect non-motorists. Over the last few years, this has been reflected in the number of pedestrian and bicyclist fatalities increasing in both absolute and relative terms (up over 15% since 2010 for pedestrians and nearly 20% for bicyclists). In 2010 there were 618 bicyclists killed and an estimated 52,000 bicyclist injuries. This increased to 749 bicyclist fatalities in 2013 and 818 in 2015 with an estimated 45,000 injuries [2, 3, 4]. These trends are summarized in Figure 1.
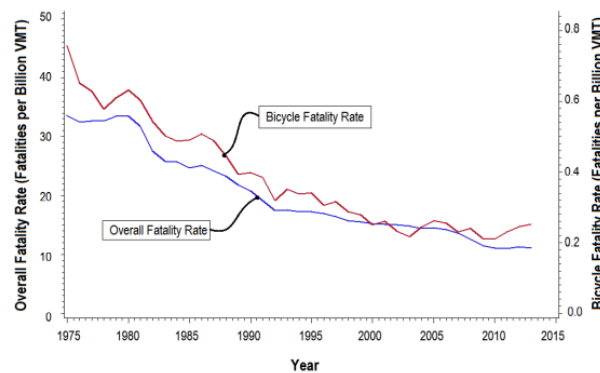

Figure 1. US traffic fatality rate and the percentage of bicyclist fatalities over time

While increasing and becoming more lethal, US, bicycle crashes are a relatively small part of the road safety with 2.3% of roadway fatalities. In most of Europe and China bicyclist fatalities compared to total fatalities is approximately 10%. In Japan, bicyclists make up 14% of traffic fatalities. In Netherlands, they comprise 32% of roadway fatalities [5].

Around the world, the typical cyclist varies widely. In the US, there is a tendency for bicyclist crashes to be viewed as something that affects children. Figure 2, shows that the demographics of those killed in bicycle crashes has changed dramatically over time. Over the last forty years,, the average cyclist fatality has changed from mid-teens to over 45 as more older Americans turn to cycling as a form of fitness and recreation rather than mobility.
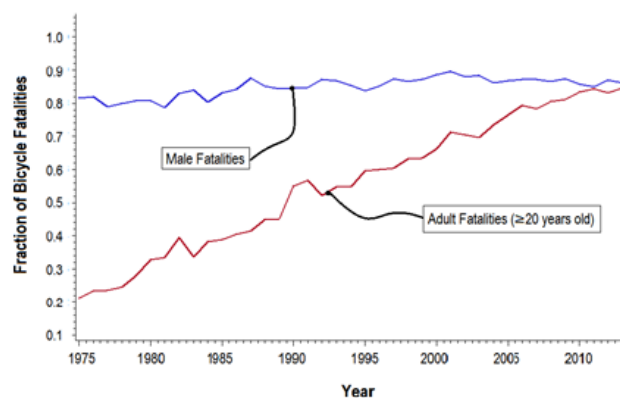

Figure 2. Demographic composition of bicyclist fatalities (FARS 1975-2015)

The objectives for safer vehicles has also changed from crashworthiness to crash avoidance. The first generation of crash imminent braking systems (CIB) focused on preventing rear end collisions. Detecting these imminent crashes is relatively simple. In comparison, the newer generations of CIB systems have been developed to recognize and mitigate non-motorist collisions where victims are harder to detect and behaviors much more complex.

In a previous paper we evaluated the benefits associated with CIB systems designed to mitigate pedestrian crashes [1]. We follow a similar approach here. Pedestrian crash geometries are more complex since they have a wider range of behaviors than are exhibited in rear end collisions and these behaviors can affect system performance quite a bit. Bicyclist crashe geometries are still more complex since bicycles bring significant speed to the crash and have a wider variety of maneuvers (they appear from the street or sidewalk, they may execute turns, etc.) Cyclists can legally occupy the travel lane and in some cases the sidewalk. As a result, many more scenarios need to be tested to fully evaluate system capabilities.

Evaluation of the full range of scenarios is beyond the scope (and budget) of our project and instead we focus on the potential to mitigate social loss in only the most important scenarios. The test track simulation approach we take is likely to be the only practical mechanism for evaluation since bicycle crashes are rare and statistical power from field operational trials is extremely low.

The rest of the paper is organized as follows. In Section II we develop a classification scheme for bicycle crash scenarios based on publicly available data. These are validated with GES from GES/FARS for 2015. In Section III, we briefly describe our models for determining the consequences of particular crashes. We also estimate a performance model based on 100 test track simulations using our surrogate target. In Section IV we develop models to be used for evaluating the effectiveness of the tested CIB system. In Section V we discuss the results and develop a set of conclusions and some steps for future work. Our analysis is limited by key missing variables. As a result, we can only talk about the performance of the system uncer best case assumptions and interpret our findings as the "potential benefits" of this type of CIB system. We find that under the best of circumstances that the benefits are rather limited, and are most likely to accrue only to the oldest cyclists because of their frailty.

2.4.2 Testable Crash Scenarios Based on Publicly Available Data

A. Defining CIB Relevant Crashes

Our analysis starts with GES (General Estimates System) and FARS (Fatal Accident Reporting System) for 2014 and 2015. We restrict our use to this data because they are more closely harmonized than in previous years, they provide a better evaluation of fatalities and are similar to the results produced using other approaches and provide sufficient detail about the bicycle crash geometry. For these two years there were on average an annual number of 54,000 bicyclist involved crashes (from GES) and include involvement by 56,000 cyclists. The average annual number of fatalities is 766. Our analysis also includes a measure of social cost that comprises the tangible costs associated with a crash (congestion, property damage, lost wages, loss of functional capacity as well as the intangible costs (loss of life or diminished enjoyment of life) that are based on quality adjusted life year analysis. DOT regulatory guidance offers 9.1 million dollars as the complete value for a lost life [6]. This value of life incorporates what people would be willing to pay or forego to achieve a small reduction in the probability of life lost. It is not an accounting measure of lost wages or insurance settlements. The document also provides guidance about how to value injuries based on Abbreviated Injury Scale values (AIS). Fatalities comprise 62% of the $10 billion annual social cost of bicycle crashes.

Our analysis narrows down the number of CIB relevant crashes that can be reasonably evaluated by eliminating some crashes 1) involving a single vehicle and a single non-motorist who is a cyclist; 2) only light vehicles in transport (no parked cars, heavy trucks, busses, motorcycles, special or emergency vehicles); 3) vehicle in forward motion that has not lost control or recovering from another evasive maneuver; 4) crashes where the bicyclist strikes the motor vehicle from behind. The remaining crashes comprise about 70% of the crashes, fatalities and social cost.

Classification of Bicyclist Crashes

We base the testable scenarios for bicyclist CIB systems on two different analyses: harmonized GES/FARS data for 2010-2011, a period where there was enhanced data collection for both pedestrians and more extensively for bicyclists; 2) some state level data for Michigan and Indiana where we have access to the police crash reports (PAR) and can reevaluate the coding of crashes as a form of quality control.

It is important to keep in mind that the purpose of the PAR is not as a scientific instrument, but to determine liability and potential criminal fault surrounding the crash. Neither pedestrian nor cyclist crashes are systematically investigated as a part of the Federal data gathering process. These PAR are the sole source of information for both GES and FARS. From out analysis of data with both actual PAR information and the way that they were coded, we find that many important features are often not described in the PAR crash narrative and key features may be left of out the report since they are unrelated to culpability.

Our approach is to this potentially missing data is to develop a three tier classification scheme for bicycle crashes. The first tier is gross geometry, tier two includes vehicle maneuver and the third tier involves cyclists maneuvers. We find that it is almost always possible to identify tier 1 from the PAR, usually possible to identify tier 2 classifications and sometimes tier 3 is a hunch based on subtleties of the scene diagram. While these are sometimes little more than a hunch. These are summarized in Figure 3.

As a way to shorthand sometimes complex scenarios we use either CP, PP or UP to classify tier 1 (crossing path, parallel path or unknown/unclear path) to specify the pre-crash
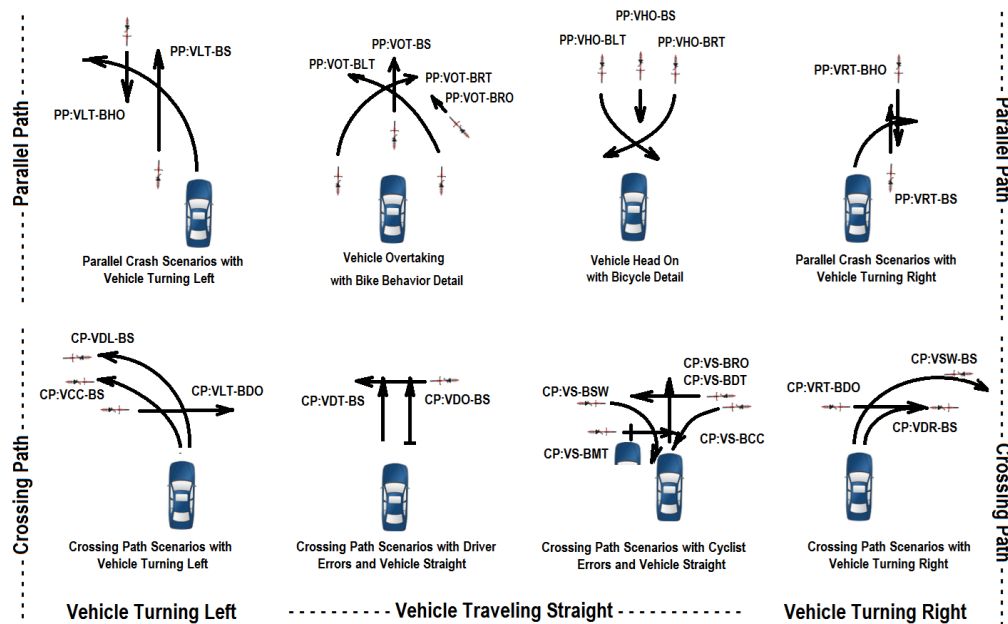

Figure 3 ThreeTier Testable Bicycle Crash Scenarios

paths of the vehicle and bicycle relative to one. UP are those where there is no clear direction to the bicycle for example while a riding in a parking lot. In tier 2 we identify the vehicle motion prior to the crash and use VOT, VHO, VRT, VLT, VS or VDO (to indicate the vehicle is overtaking the bike, approaching the bike head on, turning right or left, or going straight or driving out, stopping then going). Finally, individual elements in the figure incorporate subtleties of bicyclist behaviors and maneuvers. In Figure 3, the three tiers are represented as rows (gross geometry), columns (vehicle action) or individual elements (cyclist behavior).

Our analysis suggests that out of the 24 identifiable bicycle crash scenarios, the most serious scenario, PP:VOT-BS (vehicle striking the bicyclist from behind) involves 26% of social cost, 34%

of fatalities but only 12% of the number of crashes. The second most serious crash scenario, CP: VS-BRO (vehicle striking the bicyclist as they ride out in the vehicle path after stopping) involves 17% of the crashes, 17% of the fatalities and 17% of the social cost. This makes sense since vehicles are likely to have slower speeds in areas where they face frequent intersections. Scenarios where the vehicle is turning have much lower potential for harm because vehicle speeds are lower. In addition, CIB systems typically are disabled when the vehicle is under active maneuver such as in a turn. This is clearly stated in the owner's manual as is the relative ineffectiveness in crossing scenarios.

Our analysis focuses on the PP:VOT-BS scenario since it is both the most important, and the vehicle manufacturer claims to have some effectiveness in these situations.

Bicyclist Crash Surrogate

Our cyclist surrogate is designed to visually look like an adult cyclist, 174 cm tall (a weighted average of males and females involved in crashes) and appear to weigh (volume) 73 kg with a BMI of 24. This is a little chubbier than the Hybrid III adult male designed in the 1970s as BMI have risen considerably since then with sizing developed from current American anthropometric data in NHANES [7]. The mannequin is covered with a metal fabric skin that provides the same radar cross section at 77GHz as a human would and rides on a 26" mountain bike [8] and rides on a carrier that is both durable enough to accommodate vehicle impacts and unobtrusive [9]. The developed surrogate is light, durable and unlikely to cause vehicle damage on collision [10]. Instrumentation to predict injuries conflicts with these goals.

An Analysis of Vehicle and Cyclist Speeds

Unfortunately, bicycle crashes are not systematically investigated and compiled in Federal databases in the US (with methodologies such as the CDS, now CISS). While there are plans to do so, the data are not expected to be available until after 2020. Vehicle speed is clearly a dominant variable in both the extent of cyclist injury and in system effectiveness. It is anticipated that faster vehicle speeds will provide less system reaction time, and lead to greater injuries. The best surrogate for vehicle speed for cyclist crashes is to examine vehicle speed for pedestrian crashes from the most recent systematic study, the Pedestrian Crash Data Study, PCDS [11]. This proxy is intended to identify general characteristics about speed rather than provide exact benefit information.

In previous work we have analyzed several factors that allow better prediction of vehicle traveling speed just prior to pedestrian crashes [12]. Unlike there, there is no source of investigated crashes like PCDS where traveling speed can be reconstructed.

Figure 4 shows the speed at impact for those situations in terms of crash frequency (top) and crash severity (bottom). This reinforces the notion that speeds for vehicles traveling straight, particularly when they are not at intersections, leading to increased likelihood of serious injury or fatality.
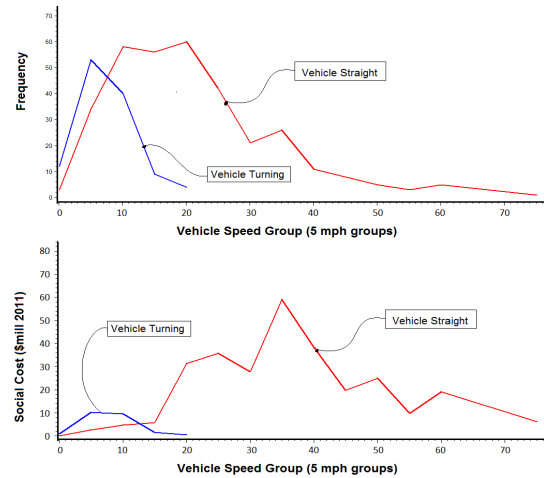
Figure 4. Vehicle traveling speeds and crash frequency (top) and social costs (bottom) for pedestrian crashes involving the vehicle turning and going straight

Our cyclist speed information is generated by examining bicyclists from footage from our naturalistic driving study [10]. For 1000 adult cyclists, median speeds were 12.5 mph with upper and lower quartiles at 16 and 9 mph. The mannequin can also reflect leg motion (pedaling) as was also observed during this study and is reflected in mannequin movement.

E. Other Test Factors

The vast majority of crashes occur during daylight hours. Children are involved primarily in crossing crashes. While a child mannequin was developed, it was not used for this round of testing. Cyclists are relatively unlikely to ride during inclement weather. Obscuring objects are present in only about 9% of crashes. These are typically widely distributed over most crash types with a common occurrence only where the cyclist is trapped, facing multiple threats (CP: VS-BMT).

2.4.3 System Performance Testing

A. Testing and Test Site

All cyclist crash imminent braking systems were conducted on the 13 m wide asphalt test track in Columbus, Indiana. 89 tests were performed with usable information under a variety of conditions: varying bicycle speed, vehicle speed, pedaling behavior and cyclist position relative to the vehicle.

Econometric Modeling of System Performance

The performance of a cyclist CIB system must determine a vehicle speed at impact. We use a doubly truncated Tobit model that posits an underlying latent index identifying the challenge posed for detection system and its capacity to meet that challenge. The measure of effectiveness is defined by:

$$Effectiveness = \frac{Travel\,Speed - Impact\,Speed}{Travel\,Speed}$$

95

This functional form identifies the effects of other variables in the test scenario to be proportional to travel speed. In addition to providing better fits for the data, the model is less subject to problems of heteroskedasticity (the variance of the error term being related to regressors which leads to inefficient estimates and tends to bias standard errors, invalidating confidence intervals and implied hypothesis tests) [13]. We use a maximum likelihood estimator where

$$ y* = \beta \cdot x + \varepsilon \quad with \quad y = \begin{cases} 1 & if\ y* > 1 \\ y* & if\ 0 \leq y* \leq 1 \\ 0 & if\ y* < 0 \end{cases} $$

and a log-likelihood function defined by

$$ \log \mathcal{L}(\beta, \sigma, \alpha | x, y) = $$
$$ \sum_{y=0} \log \Phi\left(\frac{\alpha + \beta \cdot x}{\sigma}\right) + \sum_{y=1} \log \Phi\left(\frac{1 - \alpha - \beta \cdot x}{\sigma}\right) + \sum_{0 < y < 1} \log\left[\frac{1}{\sigma} \varphi\left(\frac{y - \alpha - \beta \cdot x}{\sigma}\right)\right] $$

Here Φ and φ represent the standard normal cdf and density respectively. The model estimates for our system effectiveness measure are based on 89 simulated crashes using a vehicle equiped with a cyclist CIB system and our PP:VOT-BS crash scenario. Estimates are in Table 1.

Table 1. Tobit estimates for system performance model

variable	Quadratic Expansion Model			Linear Expansion Model		
	estimate	std err	p-val	estimate	std err	p-val
intercept	.70563	.01934	.002	.71839	.30641	.022
vehicle speed	-.12329	.00233	.000	-.12415	.22888	.000
veh speed^2	-.00387	.00233	.101	--	--	--
cyclist speed	.05601	.02804	.050	.17393	.03492	.000
cycl speed^2	-.01374	.00485	.004	--	--	--
centered	.52108	.22265	.022	.17993	.25831	.530
limb motion	-.00033	.22126	.998	. 07474	.21503	.729
sigma	.43383	.06769	--	.60314	.09652	--
chi-sq (df)	80.00	6	.000	53.72	4	.000
Pseudo-R^2	.5552			.3728		

The objective behind the final models estimated is not to identify individual factors that we can prove are related to system performance but to predict the system performance over a variety of scenarios using the best available predictor. As a result, our analysis maintains some variables in the formulation that are not statistically significant because they provide valuable controls for an unbalanced factorial design and better reflect outcomes in real world implementation. We find that a quadratic model (second order Taylor series in the kernel) fits substantially better than a linear model (increase in Rsquare from .37 to .55, p-value of .000). Dominant variables in the model are *vehicle traveling speed*, *cyclist speed*, and *whether the cyclist was centered on the front of the*

vehicle or offset 25% of the way from the right front corner (a common point of impact). *Limb motion* matters little. A graphical representation of performance incorporating vehicle and cyclist speed is presented in Figure 5. Our estimates indicate that the system is most effective for bicycle speeds of approximately 12 mph. In other words, it is well tuned for the kind of riders that were encountered during our naturalistic driving study.

For our scenario, if the vehicle is traveling slower than the bicycle, no crash will occur. We anticipate that the faster the relative speed difference the more serious injuries are likely to be. The difference in vehicle speed and cyclist speed, delta-V, has a long history as an injury severity predictor for injuries caused by the inelastic collision with the cyclist [14, 15].

Crashes are averted (cyclist delta-V of 0) if the system is effective enough to slow the vehicle to less than the cyclist speed before impact. In Figure 6. the difference between the solid line and the dashed line shows how much delta-V has been reduced as a result of the CIB system effectiveness.
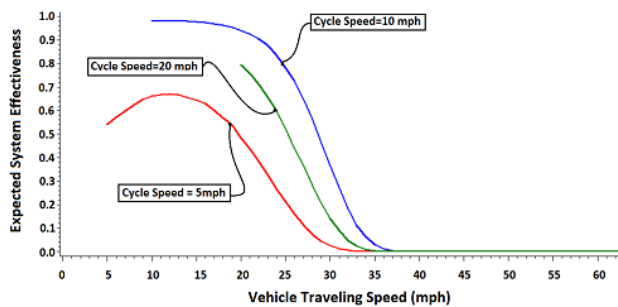

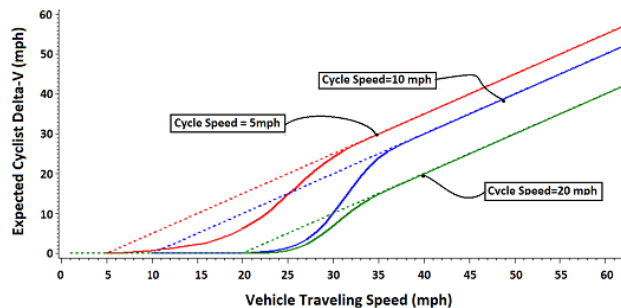Figure 5. Comparison of system effectiveness for cycling speeds.

Figure 6. Cyclist Delta-V for vehicle and cyclist traveling speeds

2.4.4 Proxying Bicyclist Crash Outcomes

A. Consequence Assessment.

Several authors have previously estimated the effects of factors on the severity of pedestrian injuries [16,17]. There are relatively few empirical models developed specifically for bicyclists. Among the best work examining both [18], they do not account for key variables such as cyclist speed, crash geometry (e.g., overtaking vs head-on) or, cyclist age (frailty). This makes it difficult to translate this work from the German to the American context. To complement that work we use a detailed model of pedestrian crashes and adjust the results to bicyclists. Our analysis is based on PCDS [18, 19] and includes variables such as non-motorist age, and a geometry regarding how the pedestrian was struck in addition to vehicle speed.

Because of the number of variables, parsimony requires estimating an ordinal probit model predicting the extent of injury as measured by the Maximum Abbreviated Injury Scale (MAIS). Because the investigation of cases in PCDS does not match the distribution of all crashes well (PCDS tended to investigate crashes with more severe consequences more heavily), we weight the observations in our maximum likelihood estimates proportionately to the occurrence of severities in GES for sample (e.g., crash severities that are over-represented get weights of less than 1 while crash severities that are underrepresented get weights greater than 1). These estimates are presented in Table 2.

Parameter	Estimate	StdError	P-value		
Intercept1	-0.8224	0.2113	<.0001		
Intercept2	2.3008	0.1588	<.0001		
Intercept3	3.0021	0.1661	<.0001	Number of Observations	447
Intercept4	3.7252	0.1788	<.0001	Log Likelihood	-575.926
Intercept5	4.2002	0.1914	<.0001	Model LR Test (7df)	231.707
Intercept6	5.2847	0.2425	<.0001	Pseudo R-square (McFadden)	.171
ImpactSpeed	-0.0653	0.0050	<.0001	Pseudo R-square (Cox/Snell)	.404
PedAge	-0.0110	0.0026	<.0001		
WithPath	-0.3504	0.1373	0.0107		
AgainstPath	-0.2076	0.4923	0.6732		
PedSpeed	-0.0316	0.0405	0.4355		
Dark	-0.3224	0.2387	0.1767		
DarkLit	-0.0990	0.1180	0.4015		

Table 2. Parameter estimates for ordinal probit model

For a simplified exposition, a comparable model is estimated using a probit model for pedestrian fatality using the same predictor variables. The parameter estimates are similar to those in Table 2 but without cutpoints. The main argument for the usability of these results is that speed at impact for pedestrians is a proxy for the delta-V for cyclists. In Figure 6, the probability of fatality is shown for different pedestrian aged 20, 45 and 70. The frailty of a 70 year old compared to a 20 year old is like a 10 mph increase in speed at impact. For a 40 mph delta-V, increases fatality risk from .2 to .5.
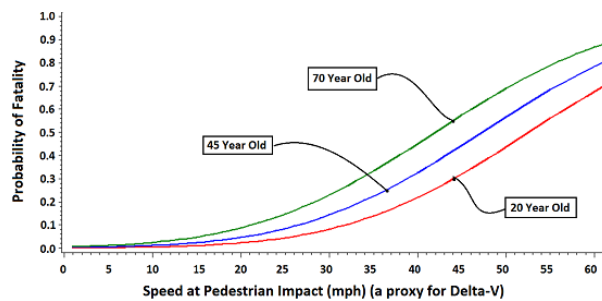

Figure 6. Probability of Fatality as a function of Pedestrian Speed at Impact (a Proxy for Cyclist Delta-V)

System integration

Integrating the model of system performance with the model of injury causation is summarized in Figure 7 for a cyclist traveling speed of 10mph, close to the system's "sweet spot" or most effective cyclist speed. The use of a cyclist CIB system shows benefits for different ages of riders and different vehicle speeds. For a twenty year old cyclist in a crash with a vehicle that is not CIB equipped (solid red line) there is little difference from one with CIB (dashed red line). Similarly, the solid blue and green lines indicate the delta-V for a 45 year old and 70 year old encountering a

vehicle that is not cyclist CIB equipped while the corresponding dashed lines represent the same scenario with a CIB equipped vehicle. This represents a near best case scenario.
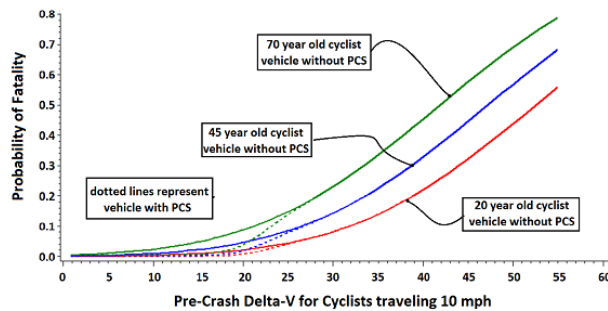

Figure 7. Life-saving potential of cyclist CIB system

The biggest benefits occur when the solid and dashed lines are the farthest apart. This occurs for pre-crash delta-V (closing speeds) of around 18 mph for all age groups. By the time closing speeds are 25mph the system loses any effectiveness (the lines converge). These cases occur when vehicle speed is around 28 mph for maximum benefit and by 35 mph the life saving benefits are exhausted for all age groups.

For younger bicyclists, in the delta-V range where the PCS system is effective, the probability of fatality is small enough, (only two or three percent), that relatively few lives will be saved by such a system. For older riders, the probability of fatality is nearly three times as high in delta-V ranges where the system is effective, with much more lifesaving. For a cyclist traveling at 10 mph, the maximum benefit is obtained with a closing speed of 19 mph. The reduction in fatalities at this most effective speed is 1.9% reduction in the probability of a 20 year old fatality, 2.7% reduction for a 45 year old, and 5.2% for a 70 year old. As older Americans continue cycling as a way to keep active and fit, this will be increasingly important.

2.4.5 Summary and Conclusions

In this paper we identified the most important bicyclist crash scenarios for crash imminent braking systems. Our tested scenario involved a crash geometry that is responsible for approximately a quarter of cyclist social cost and a third of cyclist fatalities in single light vehicle crashes. Its primary contribution is that it is based on actual test track data, rather than optimistic simulated performance. As such it embodies key crash features such as time to collision, vehicle speed, and importantly, the speed that cyclists bring to the collision.

We developed a model of cyclist injuries based on injuries incurred by pedestrians, and adapted the results using delta-V in pace of vehicle speed at impact. We intend this as suggestive rather than definitive since it allows us to incorporate other modifying variables such as age and geometry.

Our results are limited in that they examine only one scenario (albeit the most deadly) and only one manufacturer's vehicle. Still, they are suggestive about the limited co-benefits available in bicyclist CIB systems compared to pedestrian systems. The results lay out a methodology for the evaluation of other systems and scenarios. The design and enhancement of CIB systems, like our analysis, remain a work in progress.

2.4.6 References

[1]   Good, D. H., S Chien, L Li, K Krutilla and Y Chen (2015) Preliminary Benefit Analysis for Pedestrian Crash Imminent Braking Systems. IEEE 18th International Conference on Intelligent Transportation Systems 1123-8.

[2, 3, 4] USDOT, NHTSA (2012-17) Traffic Safety Facts: Bicyclists and Other Cyclists 2010-15. Publication numbers DOT HS 811 624, DOT HS 812 151 and DOT HS 812 151

[5]   World Health Organization (2015) Global Status Report on Road Safety United Nations, 2015.

[6]   USDOT (2014) Memorandum from Under Secretary RE Treatment of the Economic Value of a Statistical Life in Departmental Analyses – 2014 Interim Adjustment
[7] Centers for Disease Control and Prevention (2005-2011). National Health and Nutrition Examination Survey Data. Hyattsville, MD: U.S. Department of Health and Human Services,

[8]   Belgiovane, D.J and C-C Chen (2016) RCS Measurements of Bicycles and Human Riders for Automotive Radar No 2016-01-0168 SAE Technical Paper.

[9]   Rini Sherony, Qiang Yi, Stanley Chien, Jason Brink, Mohammad Almutairi, Keyu Ruan, Wensen Niu, Lingxi Li, Yaobin Chen, and Hiroyuki Takahashi, "Development of a Bicycle Carrier for Bicyclist Pre-Collision System Evaluation," No. 2016-01-1446, SAE Technical Paper, 2016.

[10]   Chen, Y., X. Chien, L. Li, H. Yokota, L. Christopher, J. Zheng, R. Tian, D. Good, C-C. Chen. (2016) Development and Testing of Standard Bicyclist Crash Scenarios. Final Report. Transportation Active Safety Institute. 219pp.

[11]   NASS Pedestrian Crash Data Study 1994-1998, version 03-Mar-2001, The University of Michigan Transportation Research Institute

[12]   Good, D and Abrahams, R. (2014) Vehicle Speeds for Pedestrian Pre-Crash System Test Scenarios. ITSC 2014 Proceedings.

[13]   Madalla, G. (1983) Limited Dependent Variables in Econometrics. Cambridge University Press

[14]   Shelby, S. 2011. Delta-V as a Measure of Traffic Conflict Severity, Transportation Research Board annual Meeting, 2011.

[15]   Svensson, A. and Hyden, C., Estimating the severity of safety related behaviour. Accident Analysis and Prevention, Vol. 38, pp. 379-385, 2006.
[16] Rosen, E., & Sander, U. (2009). Pedestrian fatality risk as a function of car impact speed. Accident Analysis & Prevention, 41(3), 536-542.

[17]   Wisch M, Seiniger P, Pastor C, Edwards M, Visvikis C. (2013) Scenarios and weighting factors for pre-crash assessment of integrated pedestrian safety systems. 2013

[18]   Rosén, E. (2013) Autonomous Emergency Braking for Vulnerable Road Users, IRCOBI Conference 2013 (paper IRC-13-71)

[19]   Simms, C. and D. Wood (2009) Pedestrian and Cyclist Imact: A Biomechanical Perspective (Springer).

3 Synergistic Activities (E.G., Collaborations with Others Outside the UTC And Using Data from Previous Research to Develop Driver Models)

TASI has been collaborating with Toyota North America for the AEB system testing system development and AEB system evaluation for pedestrians and bicyclists before and concurrent with this UTC project. All vehicle test data were used in this UTC project for developing the pedestrian and bicyclist models for simulation. The insights obtained from the Toyota project also helped in formulating the V2V-AEB idea. TASI has also been collaborating Delphi for the development of evaluation methods and subject testing of the driver status monitoring systems.

TASS International had provided an in-kind support of the PreScan vehicle simulation software to TASI for the development of the simulation model and pedestrian V2V-AEB simulation.

Faurecia Emission Control Technologies, USA, LLC provided vehicle test track for TASI to perform testing of the developed AEB performance evaluation system and enabled TASI to collect real-time AEB performance data for model development.

Indiana University internally funded an eighteen-month $72K grant for bicyclist naturalistic riding study led by Dr. David Good with assistance of several TASI faculty members (Lauren Christopher, Stanley Chien, and Yaobin Chen) along with graduate student David Emerson. This study developed new equipment to be used to determine visually the distance to objects using depth from defocus technology. This system was designed for use on bicycles where power, weight, and unobtrusiveness are key elements in determining the level of natural behavior on the part of the bicyclist. To encourage natural behavior, design criteria included participants using their own bicycles, minimal interaction with the system (it was designed to operate for a week, turning itself on and off without any participant interaction) and be unobtrusive enough that the system would not be stolen or the bicyclist being constantly reminded that their behavior was being recorded. With only ten participants, our small-scale study did not generate sufficient data for detailed statistical analysis of cyclist behaviors.